

Isolation, engineering, and characterization of intracellular antibodies specific for the huntingtin protein

by David W. Colby

B.S.Ch.E, Virginia Commonwealth University, 2000

B.S., Virginia Commonwealth University, 2000

Submitted to the Department of Chemical Engineering in Partial Fulfillment of the Requirements for the Degree of

DOCTOR OF PHILOSOPHY
in Chemical Engineering

at the

Massachusetts Institute of Technology

March 2005

(C) 2005 Massachusetts Institute of Technology
All rights reserved

Signature of Author _____
Department of Chemical Engineering
March 2005

Certified by _____
K. Dane Wittrup
J.R. Mares Professor of Chemical Engineering and Bioengineering
Thesis co-Supervisor

Certified by _____
Vernon M. Ingram
John and Dorothy Wilson Professor of Biology
Thesis co-Supervisor

Accepted by _____
Daniel Blankschtein
Professor of Chemical Engineering
Chairman, Committee for Graduate Students

Isolation, engineering, and characterization of intracellular antibodies specific for the huntingtin protein

By David W. Colby

Submitted to the Department of Chemical Engineering on
March 23, 2005 in Partial Fulfillment of the Requirements for the
Degree of Doctor of Philosophy in Chemical Engineering

ABSTRACT

Huntington's Disease (HD) is an autosomal dominant neurodegenerative disorder caused by an expansion in the number of polyglutamine-encoding CAG repeats in the gene that encodes the huntingtin (htt) protein. A property of the mutant protein that is intimately involved in the development of the disease is the propensity of an N-terminal proteolytic htt fragment containing the glutamine-expanded region to misfold and adopt a conformation which is prone to aggregation. Intracellular antibodies (intrabodies) against htt have been shown to reduce htt aggregation by binding to the htt fragment and inactivating it or preventing its misfolding. Intrabodies may therefore be a useful gene therapy approach to treatment of the disease. However, high expression levels of previously reported intrabodies have been required to obtain even limited reductions in htt aggregation. We have used yeast surface display (YSD) of antibodies combined with fluorescence activated cell sorting (FACS) to isolate novel single-chain antibody (scFv) clones against huntingtin from a non-immune human antibody library; these scFv's did not inhibit htt aggregation. Engineering analysis, including the derivation of equations that describe the probability that cells will form htt aggregates as a function of time and concentration, were used to estimate the intracellular expression level and binding affinity required for robust aggregation inhibition. The pool of antibodies isolated was used as the starting point for engineering an intrabody with appropriate properties for intracellular activity. We then applied YSD to affinity mature this scFv pool for binding to the first 17 aa of htt and analyze the location of the binding site of the intrabody mutant with the highest affinity. Interestingly, the paratope was mapped exclusively to the variable light chain domain of the scFv. A single domain antibody was constructed consisting solely of this variable light chain domain, and was found to retain full binding activity to huntingtin. Cytoplasmic expression levels of the single domain were at least five-fold higher than the scFv, enabling mild aggregation inhibition. However, antibodies expressed in the cytoplasm do not form intradomain disulfide bonds as they do when secreted from cells. By mutating the cysteine residues that form the disulfide bond in the single-domain antibody to hydrophobic amino acids, we found that antibody binding affinity was drastically reduced in the absence of the disulfide bond. Effectiveness of the single-domain intrabody was improved by increasing its affinity in the absence of a disulfide bond. The engineered intrabody, V_L12.3, eliminated toxicity in a neuronal model of HD. We also found that V_L12.3 inhibited aggregation and toxicity in a *S. cerevisiae* model of HD. V_L12.3 is significantly more efficient than earlier anti-htt intrabodies, and is a potential candidate for gene therapy treatment for HD. The approach demonstrated to improve intrabody potency through the use of highly expressed single-domain antibody fragments and disulfide bond-independent binding suggests a generally applicable approach to the development of effective intrabodies against other intracellular targets.

Thesis Supervisors: K. Dane Witttrup, J.R. Mares Professor of Chemical Engineering and Bioengineering, and

Vernon M. Ingram, John and Dorothy Wilson Professor of Biology

This work is dedicated to my daughters, Nora and Audrey, and to those in my family who have lived with HD: Carrie, Ramsay, and Grandpa (Bill). Together, you have provided me with the motivation for this undertaking.

Acknowledgements

This work could not have been completed, or even undertaken in the first place, without the support of many people. My advisors, Dane Wittrup and Vernon Ingram, both played invaluable roles in my education and in guiding research. Dane taught me to be realistic, both when I was overly optimistic and when I was too pessimistic. He kept me focused on what was important, but gave me the freedom to fool around some of the time. Perhaps most important, he was the chief cheerleader for my project, propping me up every time I came into his office discouraged and dejected. Vernon kept my arguing skills sharp, let me take no assumption for granted, and scrutinized my every move. It wasn't always fun, but it taught me to do my work to the highest scientific standards.

The support and helpful comments of the additional members of my thesis committee, Profs. Susan Lindquist and Daniel Wang, are greatly appreciated.

My coworkers in both labs provided a helpful and stimulating atmosphere. I especially want to thank my good friend Andy Rakestraw, for patiently listening to the day-to-day minutiae of my research, and acting as a sounding board for numerous half-baked ideas. The students who came before me in the Wittrup lab helped me get started: Christilyn Graff, Katarina Midelfort, Bala Rao, Andy Yeung, and Jeff Swers. I have to thank Jason Burbank for leaving me with the erroneous impression that 'anything goes' in the Wittrup lab; it might not have been correct, but it definitely took the pressure off that first year or two. The students who came after me were also helpful: Stefan Zajic, Ginger Chao, Greg Thurber, Shanshan Wu Howland, and Steve Sazinsky. My coworkers in the Ingram lab were always helpful; thanks to Barbara Blanchard for teaching me cell culture, and thanks to Tina Holden and John Bankston for helping with protein production. Finally, I'd like to acknowledge the help of several postdocs in both labs: Brenda Kellogg, Peter Thumfort, Jennifer Cochran, Mark Olsen, Yong-Sung Kim, Dasa Lipovsek, and Andrea Piatesi. I especially want to thank Jennifer helping me out repeatedly with basic lab techniques and being a friend and colleague.

Some of my undergraduate assistants helped generate data, others just generated more work for me to do, but I'd like to thank all of them for teaching me how to teach others to perform research: Dobrin Dragonov, Nancy Chen, Colin Chu, Payal Garg, Katarzyna Puchala, John Cassady, Grace Lin, and Christine Nee.

Many thanks to past and current collaborators, including Sue Lindquist, Anne Messer, Troy Littleton, Beverly Davidson, Arne Skerra, Martin Duenwald, Helen Zazulak, Jack Webster, and Mimi Lee.

Gary Wnek, one of my undergraduate research advisors, gave me my first research opportunity. I wouldn't be where I am today without his support and encouragement.

Finally, I am grateful for the financial support of the National Science Foundation Graduate Research Program, the Hereditary Disease Foundation, and the HighQ Foundation.

Table of Contents

TABLE OF FIGURES.....	7
ABBREVIATIONS USED	8
CHAPTER 1. INTRODUCTION.....	9
<i>Huntington's Disease</i>	<i>9</i>
<i>Mechanism of huntingtin aggregation</i>	<i>10</i>
<i>Intracellular antibodies</i>	<i>11</i>
<i>Yeast Surface Display</i>	<i>13</i>
<i>Thesis Outline.....</i>	<i>14</i>
CHAPTER 2. ISOLATION AND CHARACTERIZATION OF ANTIBODIES FROM A DIVERSE YEAST SURFACE DISPLAY LIBRARY.....	19
<i>Introduction</i>	<i>19</i>
<i>Materials and Methods</i>	<i>20</i>
<i>Results.....</i>	<i>25</i>
<i>Yeast HD FRET system.....</i>	<i>26</i>
<i>Discussion.....</i>	<i>28</i>
CHAPTER 3. ENGINEERING ANALYSIS OF INTRACELLULAR HUNTINGTIN AGGREGATION AND ITS INHIBITION BY INTRACELLULAR ANTIBODIES.....	37
<i>Derivation of a mathematical model describing the probability that a cell will form an htt aggregate</i>	<i>38</i>
<i>Experimental validation of the model.....</i>	<i>44</i>
<i>Estimation of aggregation inhibition by intracellular antibodies.....</i>	<i>46</i>
<i>Conclusions of engineering analysis.....</i>	<i>48</i>
CHAPTER 4. AFFINITY MATURATION OF ANTIBODIES	58
<i>Materials and Methods</i>	<i>58</i>
<i>Results.....</i>	<i>59</i>
<i>Discussion.....</i>	<i>62</i>
CHAPTER 5. DEVELOPMENT AND CHARACTERIZATION OF A SINGLE DOMAIN ANTIBODY AGAINST HTT	66
<i>Materials and Methods</i>	<i>66</i>
<i>Results.....</i>	<i>68</i>
<i>Discussion.....</i>	<i>73</i>
CHAPTER 6. DEVELOPMENT AND CHARACTERIZATION OF A HIGH AFFINITY SINGLE DOMAIN INTRABODY LACKING A DISULFIDE BOND	82
<i>Materials and Methods</i>	<i>82</i>
<i>Results.....</i>	<i>85</i>
<i>Discussion.....</i>	<i>91</i>
CHAPTER 7. CONCLUSIONS	99
APPENDIX 1: METHODS FOR AFFINITY MATURATION BY YEAST SURFACE DISPLAY....	103
APPENDIX 2: RESULTS FROM THE MESSER LAB.....	117
<i>Materials and Methods</i>	<i>117</i>
<i>Results.....</i>	<i>118</i>
APPENDIX 3: RESULTS FROM THE LINDQUIST LAB	122

<i>Materials and Methods</i>	122
<i>Results</i>	123
APPENDIX 4: GENBANK SUMMARY OF V_L12.3	126
REFERENCES	128
CURRICULUM VITAE	135

Table of Figures

Figure 1.1.....	16
Figure 1.2.....	17
Figure 1.3.....	18
Figure 2.1.....	29
Figure 2.2.....	30
Figure 2.3.....	31
Figure 2.4.....	32
Table 2.1.....	33
Figure 2.5.....	34
Figure 2.6.....	35
Figure 2.7.....	36
Figure 3.1.....	50
Figure 3.2.....	51
Figure 3.3.....	52
Figure 3.4.....	53
Figure 3.5.....	54
Figure 3.6.....	55
Figure 3.7.....	56
Figure 3.8.....	57
Figure 4.1.....	63
Table 4.1.....	64
Table 4.2.....	65
Figure 5.1.....	77
Figure 5.2.....	78
Figure 5.3.....	79
Figure 5.4.....	80
Figure 5.5.....	81
Figure 6.1.....	93
Figure 6.2.....	94
Figure 6.3.....	95
Figure 6.4.....	96
Figure 6.5.....	97
Figure 6.6.....	98
Figure A1.1.....	116
Figure. A2.1.....	120
Figure A2.2.....	121
Figure A3.1.....	125

Abbreviations Used

20aa-biotin, biotinylated peptide consisting of the first 20 amino acids of huntingtin

$C(\text{subscript htt})$, concentration of properly folded htt

$C(\text{subscript htt}^*)$, concentration of misfolded htt

CDR, complementarity determining region

CMV, cytomegalovirus

ex1, exon 1

FACS, fluorescence activated cell sorting

FRET, fluorescence resonance energy transfer

GFP, green fluorescent protein

GST, glutathione-S-transferase

HD, Huntington's Disease

htt, huntingtin protein

htt_{ex1-Q_n}, the first exon of huntingtin containing n contiguous glutamines

$k(\text{subscript dimerization})$, rate constant for conversion of a misfolded htt monomer into a dimer

$K(\text{subscript m})$, equilibrium constant between misfolded and properly folded mutant huntingtin

$k(\text{subscript misfolding})$, rate constant for conversion of properly folded htt to misfolded conformation

$k(\text{subscript refolding})$, rate constant for conversion of misfolded htt to properly folded conformation

K_d , dissociation constant

λ , characteristic rate in poisson distribution

$P(\text{subscript dimerization})$, probability that a misfolded htt monomer will form a dimer

P , probability that an aggregate has not formed

PBS/BSA, Phosphate buffered saline with 0.1% bovine serum albumin

PE, phycoerythrin

$r(\text{subscript dimerization})$, rate of htt dimerization

$r(\text{subscript misfolding})$, rate of htt misfolding

$r(\text{subscript refolding})$, rate of htt refolding

scFv, single-chain fragment variable

$V(\text{subscript cell})$, volume of cell

YFP, yellow fluorescent protein

YSD, yeast surface display

Chapter 1. Introduction

Huntington's Disease

Huntington's disease (HD) is a neurodegenerative disorder affecting 30,000 people in the United States, with an estimated 60,000 more at risk of developing the disease.

Clinically, HD has both psychological (e.g. dementia) and physical components, with uncontrollable dance-like movements (chorea) being a hallmark of the disease.

Individuals who have the disease begin showing symptoms on average in their mid 30s; these symptoms worsen progressively, resulting in death approximately 15 years after onset. Currently, there is no treatment to stop the underlying degenerative process in HD.

HD is a genetic disorder, passed on in an autosomal dominant fashion (if either parent is affected, each child has a 50% chance of acquiring the disease). The genetic mutation responsible for the disease was first identified in 1993 as an expansion in the number of CAG repeats in exon 1 of a gene encoding a protein called huntingtin (htt)¹. CAG encodes for glutamine (Q), so the resulting protein contains a polyglutamine stretch (polyQ). In normal individuals, the gene contains a stretch of less than 35 contiguous CAG codons (the number varies between alleles and individuals), whereas in individuals with HD the gene contains a stretch of 35 or more CAG repeats. Longer polyQ stretches result in an earlier age of onset, while polyQ stretches just over 35 long result in a later age of onset (see figure 1.1).

In HD, a proteolytic fragment of the huntingtin protein misfolds and forms aggregates, which are likely rich in beta sheet content.² The formation of nuclear

inclusions, containing the N-terminal proteolytic fragment of htt as well as other proteins, is observed in the medium spiny neurons of the striatum in patients with HD.³ The proteins which co-aggregate with the mutant htt include wt htt.^{4;5} There are several hypotheses as to the molecular structure of the aggregates. Aggregates formed of polyglutamine may have a beta-sheet structure consisting of an anti-parallel arrangement;⁶ it has also been suggested that the beta-sheet structure may arise from a parallel arrangement of the polypeptide strands, resulting in the formation of nanotubes (see figure 1.2).⁷ The beta-sheet structure is thought to form amyloid-like fibrils, which have been observed *in vitro*.⁸ It has been hypothesized that the formation of these aggregates, accompanied by depletion of key transcription factors which co-aggregate with htt, lead to neuronal dysfunction.⁹ It has also been shown that these aggregates tie up the protein degradation system.¹⁰

Mechanism of huntingtin aggregation

The underlying molecular mechanism that leads to aggregation is not well understood. The generation of the proteolytic fragment is assumed to occur before aggregation, although no evidence exists for this assumption. The aggregation process (whether involving full-length htt or just httx1) likely proceeds via a two-step process, nucleation and aggregate growth. The presence of the nucleation step is confirmed by the occurrence of a lag phase in *in vitro* kinetic studies of the aggregation of an N-terminal htt fragment.¹¹ Since the duration of the lag phase is dependent on the length of the polyglutamine stretch, it has been suggested that this accounts for the inverse relationship observed between polyglutamine length and age of onset.¹² Under this hypothesis,

nucleation is the rate-limiting step and aggregate growth occurs quickly afterwards, leading to cell death.

It is also important to consider that the model systems used in this work and by others in the field are significantly different from the human disease with respect to the time scale involved for aggregation and toxicity. Laboratory models exhibit aggregation and toxicity in days (cellular models) to a few years at most (animal models). In the human case, dysfunction is most often not observed until 35 or more years of age. The reason for the difference is that the model systems have been modified to have very long polyQ repeats, or very high htt1 concentrations, to accelerate the time scale required for experimentation. The fact that most model systems use a truncated htt fragment consisting of the first exon only may also accelerate the aggregation process.

Intracellular antibodies

Intracellularly expressed antibodies, or intrabodies, are powerful tools for studying cell biology^{13;14} and hold promise as potential therapeutics to be delivered via gene therapy.¹⁵ The DNA encoding the antibody sequence must be introduced into the cell in order for expression of the protein. Antibodies against htt have been shown to partially ameliorate the protein's aggregation. This has been shown in a cell-free aggregation assay using a monoclonal anti-polyglutamine antibody¹⁶, in cellular HD models using a single-chain Fv intrabody,^{14;17} and in an organotypic slice culture model of the disease.¹⁸ However, high intrabody expression levels have been required to obtain moderate reductions in aggregation and toxicity. This has proven to be a barrier to the development of a treatment for HD with intracellular antibodies via gene therapy, given the limited ability of viral vectors to deliver genes to the CNS.

Although intracellular targets abound, only a small handful of functional intracellular antibodies have been reported to date, potentially due to the difficulties in isolating antibody fragments that are expressed well and are functional in cytoplasm. One approach that has been employed in the isolation of intrabodies is the selection of single-chain antibodies (scFvs) from phage display libraries followed by screening large numbers of clones for expression in *E. coli* or function in mammalian cells.^{17; 19; 20} The yeast two-hybrid system has also been used to isolate intracellular antibodies.^{21; 22} A key problem arises from the conditions under which antibodies against intracellular targets are isolated and engineered. With the exception of the yeast two-hybrid approach to intrabody isolation²³, antibodies are isolated and engineered under oxidizing conditions by yeast or phage display^{19; 20; 24}, where stabilizing disulfide bonds form; however, disulfide bonds do not form as readily in the reducing environment of the cytoplasm, where intrabodies are intended to function. Although the yeast two-hybrid approach does result in intrabodies with some function, this system is not well suited for isolating variants with incremental improvement in functional capability. One of the significant contributions of this work is the development of an approach which allows one to optimize intracellular antibodies for improved function, using yeast surface display (described in the next section).

In most previous work, intrabodies have consisted of single chain antibodies, which contain both the heavy and light chain variable domains connected by a flexible linker; several effective intrabodies have been developed in this format (for example^{17; 19; 21; 22}). Intrabodies consisting of single domains may also be able to specifically recognize antigens without the need for interdomain interactions^{25; 26; 27}. Recent studies suggest that

single heavy chain variable domains alone may be useful as intrabodies, with improved intracellular expression.^{28;29} In this work, we show that an isolated variable light chain domain antibody can be engineered as a functional intrabody.

One potentially significant application of intracellular antibodies is in the treatment of autosomal dominant genetic disorders, such as HD, by gene therapy. Currently, gene therapy is limited to the delivery of new genes to induce an immune response or cell death, as is the case in cancer treatment, or to complement the host's genetic makeup, which is useful in the treatment of recessive genetic disorders³⁰. However, autosomal dominant disorders arise from "gain of function" genetic mutations. To treat these diseases by gene therapy, it is necessary to identify appropriate therapeutic genes and their corresponding proteins that should be delivered to the affected cells. Intracellular antibodies have the ability to bind to mutant proteins and inactivate their abnormal gained function, and therefore are well suited for the treatment of such disorders.

Yeast Surface Display

Yeast surface display (YSD,³¹) is a technique for isolation of novel antibodies³², improving protein function^{33;34;35;36}, and analysis of protein properties^{24;37;38;39}. In this system, the gene for a protein of interest is fused to the gene for the yeast mating protein (Aga2p) and to epitope tags, such as c-myc, for detection (see figure 1.3). When transformed into an appropriate yeast strain, the protein is displayed on the yeast cell wall, where it is accessible to antigens or other interaction partners and immunofluorescent reagents in solution. In this way, the properties of individual proteins

may be analyzed by flow cytometry, or libraries of expressed proteins may be sorted to isolate clones with desired properties by fluorescence activated cell sorting (FACS).

YSD has been successfully applied to several facets of antibody engineering including improvement of antibody binding affinity resulting in the highest affinity antibody reported to date.³⁶ It has also been applied to antibody stability optimization.⁴⁰ One advantage to engineering protein affinity by YSD is that yeast cells can be sorted by Fluorescence Activated Cell Sorting (FACS), allowing quantitative discrimination between mutants.⁴¹ Traditional panning methods have also been used with YSD, including magnetic particle separation.⁴² Since first described by Boder and Wittrup,³¹ YSD has been employed successfully in engineering a number of antibodies,^{36; 43} as well as T-cell receptors,^{44; 45; 46} and cytokines.³⁵

In YSD, protein properties such as stability and affinity, can be quantitatively measured using fluorescently labeled reagents and flow cytometry. Equilibrium binding constants and dissociation rate constants measured for yeast-displayed proteins are in quantitative agreement with those measured for the same proteins *in vitro* by surface plasmon resonance (BIAcore) or antibody immobilization.

Thesis Outline

The objective of my thesis work was to isolate and engineer antibodies that could efficiently inhibit mutant httx1 aggregation in an intracellular context. We accomplished this by making extensive use of the yeast surface display system. First, we isolated antibodies against exon1 of htt from a yeast surface display library of human single-chain antibodies.³² However, these antibodies were ineffective at blocking htt aggregation (Chapter 2). We then analyzed the intrabody-htt system to determine why the intrabodies

were ineffective. This included the development of mathematical models to assist in the analysis (Chapter 3). Having determined that antibody binding affinity, intracellular expression, and dependence of binding affinity on the presence of disulfide bonds were critical to the function of intrabodies, we set out to engineer the isolated antibodies for function. First, we improved the binding affinity of one of the antibodies by ~4 orders of magnitude (Chapter 4). We then discovered that the light chain variable domain alone retained binding affinity and had improved intracellular expression (Chapter 5). Finally, we mutated the cysteines that form the disulfide bond to hydrophobic residues, only to discover that the binding affinity was drastically lowered as a result. We corrected this by improving the binding affinity of the mutant that lacked a disulfide bond. The resulting intrabody, which we named V_L12.3, strongly inhibited htt aggregation, and was at least 10-fold more efficient at doing so than previously reported intrabodies against htt (Chapter 6). Most of the work in this thesis is contained in three publications,^{33; 47; 48} although some unpublished results and results to be published later are also included.

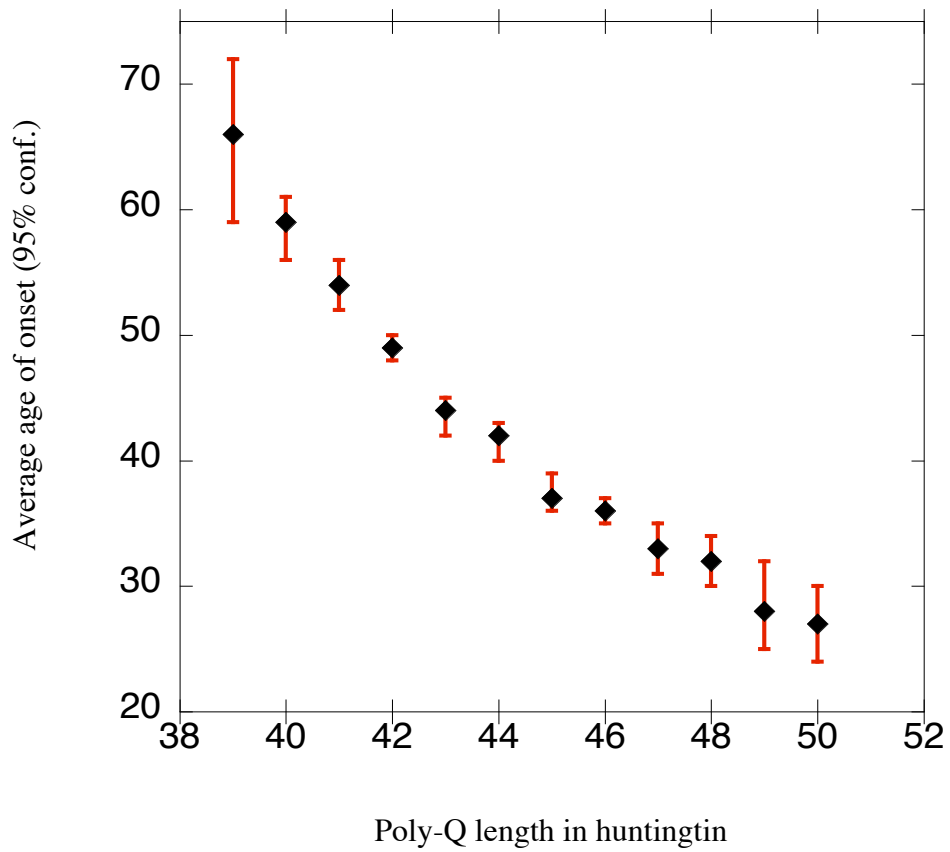


Figure 1.1.
Correlation between length of CAG/PolyQ repeat in htt exon1 and age of onset for HD (data from “A Physician’s Guide to the Management of Huntington’s Disease, 2nd ed).

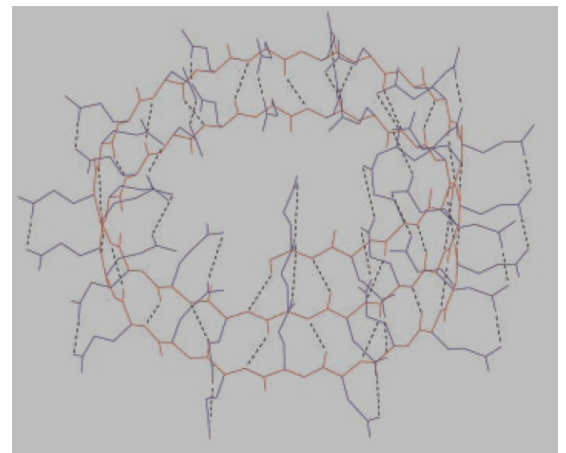
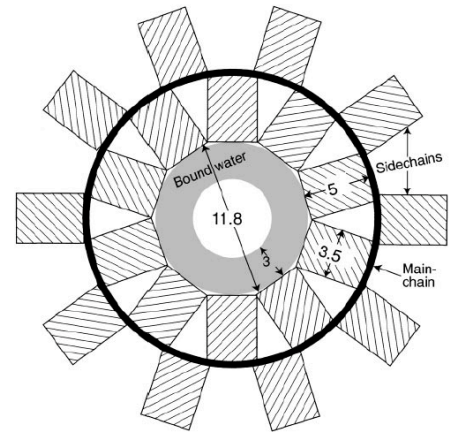
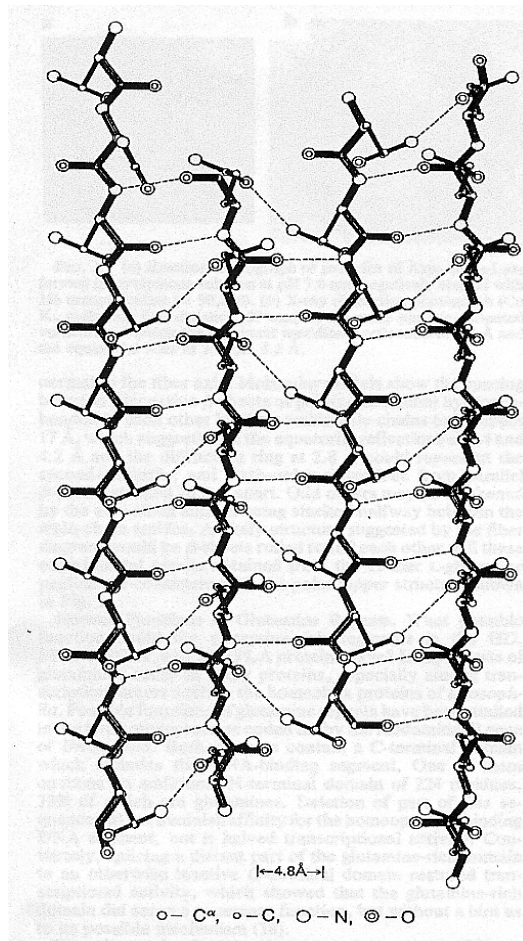
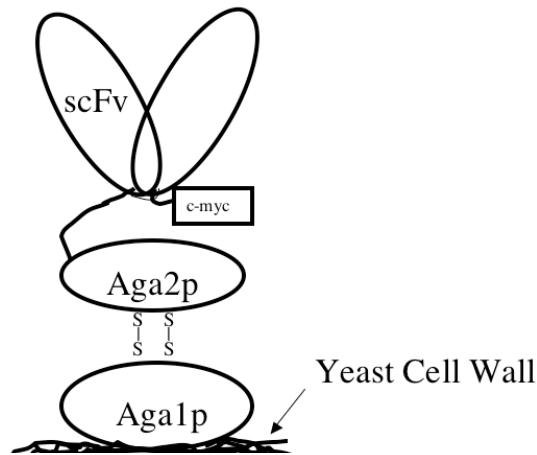


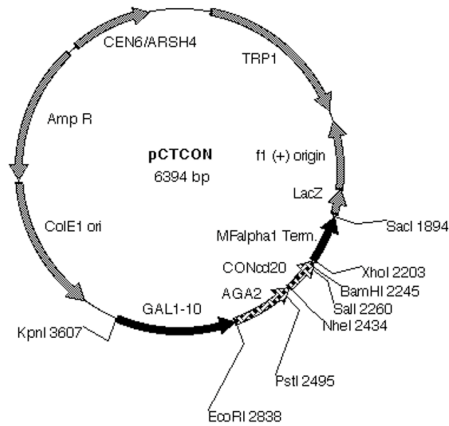
Figure 1.2.

Hypothesized structures of polyglutamine beta-sheet structure. Left, anti-parallel beta-sheets (from Perutz, 1994⁶). Original legend read “computer-generated structure of two paired antiparallel beta-strands of poly(L-glutamine) linked together by hydrogen bonds between the main-chain and side-chain amides.” Right, parallel beta-sheets resulting in nanotubes (from Perutz, 2002⁷). Original legends read “Diagrammatic projection of a helical fiber with 20 residues per turn on a plane normal to the fiber axis,” and “Computer-generated model of a poly-L-glutamine helix with 20 residues per turn (stereo pair). The main chain is black and the side chains are red. Hydrogen bonds are broken lines. The main chain conformational angles of this model are all in or near allowed regions of the Ramachandran plot.”

A



B



C

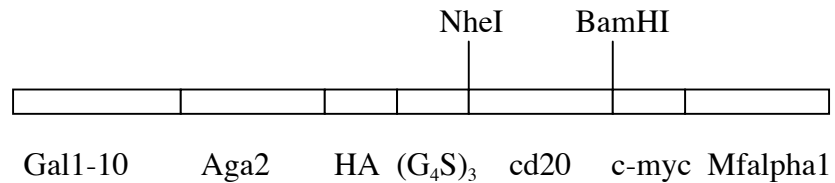


Figure 1.3.

Yeast surface display schematic and map of a sample plasmid used for YSD. A. An scFv is expressed as a fusion to the Aga2 mating protein. C-myc and HA epitope tags are present to quantify expression by immunofluorescence. B. Plasmid map of pCTCON, CON cd20 is expressed from the plasmid as a fusion to the yeast mating protein Aga2. C. Detail of pCTCON.

Chapter 2. Isolation and characterization of antibodies from a diverse yeast surface display library

Introduction

The antibodies discussed in this thesis were isolated from a non-immune yeast surface display library described in detail elsewhere.³² The term “non-immune” simply means that the people who donated the genetic material for synthesis of the library were not directly immunized with the antigens that the library is screened against. My role in the creation of the library was limited to assisting in the many yeast transformations required, and in protocol development. Therefore, I will only describe the background of the library briefly in this thesis. Human mRNA from spleen and lymph node tissues was purchased from a commercial source. Antibody variable domain genes were amplified by PCR to isolate variable heavy (V_H) and variable light (V_L) gene fragments. These fragments were ligated together randomly in a yeast surface display vector to make scFv's connected by a Gly₄Ser linker. The resulting plasmid library was transformed into the yeast strain EBY100 to make a yeast surface display library with a diversity (i.e. number of unique members) of approximately 10^9 .

In this chapter, isolation of antibodies against htt from this library is discussed, as well as their characterization, in terms of sequence analysis and performance in intracellular htt aggregation assays in yeast. Intracellular htt aggregation assays included use of fluorescence microscopy and a new, HD FRET (fluorescence resonance energy transfer) assay.

In order to rapidly assess the impact of intrabodies on htt aggregation, a yeast FRET HD model was constructed. In FRET, energy is transferred from one fluorophore to a second fluorophore whose excitation spectrum overlaps the emission spectrum of the first (see figure 2.1). However, energy transfer can only occur when the two fluorophores are in very close proximity, as may occur during protein aggregation.

We fused httex1 fragments to CFP and YFP, which form a fret pair. Fluorescence spectroscopy was used to measure FRET by exciting CFP and observing the emission spectrum across the range of CFP and YFP emission.

For the yeast HD FRET model, the seven constructs shown in figure 2.2 were assembled. The first two constructs, containing htt-x1 Q97 fused to CFP or YFP, would be co-transformed into yeast (on different selectional markers) as an HD positive model. The next two constructs, containing htt-x1 Q25 fused to CFP or YFP, would be co-transformed into yeast as an HD negative control. FRET control plasmids were also assembled to determine the extent to which FRET occurred in the HD model. The FRET negative control consists of CFP and YFP co-transformed into yeast. Since GFP variants do not interact, no FRET signal should be obtained. As a positive control, a plasmid containing CFP fused directly to YFP was assembled.

Materials and Methods

Production of GST-GFP, GST-htt_{x1}-Q₆₇-GFP, and GST-htt_{x1}-Q₆₇

Genes encoding GFP, htt_{x1}Q₆₇-GFP, or htt_{x1}Q₆₇ were subcloned into pGEX4T (Amersham) by a postdoctoral fellow (Peter Thumfort); pGEX4T encodes GST followed by a thrombin cleavage site on an IPTG-inducible promoter. These constructs were

transfected into BL21 (DE3) *E.coli*, which were then used to inoculate 2XYT with glucose and ampicillin. Overnight cultures were diluted 1:100 and grown to an OD₆₀₀ of 0.6-0.8 at 37 °C, followed by induction with 0.2 mM IPTG for 3 hours at 20 °C. Cells were collected, lysed by sonication, and centrifuged to remove cell debris and aggregated protein. The supernatant was purified using a GSH affinity column (Amersham Pharmacia). GST-httx1-Q₆₇-GFP, which had a C-terminal his tag, was further purified using a nickel affinity column. Purity was measured by SDS-PAGE (typically proteins were at least 75% pure), and the BCA kit (Pierce) was used to measure concentration. The protein was produced and purified by myself, Peter Thumfort, or Tina Holden (a lab technician).

Labeling and analysis of yeast surface display libraries and clones

Libraries and clones were labeled according to published protocols.⁴⁹ In brief, 0.2 OD₆₀₀-ml (approximately 2 million cells) of yeast were collected following overnight induction of intrabody expression with galactose, rinsed in PBS/BSA, resuspended in 500 µl PBS/BSA with antigen (either biotinylated peptide or GST fusion protein) at appropriate concentration and mouse monoclonal anti-c-myc antibody (9E10, Covance) at 1:100 dilution. Following an incubation step of 30 minutes or longer at 37 °C, cells were rinsed with PBS/BSA and resuspended in PBS/BSA with either anti-GST polyclonal-PE conjugate (Prozyme) or Streptavidin-PE (Molecular Probes) and goat anti-mouse FITC conjugate (Sigma), at a 1:50 dilution. After an additional 30 minute incubation, cells were rinsed and analyzed on an Coulter Epics XL flow cytometer, or taken to the MIT Flow Cytometry Core Facility for FACS.

Library screening

The library was sorted using a MoFlo FACS machine at the MIT Flow Cytometry Core Facility. 5×10^8 cells were labeled as described above with GST-httx1Q₆₇-GFP and the most brightly PE labeled (top 0.1%) were collected. Collected cells were amplified by growth, induced and sorted two more times, at which time a bright, double labeled population was obtained. This population was depleted of antibodies against GST-GFP by labeling with this reagent followed by sorting cells which expressed c-myc tagged antibodies but did not bind GST-GFP.

Sequencing and sequence analysis

Plasmids were recovered from yeast using a Zymoprep kit (Zymo Research), and sequenced by the MIT Biopolymers Laboratory. Sequences were analyzed using the Biology Workbench (<http://workbench.sdsc.edu>) and NIH's IgBlast (<http://www.ncbi.nlm.nih.gov/igblast/>).

Intracellular expression of antibodies in yeast

ScFv genes were subcloned into p416 (ATCC), a galactose-inducible yeast shuttle plasmid, using PCR primers that included a start codon to initiate protein synthesis. The resulting plasmids were used for expression in both the strains for microscopy and FRET analysis. Control intrabodies were picked at random from the non-immune library.

Microscopy and aggregate quantification

Yeast co-expressing the intrabodies and httex1Q103-GFP were grown to mid-log phase before induction in galactose containing media. Cells were analyzed 18-hours post-induction for the presence of aggregates. The samples were examined with a Nikon TE200 inverted microscope equipped with an excitation source and appropriate filter sets for imaging GFP (FITC filter sets were used) as well as a DeltaVision 12-bit CCD camera. A 10x objective is used in order to get a large population of cells (approximately 100) in a single image. All images contained approximately the same number of cells, being completely saturated with cells covering the entire field of view. At least three separate fields of view are captured for each sample.

Image analysis is performed using a software package called SoftWorx, which is supplied with the DeltaVision system. Diffuse, non-aggregated material has a much lower fluorescence intensity per pixel than the dense, punctate aggregates. Pixel values for aggregates are up to ten times as high as those for soluble material, sometimes more. Therefore, a threshold is applied to differentiate between soluble and aggregated protein. Images of cells expressing the control fusion protein (htt-25Q-EGFP), are used in order to identify an appropriate, non arbitrary threshold. The threshold chosen is a value 10% higher than the highest pixel value observed for the control cells. The expression levels of the fusion protein in the control cell line are identical to those observed in the HD cell line, as shown by flow cytometry (see figure 2.3). Once a threshold is chosen, the software identifies contiguous regions above the threshold as objects, and determines the total fluorescence for each. This information may then be saved as a list of values that

can be opened in Microsoft Excel. Total fluorescence of aggregates observed was used as a measure of aggregation.

Yeast FRET System

Plasmids were constructed containing httex1 fragments fused to cyan fluorescent protein (CFP) or yellow fluorescent protein (YFP). The parent vectors used were p414 (for YFP fusions) and p415 (for CFP fusions); both parent vectors were purchased from ATCC. Htt-x1-Q97 and htt-x1-Q25 were obtained from the Lindquist lab in the form of GFP fusions on the plasmid p416. Plasmids containing CFP, YFP, and CFP-YFP were obtained from the Yeast Resource Center at the University of Washington. CFP, YFP, and CFP-YFP were amplified by PCR with primers containing a 5' BamHI site and a 3' XhoI site. Htt-x1-Q97 and htt-x1-Q25 were excised using 5' EcoRI and 3' BamHI. Both PCR products and digestion products were gel purified. Htt and the GFP variants were fused via the BamHI sites present on each. The resulting ligation product was amplified by PCR using primers with both 5' and 3' XhoI sites. The products were gel purified, digested with XhoI, and ligated into p414 (a yeast shuttle vector with a tryptophan selection marker) for the YFP variants and p415 (leucine selection) for the CFP variants. CFP, YFP, and CFP-YFP were ligated directly into the appropriate plasmid. Each plasmid was sequenced over the area of interest and found to be free of mutations.

Plasmids were transformed into BJ5464-alpha using the EZ yeast kit by Zymo research to make the following strains: FRET- (pCFP and pYFP), FRET+ (pFRET+), HD- (pC25 and pY25), HD+ (pC97 and pY97). These strains were grown overnight and then induced in galactose containing medium for approximately 18 hours. Cells were

rinsed in PBS/BSA, and diluted to a concentration of $\sim 10^7$ cells/ml in PBS/BSA. The fluorescence spectra of the cells were then collected using a Varian fluorescence spectrophotometer. Excitation was set to 430 \pm 5 nm, and emission was observed from 450 to 550 nm.

Results

Isolation of a panel of single-chain antibodies against multivalent glutathione-S-transferase huntingtin exon 1 fusion protein

Single chain antibodies against exon 1 of huntingtin were isolated from a yeast-displayed non-immune human scFv library by Fluorescence Activated Cell Sorting (FACS).³² Due to the difficulty in isolating scFvs against self-antigens and the aggregation-prone nature of huntingtin exon 1 (httex1) fragments with pathological-length polyglutamine tracts (here we use 67 glutamines, httex1-Q₆₇), a multivalent glutathione-s-transferase (GST) fusion protein with improved solubility was used as the antigen, GST-httex1-Q₆₇-GFP. GST is a dimer in its native state. Therefore, fusion proteins containing GST present multivalent epitopes and consequently allow isolation of weak initial binders by avidity-increased affinity. Screening was performed using 800 nM antigen, while screening attempts at lower antigen concentrations were unsuccessful, demonstrating the benefit of screening against the multivalent antigen.

The antibody panel isolated against GST-httex1-Q₆₇-GFP contained antibodies against epitopes in GST and GFP, which were depleted from the pool by labeling with a GST-GFP fusion protein and further FACS sorting. The panel of yeast surface-displayed scFvs resulting from several rounds of enrichment against GST-httex1Q₆₇-GFP and

depletion against GST-GFP was labeled for analysis with each of the two proteins (Figure 2.4). Strong preference for the protein containing httex1 is observed, indicating that the great majority of isolated antibodies are specific for this fragment rather than GST or GFP.

Ten clones from the panel of antibodies specific for exon 1 of huntingtin were sequenced, and eight clones were unique. The germline usage and complementarity determining regions (CDRs) are shown in Table 2.1. Interestingly, all eight clones had a highly conserved light chain CDR3, pointing to its dominance in the httex1-binding paratope. The remaining non-CDR3 regions of the light chain sequences were all derived from the lambda 1 germline family. In contrast, the heavy chains in these clones were diverse members of the VH6 or VH1 families, implying flexibility in heavy chain usage compared to light chain usage.

The eight isolated scFvs were subcloned into a yeast cytoplasmic expression vector and tested for biological activity in a yeast model of HD and were found to be completely inactive in preventing aggregation (results from six of the clones are shown in Figure 2.5), as measured by fluorescence microscopy.

Yeast HD FRET system

We fused httex1 fragments alternately to CFP or YFP, which form a FRET pair, and studied whether or not polyglutamine-length dependent FRET can be observed in a yeast model of HD. pC25 and pY25 were co-transformed to create an HD- strain, while pC97 and pY97 were co-transformed to create an HD+ strain. The strains were induced for expression of the HD transgenes, and the aggregation state of the htt fusion proteins

was observed by fluorescence microscopy. The aggregation state was found to be consistent with published reports with respect to polyglutamine length (see figure 2.6).⁵⁰

We then used fluorescence spectroscopy to measure FRET emission of cell suspensions. First, FRET control strains were used to determine if the energy transfer would be observable in this system. The result is shown in figure 2.7. When excited at the excitation wavelength of CFR, the FRET- strain had an emission spectrum exhibiting a strong peak at the emission wavelength of CFP, and very little YFP emission. Under the same conditions, the FRET+ strain exhibited a strong YFP emission peak and a highly attenuated CFP emission peak, demonstrating that energy transfer had occurred and was detectable.

For the HD- strain, the emission spectrum observed was comparable to the FRET- strain (see figure 2.7B). For the HD+ strain, a significant YFP emission peak was detected, indicating that FRET does occur in a polyglutamine length dependent fashion. For a short polyQ length (Q25), the protein does not aggregate, and so the fluorophores are distant enough that FRET does not occur. For a long polyQ length (Q97), the protein aggregates, bringing CFP and YFP in close proximity, and resulting in FRET.

We then studied the effect of co-expression of the intrabodies isolated on the FRET signal observed in the HD+ strain. Intrabodies isolated at random from the non-immune library were used as a negative control. The result is shown in figure 2.7B. None of the intrabodies isolated significantly decreased the FRET signal observed, when compared to the control intrabodies.

Discussion

In this chapter, we described the isolation and characterization of single-chain antibodies against huntingtin from a yeast surface display. We were able to isolate a diverse population of antibodies against the httex1; however, none of these antibodies were effective inhibitors of htt aggregation in yeast cell models of HD. We also described a new assay for monitoring htt aggregation by FRET.

Screening a YSD library with a multivalent antigen enabled isolation of human scFvs with specificity for a human protein. Difficulties in obtaining antibodies from non-immune libraries against self-antigens have been reported elsewhere.⁵¹ This technique may prove useful when screening non-immune libraries against other self-antigens.

Unfortunately, none of the antibodies isolated were effective inhibitors of htt aggregation. Although the use of a multivalent antigen enabled isolation of anti-htt antibodies, the antibodies isolated had low affinity against the multivalent antigen and almost certainly had extremely low monovalent affinity. We surmised that this may contribute to the inability of the intrabodies to inhibit htt aggregation.

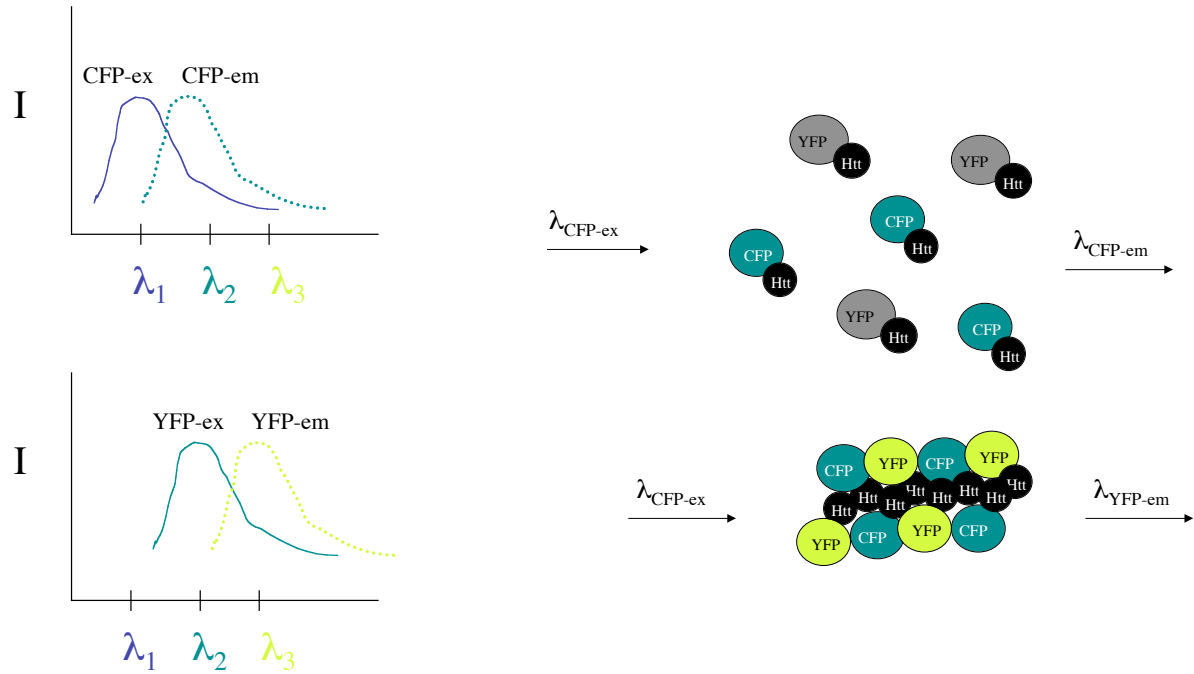
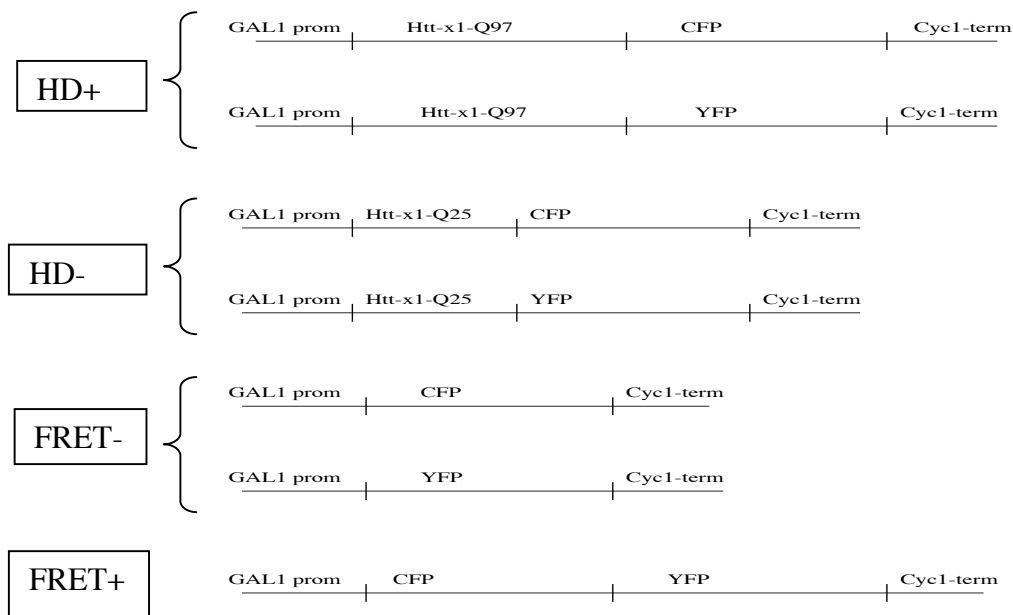


Figure 2.1.

Schematic of htt FRET system. Left, emission and excitation spectra of CFP and YFP; note overlap of CFP emission with YFP excitation, which can result in energy transfer when the two fluorophores are in close proximity to one another. Right, when htt-CFP and htt-YFP are in solution, they should not be close enough together to allow energy transfer; when they are aggregated, energy transfer may occur.



Plasmid Name	Protein Expressed	Parent Vector	Purpose
PCFP	CFP	p415	FRET negative
PYFP	YFP	p414	FRET negative
pFRET+	CFP-YFP (fusion)	p414	FRET positive
pC25	httex1Q25-CFP	p415	HD negative
pY25	httex1Q25-YFP	p414	HD negative
pC97	httex1Q97-CFP	p415	HD positive
pY97	httex1Q97-YFP	p414	HD positive

Figure 2.2.

Constructs used for yeast HD FRET model. Bracketed constructs are to be co-expressed. For HD+ constructs co-expressed in yeast, a fret signal will be observed if CFP and YFP come into close contact (as in aggregation). HD- constructs serve as a negative control to ensure that FRET signal is related to the expanded polyglutamine region, while FRET+ and FRET- controls are used to verify that FRET occurs at all.

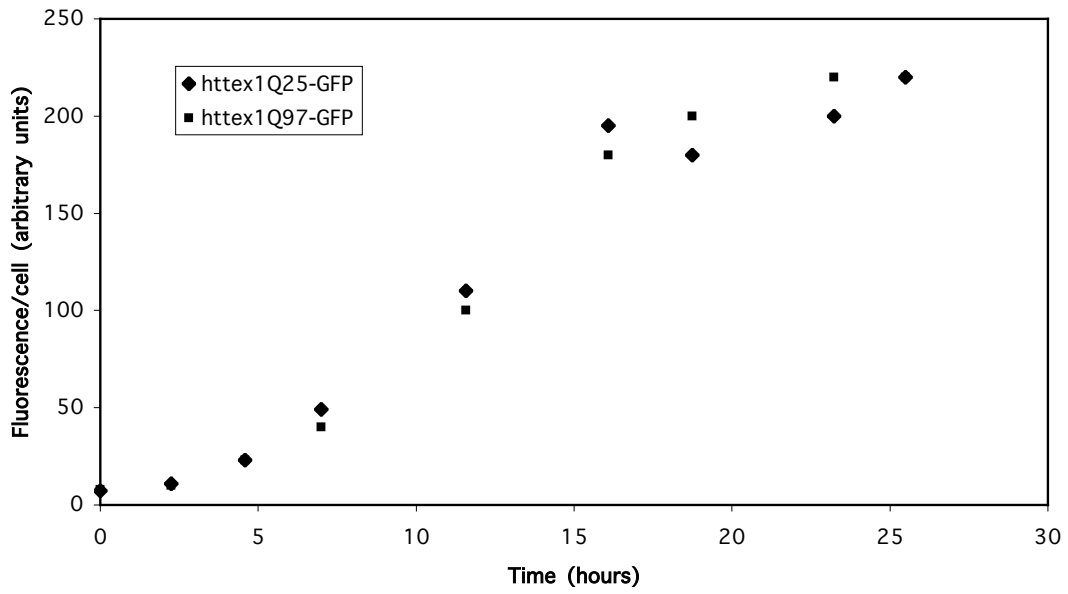


Figure 2.3.
Fluorescence of yeast cells expressing httex1-GFP with 25 or 97 glutamines.
Fluorescence intensity is not dependent on polyglutamine length.

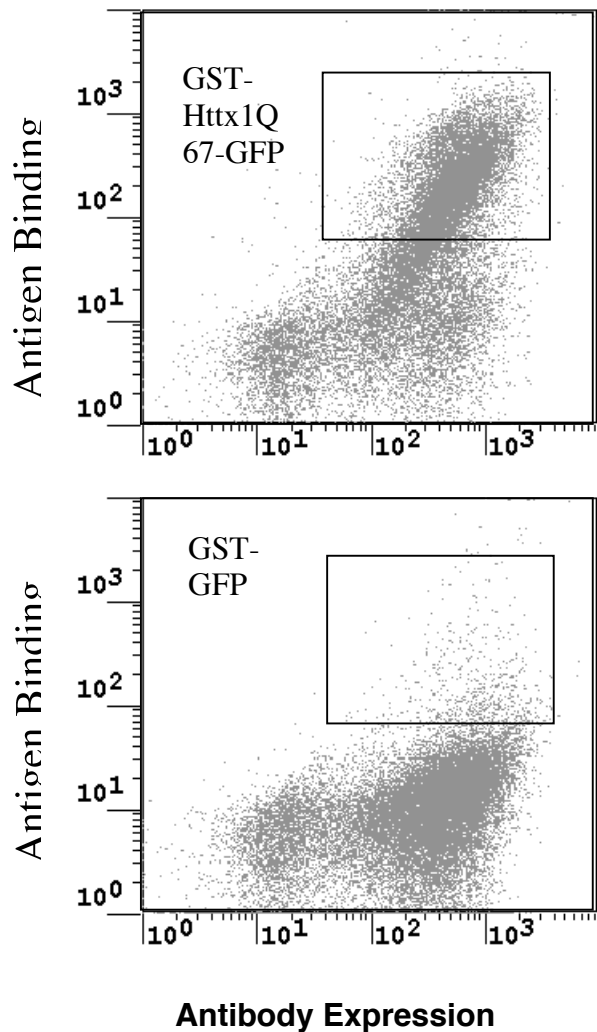


Figure 2.4.

Pool of yeast-displayed scFvs are specific for exon 1 of huntingtin, rather than GST or GFP. The pool of scFvs isolated from a human antibody YSD library by FACS sorting against GST-httex1-Q₆₇-GFP, for enrichment, and GST-GFP, for depletion, is shown here under two labeling conditions. Top, the pool is labeled with 1 μ M GST-httex1-Q₆₇-GFP and analyzed by flow cytometry. Bottom, the same pool is labeled with 1 μ M GST-GFP. The abscissa shows the expression level of C-terminally c-myc tagged scFv on the yeast surface, labeled with mouse 9E10 anti-c-myc monoclonal antibody and FITC-conjugated goat anti-mouse polyclonal antibody. On the ordinate is antigen binding, detected by anti-GST polyclonal antibody conjugated to PE. A box has been drawn to show the location of yeast that express scFv and bind httex1Q67, but not GST-GFP.

Clone	Germ-line	CDR H1	CDR H2	CDR H3	CDR L1	CDR L2	CDR L3
0.4.1	Vh6-1, V1-11	GDSVSSNTAAWY	RTYYSSKWFYD	EDD-----YGDYV	SGSTSNIGNNAVN	YDDLPS	ATWDDSLNGWV
0.4.2	VH1-69, V1-11	GGTISS--CAIS	GIIPMFDTN-	TYYHDTSDNDGTYGMDV	SGSTSNIGNNAVN	YDDLPS	ASWDDNLNGWV
0.4.3	VH6-1, V1-11	GDSVSSNSAARN	RTYYRSRWYND	DPPYV-----LSTFDI	SGSTSNIGNNAVN	YDDLPS	ATWDDSLNGWV
0.4.4	VH1-18, V1-16	GGTISS--CAIS	GIIPMFDTN-	TYYHDTSDNDGTHGMDV	SGSSSNIGSNTVN	SDNQRPS	ATWDDSLNGWV
0.4.6	VH1-69, V1-11	GGTISS--CAIS	GIIPMFDTN-	TYYHDTSDNDGTYGMDV	SGSTSNIGNNAVN	YDDLPS	ATWDDSLNGWV
0.4.7	VH1-69, V1-11	GGTISS--CAIS	GIIPMFDTN-	TYYHDTSDNDGTYGMDV	SGSSSNIGSNTVN	ADYERPS	ATWDDSLNGWV
0.4.9	VH1-69, V1-11	GGTISS--CAIS	GIIPMFDTN-	DDVVA-----TLGGFDI	SGSSSNIGSNTVN	YDALLPS	AAWDDSLDGWV
0.4.10	VH1-69, V1-16	GGTISS--CAIS	GIIPMFDTN-	TYYHTRDNDGTYGMDV	SGSSSNIGSNTVN	YDDLAS	ASWDDNLNGWV

Table 2.1.

Germline usage and sequences of complementarity determining regions (CDRs) of antibodies discussed in this work. Clones were named according to "rounds of mutation, rounds of FACS sorting, clone number." Germline sequences shown were determined using IgBlast (<http://www.ncbi.nlm.nih.gov/igblast/>). CDR H1 refers to the first CDR of the heavy chain, CDR H2 is the second, etc. Yellow shading appears due only to a formatting error and is not significant.

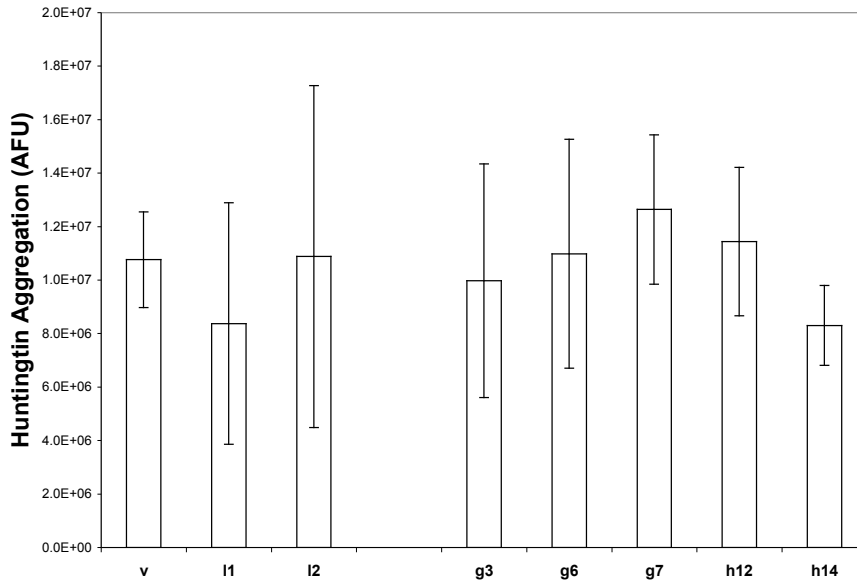


Figure 2.5.
Effect of intrabodies on aggregation of htt in a yeast model of HD, as measured by fluorescence microscopy. None of the intrabodies significantly reduced aggregation on httex1Q97-GFP when co-expressed in yeast cytoplasm.

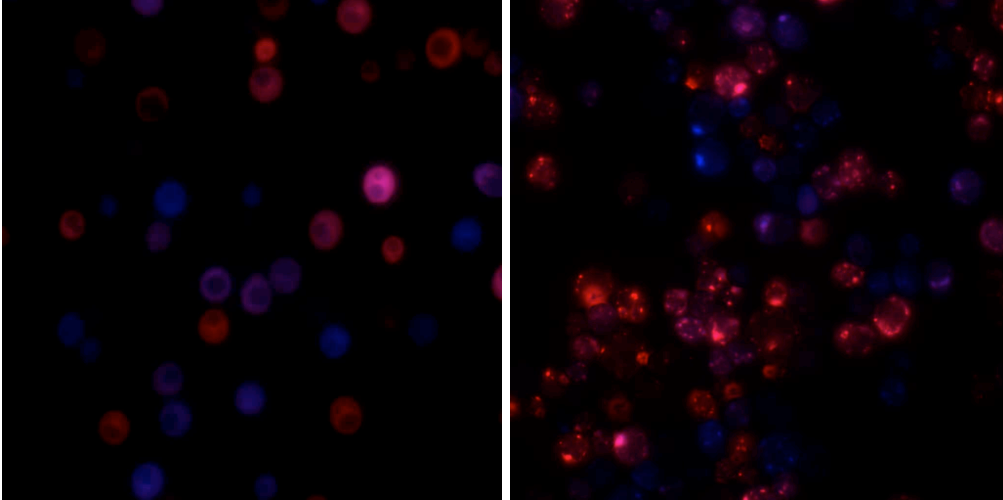


Figure 2.6.

Yeast co-transformed with htt-x1-Q25-CFP and htt-x1-Q25-YFP (left) show diffuse cytoplasmic fluorescence. CFP appears blue in this false color image, and YFP appears red. Right, yeast co-transformed with htt-x1-Q97-CFP and htt-x1-Q97-YFP. Note punctate aggregates in HD+ strain.

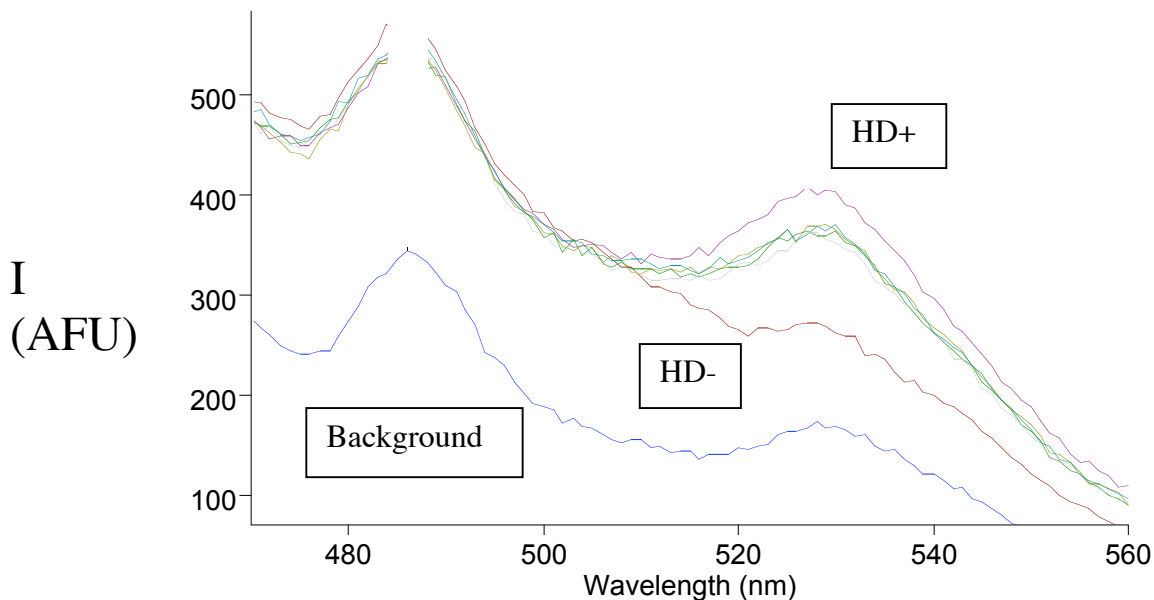
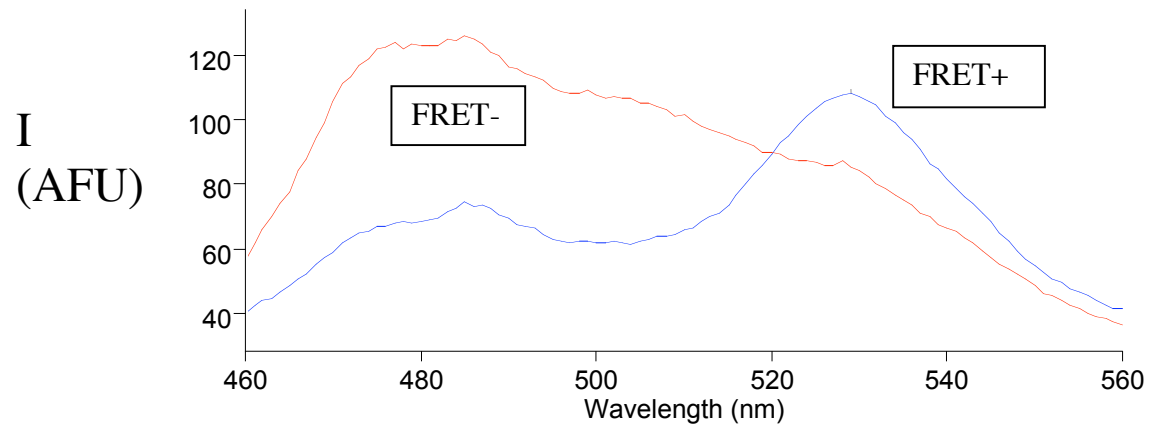


Figure 2.7.

Fluorescence spectra of yeast FRET strain cell suspensions. FRET occurs when two fluorophores are in close proximity (see figure 2.1). Cells are excited at 430 ± 5 nm, and the emission spectra is collected from 470 to 560 nm. Top, FRET- strain exhibits CFP emission only; FRET+ shows attenuated CFP emission and strong YFP emission, indicating FRET. Bottom, HD- strain exhibits no significant YFP emission, in contrast to HD+ strain. The polyglutamine-length dependent FRET signal is likely due to aggregation of the htt-CFP and htt-YFP protein. Expression of intrabodies, both randomly selected and those isolated against httex1, slightly reduce the FRET signal, but this reduction is not dependent on specificity for httex1, indicating no effect on htt aggregation.

Chapter 3. Engineering analysis of intracellular huntingtin aggregation and its inhibition by intracellular antibodies

Given the inability of the isolated intracellular antibodies to inhibit the aggregation of htt with an expanded polyglutamine tract, we began a detailed analysis of the possible causes of failure. The GST fusion protein that we had used to screen the antibody library formed an oligomer consisting of 4-8 GST-htt_{1Q67}-GFP monomers; this protein then offered redundant epitopes (i.e. it was multivalent), which can enhance apparent binding affinity by acting cooperatively. Since the clones had binding activity only at high concentrations of multivalent htt_{1Q67} protein (figure 2.4), we surmised that the affinity against a monovalent target would be much lower and likely insufficient for biological activity. Furthermore, western blotting of the intracellular scFv intrabodies revealed very poor cytoplasmic expression (figure 3.1), which would also be a dominant cause of their inactivity.^{52; 53; 54} Finally, the dependence of binding properties on the presence of a disulfide bond was also a possible shortcoming of the antibodies isolated. These qualitative problems could all be addressed through protein engineering. However, protein engineering is labor intensive and it would be beneficial to have a more quantitative understanding of the system to guide the protein engineering process. We therefore developed a mathematical description of the htt-intrabody system.

In the first section of this chapter, we derive the equation which connects the molecular mechanism of mutant htt misfolding to the stochastic nature of the aggregation process. With the assistance of an undergraduate (John Cassady) to help generate data, we then validate the equation experimentally. Finally, we couple this equation with the

law of mass action, which describes intrabody-htt interactions, in order to evaluate the effect of antibody binding and expression properties on htt aggregation.

Derivation of a mathematical model describing the probability that a cell will form an htt aggregate

It has been shown that neurodegeneration in HD is described by neuronal loss in which the probability of cell death remains constant with time.^{55;56} However, the connection between the kinetics of cell death and the molecular mechanism underlying the disease remains murky. Perutz hypothesized that nucleation of aggregates was the most likely explanation for the infrequent but steady occurrence of neuronal death, which results in adult onset of the disease.¹² Under this hypothesis, formation of a thermodynamically stable nucleus, containing several htt molecules with expanded polyQ repeats, leads to cell death or dysfunction. However, recent evidence suggests that polyglutamine peptides undergo a single-molecule conformational change.⁵⁷ In this scheme, properly folded htt is in equilibrium with its misfolded counterpart, and the formation of a stable dimer is the rate limiting, irreversible step in aggregate formation (see figure 3.2). We used this mechanistic model to derive a stochastic mathematical model describing the dependence of the probability of intracellular aggregate formation on time and on concentration of the htt protein (case 1). We then consider the case where the misfolding event is the rate-limiting step in aggregation (case 2), and develop the general equation that doesn't rely on assumptions about which step is rate-limiting (case 3).

Case 1: Misfolded htt in equilibrium with properly folded form; dimer formation the rate-limiting step in aggregation process.

Wetzel assumed that the misfolded htt protein would be in rapid equilibrium with its properly folded counterpart. Applying this assumption, and introducing

$$K_m = k_{\text{misfolding}}/k_{\text{refolding}} = C_{\text{htt}^*}/C_{\text{htt}} \quad \text{Eqn 3.1}$$

the concentration of the misfolded htt is given by

$$C_{\text{htt}^*} = K_m C_{\text{htt}} \quad \text{Eqn 3.2}$$

The rate of dimer formation is

$$r_{\text{dimerization}} = k_{\text{dimerization}} C_{\text{htt}^*} C_{\text{htt}} V_{\text{cell}} = K_m k_{\text{dimerization}} C_{\text{htt}}^2 V_{\text{cell}} \quad \text{Eqn 3.3}$$

In a cellular context, where the concentrations of most proteins are low, and where the total volume is small, there are only a discrete number of copies (perhaps a few thousand) of htt. Therefore, we cannot simply use the bulk rate of dimer formation, which applies to volumes which are sufficiently large to be treated as homogeneous, but have to use probability theory. The probability that a dimer will have formed by some time, t , is described by a Poisson distribution with characteristic parameter, λ equal to the rate above. The Poisson distribution can be used to determine the number of times an event is likely to occur, assuming the events are independent. However, in this system, the formation of an aggregate will change the soluble concentration of the protein,

decreasing the probability of a second occurrence. Further, it is experimentally difficult to determine the number of nucleation events which have occurred because cells can package multiple aggregates into a single inclusion body, and because htt fibers could break, giving the appearance of multiple aggregates from a single nucleation event. Therefore, we will focus on the probability that a nucleation event has *not* occurred, since this allows us to avoid complications involving independence and the experimental complications mentioned above. In a Poisson distribution, the probability that an occurrence happens exactly zero times is given by:

$$P = e^{-\lambda t} \quad \text{Eqn 3.4}$$

Substituting Eqn 3.3 into Eqn 3.4:

$$P = e^{-K_m k_{dimerization} C_{htt}^2 V_{cell} t} \quad \text{Eqn. 3.5}$$

Thus, the mechanistic model of Wetzel suggests that the number of cells without aggregates will exponentially decline with time in a manner that is dependent on the concentration of htt squared. This agrees with Wetzel's mechanism, in which formation of a dimer is the rate-limiting step in the aggregation process, giving second order reaction kinetics.

Case 2: Misfolding htt the rate limiting step in aggregate formation

If instead of the misfolded htt being in equilibrium with the properly folded form, the misfolding of htt is the rate-limiting step in aggregate formation, then the rate would be given by

$$r_{\text{misfolding}} = k_{\text{misfolding}} C_{\text{htt}} V_{\text{cell}} \quad \text{Eqn 3.6}$$

Substituting this rate into Eqn 3.4, we get

$$P = e^{-k_{\text{misfolding}} C_{\text{htt}} V_{\text{cell}} t} \quad \text{Eqn 3.7}$$

If misfolding of htt is the rate-limiting step, then the number of neurons without aggregates would be expected to exponentially decline with a first order dependence on htt concentration.

Case 3: General derivation without assuming a rate limiting step

The rate at which polyglutamine peptides misfold is given by Eqn 3.6. Once misfolded, the peptide may either bind to a second polyglutamine peptide in the cell, forming a nucleus consisting of a dimer, or refold to the native state. The probability that a dimer will form after misfolding of a monomer would then given by the rate of dimerization divided by the combined rate of dimerization and refolding:

$$P_{\text{dimerization}} = \frac{r_{\text{dimerization}}}{r_{\text{dimerization}} + r_{\text{refolding}}} \quad \text{Eqn 3.8}$$

Substituting in the relevant rates,

$$P_{dimerization} = \frac{k_{dimerization} C_{htt} C_{htt^*} V_{cell}}{k_{dimerization} C_{htt} C_{htt^*} V_{cell} + k_{refolding} C_{htt^*} V_{cell}} \quad \text{Eqn 3.9}$$

The initial rate of dimer formation may then be approximated by the rate of misfolding multiplied by the probability that a misfolded monomer forms a dimer. From Eqn. 3.6 and 3.9, after simplification:

$$r_{dimerization} = \frac{k_{misfolding} k_{dimerization} C_{htt}^2 V_{cell}}{k_{dimerization} C_{htt} + k_{refolding}} \quad \text{Eqn 3.10}$$

Once again, we substitute this rate into Eqn 3.4, arriving at

$$P = e^{-\frac{k_{misfolding} k_{dimerization} C_{htt}^2 V_{cell} t}{k_{dimerization} C_{htt} + k_{refolding}}} \quad \text{Eqn 3.11}$$

Equation 3.11 gives the probability that a cell will not have formed an aggregate, assuming that the formation of a dimer is essentially an irreversible step leading to the formation of an aggregate, but without stipulating which step is rate limiting.

Wetzel assumed that the misfolded htt protein would be in rapid equilibrium with its properly folded counterpart, implying that $k_{refolding} \gg k_{dimerization} C_{htt}$. Applying this assumption, and introducing $K_m = k_{misfolding}/k_{refolding}$, Eqn 3.11 reduces to:

$$P = e^{-K_m k_{dimerization} C_{htt}^2 V_{cell} t} \quad \text{Eqn. 3.5}$$

Alternately, if the rate of dimerization is fast relative to the rate of refolding, then $k_{\text{dimerization}}C_{\text{htt}} \gg k_{\text{refolding}}$, and Eqn 3.11 reduces to:

$$P = e^{-k_{\text{misfolding}}C_{\text{htt}}V_{\text{cell}}t} \quad \text{Eqn 3.7}$$

Underlying assumptions involving the cellular context of aggregation

It is useful to study reaction kinetics in the cellular context where the reaction occurs; however, there are many potentially complicating processes occurring in the cell. We have neglected to directly account for chaperone binding and the unfolded protein response (UPR). Chaperone binding and the UPR may affect the values of $k_{\text{misfolding}}$, $k_{\text{refolding}}$, and other parameters in the model derived. The UPR could result in clearance of aggregates; in this case the observed fraction of cells without aggregates would be the result of a dynamic balance between aggregate formation and clearance. We assume that the concentration of htt is constant, or close to constant, over the time period considered; currently the validity of this assumption is unknown. *In vivo*, the expression level may vary in response to cellular events. In the experimental system described below, the concentration may vary ~2-fold over the time periods considered. The model also does not account for cell growth or division.

Experimental validation of the model

[The raw data that this section is based on was generated by an undergraduate under my supervision, John Cassady]

To test the accuracy of the model derived, and try to determine which of the three equations derived was most relevant, we studied the kinetics of aggregate formation in transiently transfected ST14A cells.⁵⁸ Cells were transfected with httex1Q_n-GFP, with n varying between 25, 47, or 72 glutamines. Twenty-four hours post-transfection, FACS was used to separate cells based on GFP intensity, which is proportional to httex1Q_n-GFP concentration, assuming cells are roughly the same volume (this assumption may result in error up to 25% variation in the concentration of cells isolated; however, the cells within each population collected by FACS exhibit the same amount of variation, so the relative mean concentration should not be significantly affected by this assumption). The percentage of cells with aggregates within each cell population was then determined by fluorescence microscopy, and monitored periodically thereafter.

To eliminate the cells which had already formed aggregates at the time of FACS sorting from further analysis, the data were normalized to the fraction of cells without aggregates after FACS sorting (i.e. the measured value at each data point was divided by the initial value). The exponential time dependence of the aggregation process was confirmed by taking the natural log of the value obtained for the fraction of cells without aggregates, and plotting $\ln(\text{fraction of cells without aggregates})$ versus time (an example of this data is shown figure 3.3). The linear least squares fit was good ($R^2 > 0.85$) for most of the data obtained over the first 24 hours. The slopes of these lines were taken as the rate of aggregation, and plotted versus concentration to determine concentration

dependence of intracellular aggregation. The results from several independent experiments for the various polyQ lengths are shown in figures 3.4, 3.5, and 3.6.

Regression analysis of the data in figures 3.5 and 3.6 indicates that the fraction of cells that do not contain aggregates will exponentially decline with first-order htt concentration dependence. This implies that the conformational change of a single htt molecule is the rate-limiting step in aggregate formation, and that once the conformational change has occurred, the molecule is much more likely to continue down the aggregation pathway than to revert to the properly folded form.

The first order concentration dependence of aggregate formation is most consistent with the relatively small decreases observed in the age of onset for HD homozygotes.⁵⁹ Individuals who are homozygous for the HD gene should produce twice as much of the mutant htt as HD heterozygotes. If the rate-limiting step in the formation of toxic htt aggregates or aggregation intermediates were the formation of a dimer (second order kinetics), then the neurons of homozygotes would be four times (2 squared) as likely to degenerate as their heterozygous counterparts. First order reaction kinetics for the rate-limiting step would result in the number of degenerated neurons reaching a critical point (assumed to correspond to an age of onset) in half the time. The age of onset for homozygous is approximately 20-25% earlier than for heterozygous.⁵⁹

Although homozygotes do not have an age of onset that is half that of heterozygotes, the first order kinetics are more consistent with the decrease seen than second order kinetics. The discrepancy may be explained by the small size of the data set referenced (N=12 homozygotes), the large variation noted in age of onset, the influence of non-repeat

length genetic and environmental factors, or even differences in plasticity as the brain finishes development and ages.

Estimation of aggregation inhibition by intracellular antibodies

To evaluate the effect of co-expressing intracellular antibodies on htt aggregation, eq 3.7 must be coupled with the equilibrium binding expression for antibody-antigen interactions:

$$\frac{[Intrabody \cdot Antigen]}{[Antigen]} = \frac{[Intrabody]}{K_d} \quad \text{Eqn 3.12}$$

where K_d is the equilibrium binding constant for the interaction. An underlying assumption is that the antibody and antigen come to equilibrium on a faster timescale than the timescale required for aggregation. We assume that an htt molecule that has been bound by an intrabody is incapable of misfolding, or joining an aggregate, in the bound state. Thus, the effect of intrabody binding is to reduce the effective concentration of htt in equations 3.7:

$$P = e^{-k_{\text{misfolding}} C_{\text{htt}} V_{\text{cell}} t} \quad \text{Eqn 3.7}$$

Rearranging, we see that in this case the time taken to reach a certain degree of degeneration (a given P) is inversely proportional to the concentration of htt:

$$t = \frac{-\ln P}{k_{\text{misfolding}} C_{\text{htt}}} \quad \text{Eqn 3.13}$$

Therefore, a therapeutic antibody which bound approximately half of the htt molecules within a cell (and thereby prevented toxicity resulting from the aggregation process) would double the time for the disease to progress to a certain stage, assuming that the individual received the treatment from birth and that it could be effectively delivered to all cells within the affected neuronal populations (see figure 3.7). This would theoretically push the age of onset back from an average of about 35 years to around 70. However, the most likely scenario for use of gene therapy in this disease in the foreseeable future would be to begin treatment after the disease has already presented itself. In this case, the proposed therapy would need to robustly halt the degeneration and therefore bind 90% or greater of all htt molecules within the cells.

What levels of expression and binding affinity would be required to accomplish 90% or greater of htt molecules bound? In order to answer this we need to know the concentration of htt in human brains, which has not been experimentally determined to my knowledge. However, most proteins are expressed at a level in the nanomolar range, so assuming a concentration of 1 nM may be a reasonable approximation. The trade off between antibody affinity and expression level required for binding 90% of htt molecules (assuming 1 nM) is shown in figure 3.8. For low affinity antibodies, in the micromolar range, expression levels would need to be in the tens of micromolar to effectively bind the antigen. However, achieving such high levels of expression is difficult and may not be possible for some proteins. Further, such high expression levels increase the likelihood of nonspecific interactions, which could be toxic, as well as increase the probability of an autoimmune response against cells which express the intrabody. In

order to drive the required level of antibody expression to levels 100 nM or lower, the binding affinity should be 10 nM or lower.

In the experimental systems used in this work, such as the cell-free htt aggregation assay and genetically modified cell lines, htt concentrations are much higher than that which is likely to be present in human brains. This is so that the aggregation will occur on a time scale which is amenable to experimentation. In these systems, htt concentrations are in the hundreds of nanomolar or greater, and so effects of affinity and expression level will be somewhat different. The required antibody expression levels and affinity to bind 90% of antigen molecules assuming 500 nM htt is also shown in figure 3.x. At such high target concentrations, there is a stoichiometric effect observed at high affinities, in which high concentrations are required despite high affinity.

Conclusions of engineering analysis

The analysis presented here has important implications for the antibody engineering process. First, the differences between the experimental systems used and actual human beings are substantial. In the experimental system even high affinity antibodies will need to be expressed at high levels to be highly effective at blocking aggregation. In people, where target concentrations are lower, expression levels required are likely to be lower and there is a benefit to developing high affinity antibodies. In general, the intrabody should be expressed at concentrations at least equal to that of the target. The affinity should be as high as possible to minimize the intrabody expression level required for quantitative binding, with an affinity in the 10 nM range being

sufficient to keep required intrabody expression levels in the range of normal intracellular proteins ($\sim < 100$ nM), assuming a target protein concentration on the order of 1 nM.

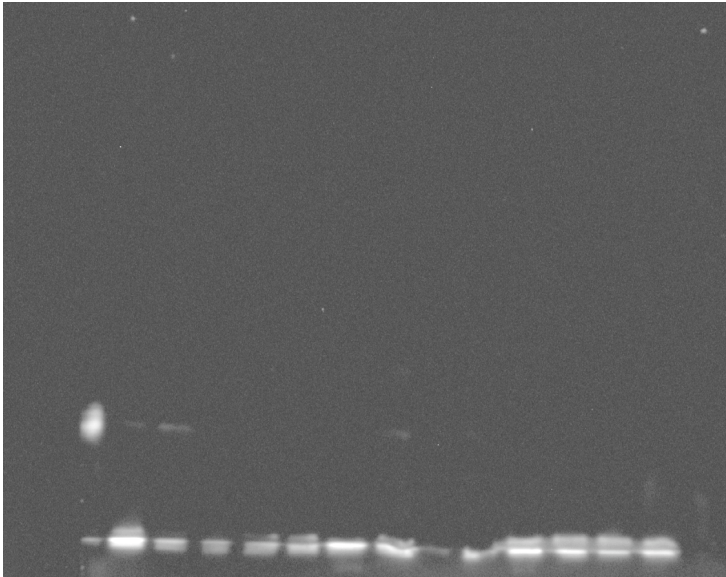


Figure 3.1.

Western blot of intracellular antibody expression. Yeast cells expressing c-myc tagged scFv fragments in the cytoplasm were lysed for western blot analysis using the monoclonal 9e10 antibody. The first visible lane (left) contains a yeast cell surface displayed Aga2p-scFv fusion as a positive control (runs higher due to fusion). The next thirteen lanes are intrabodies selected at random from the pool of anti-htt scFvs isolated. None of the intrabodies tested were present at levels significantly higher than the positive control; well expressed intracellular proteins are often present at levels 10x higher than cell surface proteins. Low expression level is later confirmed for one of the intrabodies after engineering by use of fluorescent protein fusions (chapter 5).

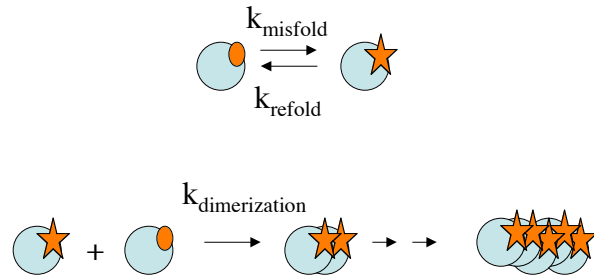


Figure 3.2.

Mechanism of htt aggregation proposed by Wetzel. Normally folded htt is in equilibrium with misfolded htt (denoted by a star). Reaction of a misfolded htt molecule with a normally folded one results in stable dimer, the formation of which is thought to be irreversible.

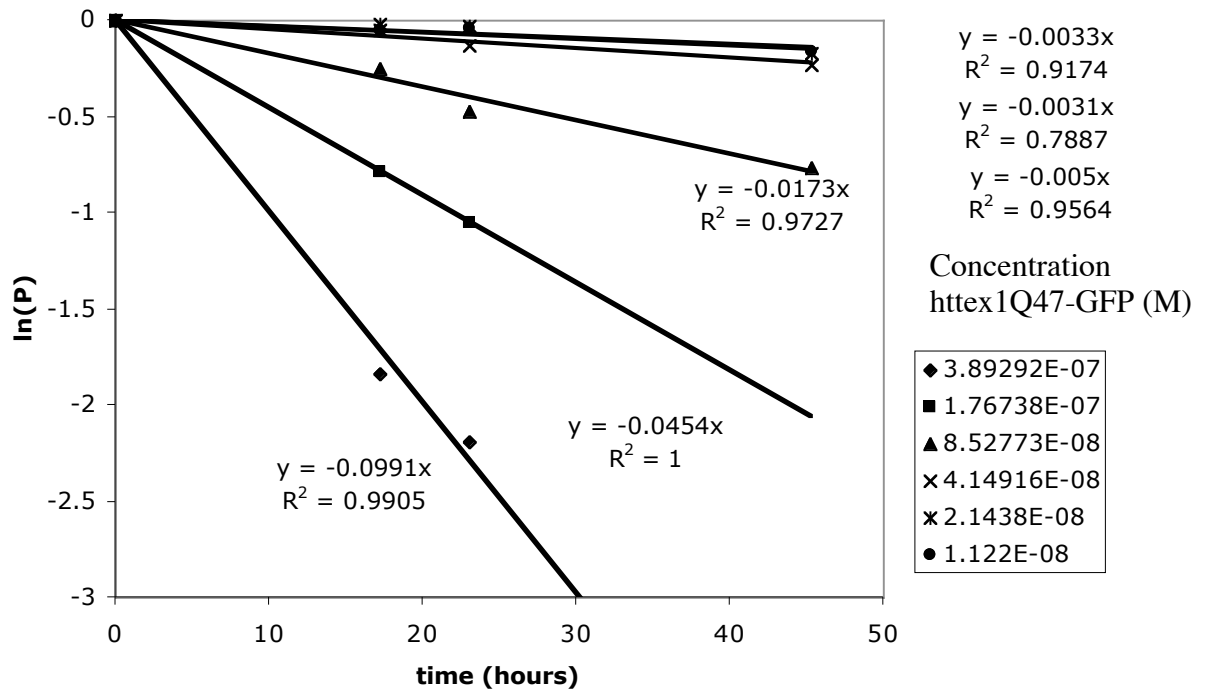


Figure 3.3.

Rate of aggregate formation from a typical experiment. Cells were sorted based on httex1Q47-GFP intensity. Intensity was used to estimate httex1Q47-GFP concentration assuming spherical cells with diameter 22 microns (measured value). The fraction of cells not containing aggregates just after sorting ($t=0$) was determined by fluorescence microscopy, and monitored periodically thereafter. Cells were returned to the incubator between measurements. Fraction of cells without aggregates at each time point were normalized to (divided by) the first measured value ($t=0$) in order to exclude cells which had formed aggregates prior to sorting. The natural log of the fraction of cells without aggregates is plotted versus time. The slope (i.e. rate) was determined by linear regression, and data having R^2 values greater than 0.85 were used to determine the concentration dependence of the rate. [The raw data that this figure is based on was generated by John Cassady under my supervision].

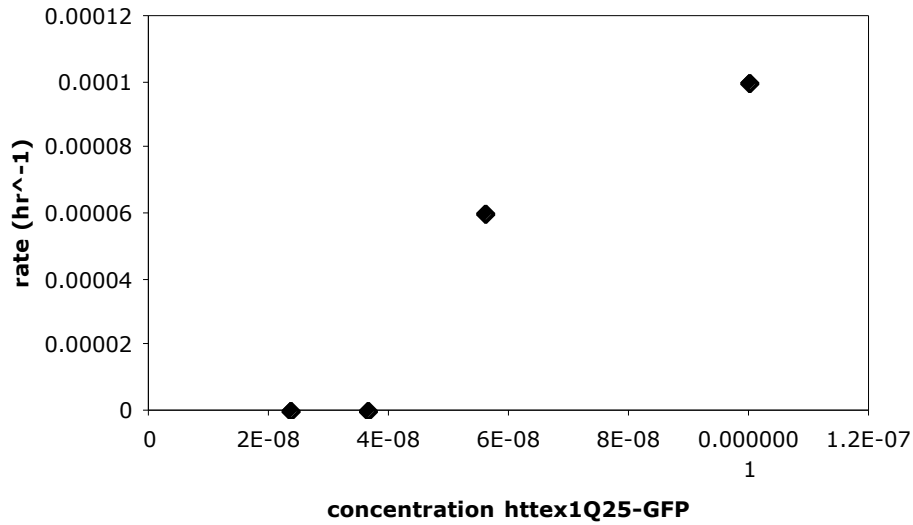


Figure 3.4.

Aggregation rates for httex1Q25-GFP as a function of concentration. Rates were determined from plots like that shown in Figure 3.3. Htt with short polyQ tracts forms aggregates at extremely low rates, measurable only at high concentration. The rates shown here correspond to the formation of less than 1% of cells having aggregates after 48 hrs (compare to rates in Figures 3.5 and 3.6). [The raw data that this figure is based on was generated by John Cassady under my supervision].

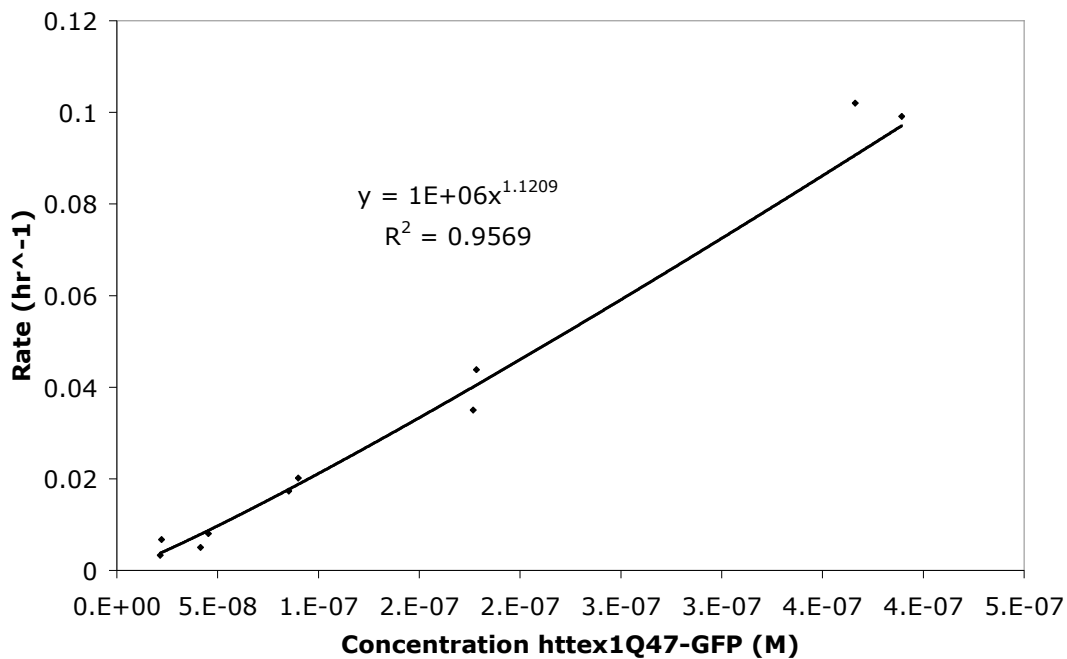


Figure 3.5.

Rate of aggregate formation as a function of httex1Q47-GFP concentration. Data have been pooled here from two independent experiments. Regression analysis indicates that the rate is approximately first order in httex1Q47-GFP. [The raw data that this figure is based on was generated by John Cassady under my supervision].

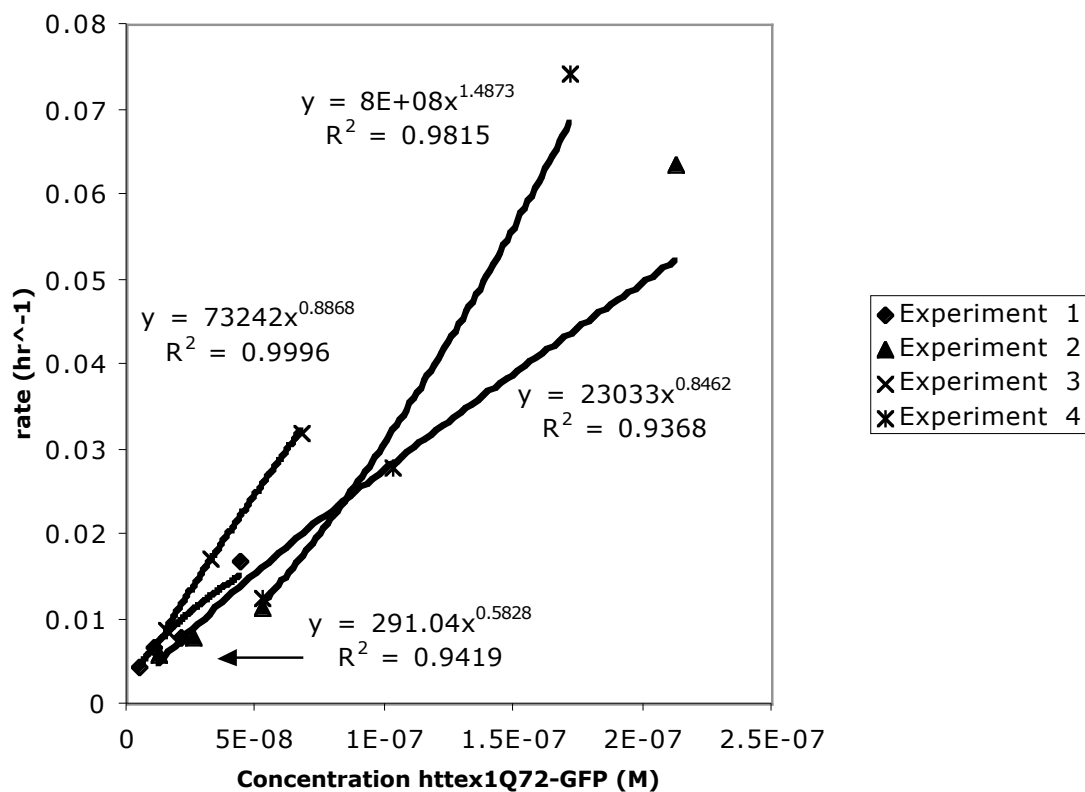


Figure 3.6. Rate of aggregate formation as a function of httex1Q72-GFP concentration. Data from four independent experiments is shown. The exponent calculated by regression analysis varied between 0.58 and 1.48, averaging approximately 0.94. This indicates that the rate is approximately first order in httex1Q72-GFP concentration. [The raw data that this figure is based on was generated by John Cassady under my supervision].

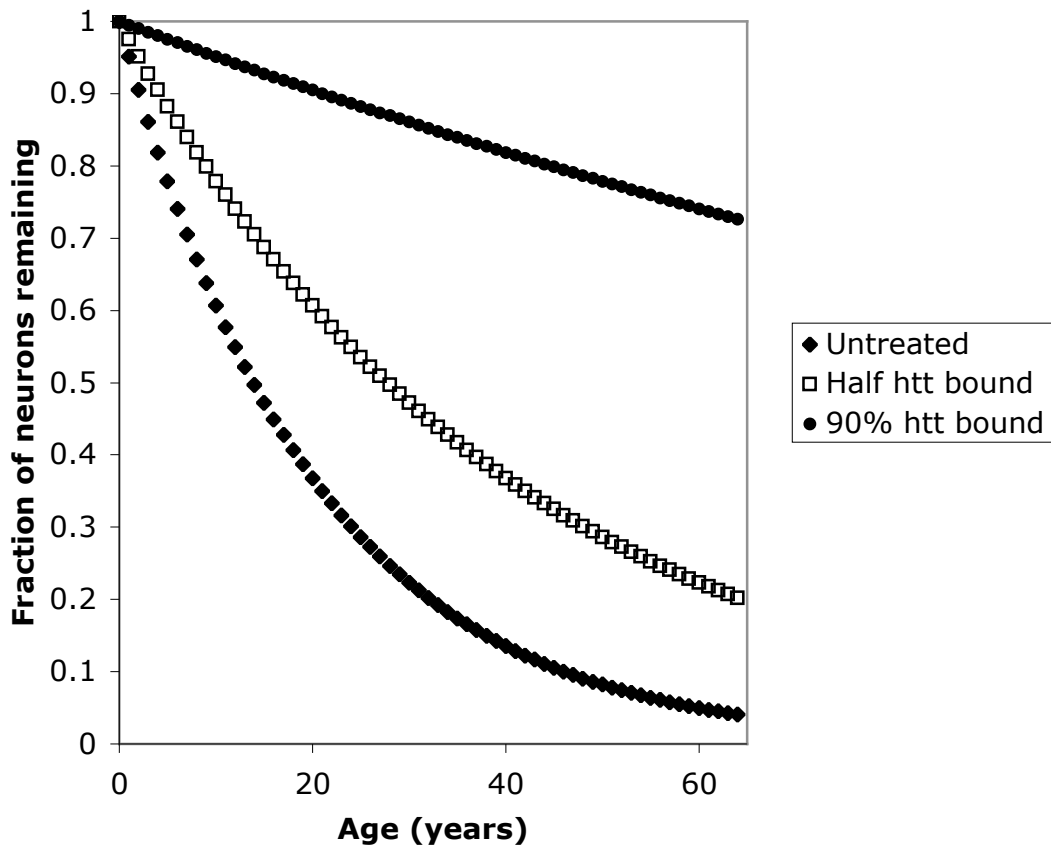


Figure 3.7. Predicted degeneration of neurons based on the model derived here (first order exponential concentration dependence), with and without intracellular antibody expression. The value of $k_{\text{misfolding}} \times C_{\text{htt}}$ was assumed to be 0.05 (chosen arbitrarily to give significant degeneration in 65 years time).

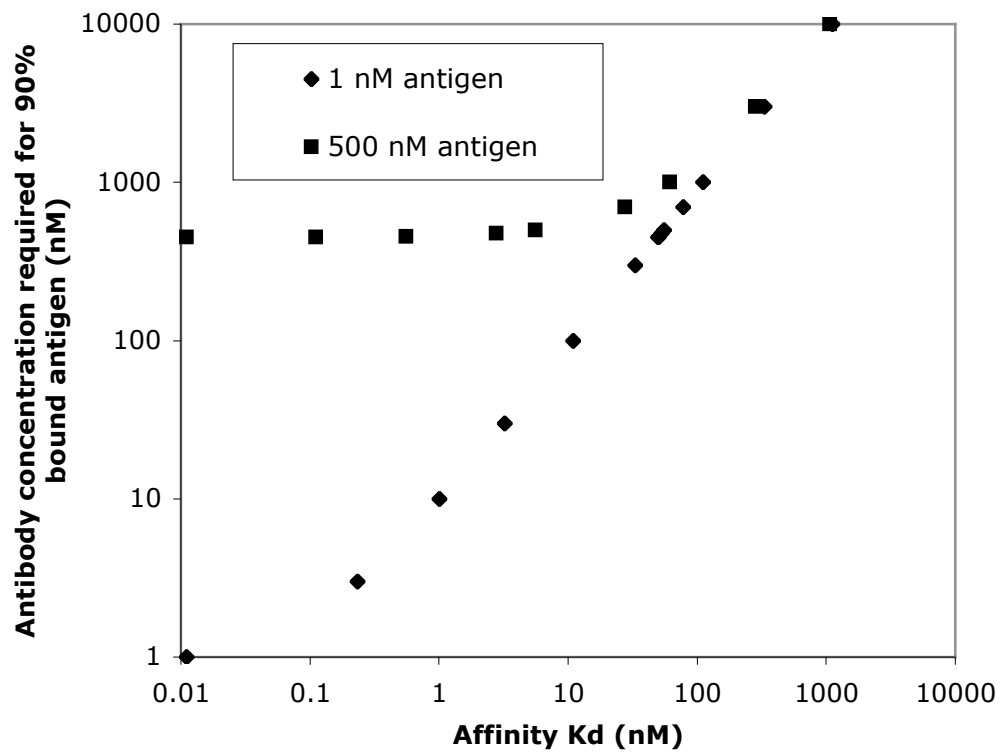


Figure 3.8. Antibody concentration required to bind 90% of htt, present at 1 or 500 nM, as a function of binding affinity. Model systems discussed in this work use htt at concentrations on the order of 500 nM. Htt is likely present at concentrations of the order of 1 nM in human brains.

Chapter 4. Affinity maturation of antibodies

The antibodies isolated in chapter 2 were engineered for improved binding affinity through mutagenesis and screening (affinity maturation).

Materials and Methods

Labeling and analysis of yeast surface display libraries and clones

Libraries and clones were labeled according to published protocols.⁴⁹ In brief, 0.2 OD₆₀₀-ml (approximately 2 million cells) of yeast were collected following overnight induction of intrabody expression with galactose, rinsed in PBS/BSA, resuspended in 500 μ l PBS/BSA with antigen (either biotinylated peptide or GST fusion protein) at appropriate concentration and mouse monoclonal anti-c-myc antibody (9E10, Covance) at 1:100 dilution. Following an incubation step of 30 minutes or longer at 37 °C, cells were rinsed with PBS/BSA and resuspended in PBS/BSA with either anti-GST polyclonal-PE conjugate (Prozyme) or Streptavidin-PE (Molecular Probes) and goat anti-mouse FITC conjugate (Sigma), at a 1:50 dilution. After an additional 30 minute incubation, cells were rinsed and analyzed on an Coulter Epics XL flow cytometer , or taken to the MIT flow cytometry core facility for FACS.

Library screening

All libraries were sorted by a MoFlo FACS machine at the MIT flow cytometry core facility. Mutant libraries were sorted as described in Appendix 1 and published elsewhere.⁶⁰

Sequencing, sequence analysis, and homology modeling

Plasmids were recovered from yeast using a Zymoprep kit (Zymo Research), and sequenced by the MIT Biopolymers Laboratory. Sequences were analyzed using the Biology Workbench (<http://workbench.sdsc.edu>) and NIH's IgBlast (<http://www.ncbi.nlm.nih.gov/igblast/>).

Results

ScFvs were affinity matured against httex1 and the N-terminal 20 amino acids of htt using the yeast surface display platform.^{31; 49; 60} A diverse library of point mutants, with mutations randomly distributed over the scFv sequences, was generated by error-prone PCR from the pool of httex1-binding scFvs initially selected from the non-immune library. This pool contained at least the eight clones whose sequences are presented in Table 2.1, but likely included many more since the entire pool was amplified for mutagenesis. Clones with higher affinity were isolated from this library by FACS, with the initial round of sorting utilizing the same GST-httex1-Q₆₇-GFP antigen used to isolate the original pool of binders. Subsequent rounds of sorting used a monovalent, biotinylated peptide consisting of the N-terminal 20 amino acids of the huntingtin protein as the antigen (MATLEKLMKAFESLKSFQQQ-biotin, here called 20aa-biotin). Use of the monovalent antigen resulted in more stringent screening by eliminating avidity effects; it also focused our screening on a region of the htt protein which has been shown to be a useful target.¹⁷

After four sorting rounds, the affinity matured scFv pool was compared with the original panel isolated from the non-immune library. The multivalent GST-htt₁-Q₆₇-GFP antigen was used for labeling during this analysis because the original panel of antibodies did not recognize the monovalent antigen with sufficient affinity to be detected (see Figure 4.1). The results are shown in Table 4.1. After affinity maturation, the fluorescence signal of binding was significantly increased, giving roughly equivalent signal at 8 nM antigen as was observed at 800 nM antigen for the original pool of binders, corresponding to an approximately 100-fold improvement in binding activity to the multivalent GST-htt₁-Q₆₇-GFP fusion protein. Both pools of yeast surface displayed scFv had comparable expression levels (data not shown), indicating that the improved signal was due to higher binding affinity.

Ten clones from the affinity matured panel were sequenced; the germline usage and CDR sequences are shown in Table 4.2. From these ten, four distinct clones were identified. Once again, the heavy chain usage varied between VH1 and VH6 family members. Unexpectedly, the light chain now belonged to the lambda 2 family instead of lambda 1. However, the third CDR showed exceptionally high homology to the lambda 1 CDR3 previously isolated, including the sequence WDDSLXXWV, further implying a strong role for this sequence in htt₁ binding activity. This lambda 2 family member derived from an scFv in the original pool which was not picked at random for sequencing, making it impossible to ascertain what mutations, if any, were responsible for improved affinity. However, its dominance in the panel of improved mutants shows the benefit of using a larger, more diverse template pool for library generation, rather than only the previously sequenced clones.

The pool of improved mutants was titrated with the monovalent 20aa peptide to estimate the scFv's binding affinity (Figure 4.1, circles). The affinity against this monovalent antigen was approximately low micromolar, predicted to be insufficient for potent intracellular activity. Comparison of the signal obtained for the affinity matured pool in Figure 4.1 relative to Table 4.1 indicates that the level of avidity improvement attributable to GST dimerization is approximately 2 orders of magnitude (approximate $K_{d,s}$ are 5 μ M for monovalent antigen and 50 nM for multivalent antigen).

To further improve binding affinity, a second round of affinity maturation was carried out. Several DNA sources were used for the library template in order to maximize diversity. This diverse DNA template consisting primarily of the pool isolated after affinity maturation (80% of template), but also included intermediate pools isolated during successive rounds of sorting the library of mutants (20% of template, 10% each of panel after one and two rounds of sorting.) These intermediate pools were included in the template to exploit any mutations which may have conferred a limited improvement in binding affinity, but were not improved sufficiently to be enriched in the final pool. Although DNase-based shuffling was not applied, it has been shown that the yeast homologous recombination method of library construction used yields inter-gene shuffling products⁶¹. This second library was sorted 4 times against the 20aa peptide, once at a concentration of 1 μ M, once at 100 nM, and twice at 10 nM.

From the panel of antibodies thus isolated, ten clones were sequenced and nine were identical replicates, with the tenth found not to exhibit improved affinity. The improved clone was named 2.4.3, and its sequence is shown in Table 4.2. The heavy chain was based on the dominant VH1 germline sequence found in both of the previously

isolated panels, and the light chain came from the lambda 1 family, which was utilized by the clones isolated from the non-immune library. Once again, the dominant improved clone was not derived from the major constituent of the template, but from a minor fraction, underscoring once again the value of carrying forward a maximally diverse pool of improved binders at each step of library construction.

The high affinity clone, 2.4.3, was titrated with monovalent 20aa peptide antigen to determine its affinity (Figure 4.1, triangles). The affinity was estimated to be roughly 30 nM, approximately 100-fold higher than the pool of mutants isolated after the first round of affinity maturation. Combined with the 100-fold improvement obtained during the first round of affinity maturation, the total improvement to affinity was approximately 10,000-fold.

Discussion

Due to the accessibility of proteins on the cell surface, the yeast surface display format is highly amenable to analysis of binding affinity and quantitative discrimination between mutants with different affinities using FACS.⁴¹ This enables significant improvements in affinity, such as the approximately 10,000-fold K_d improvement reported here during two rounds of affinity maturation.

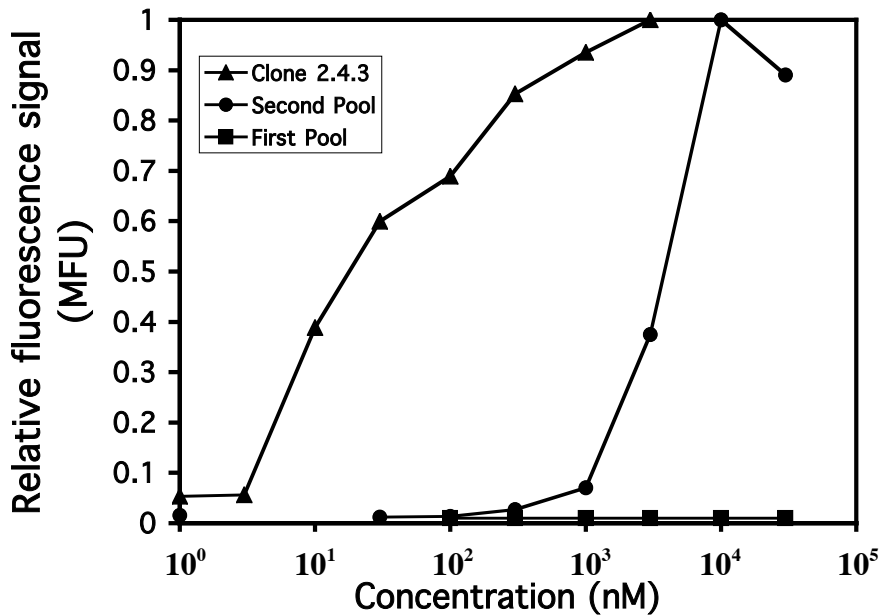


Figure 4.1

Titration against 20 aa antigen. Antibody pools and clones, displayed on the surface of yeast, were titrated with monovalent 20aa-biotin peptide antigen to demonstrate binding affinity. First pool refers to scFvs isolated from the non-immune library; Second pool refers to scFvs isolated after one round of affinity maturation. Cells were incubated with peptide at indicated concentrations, followed by labeling with streptavidin-PE, and mean fluorescence intensity was measured by flow cytometry. Cells not expressing the antibody were excluded from the analysis. Values obtained at each concentration were normalized to the highest value obtained for the clone or panel to give relative fluorescence signal in mean fluorescence units (MFU); except for the first pool, which was normalized to highest value obtained for the second panel, since the first pool did not give signals above background. The second round of affinity maturation increased the affinity by 50 to 100-fold, based on the shift in the binding curve shown.

Antigen Concentration (nM)	Pool from Non-Immune Library (MFU)	Affinity Matured Pool (MFU)
8	35	110
80	60	290
800	120	390

Table 4.1.

First round of affinity maturation resulted in an approximately 100-fold increase in affinity for GST-httx1-Q₆₇-GFP. Yeast surface displayed scFv pools isolated before and after first round of affinity maturation were labeled with GST-httx1-Q₆₇-GFP at specified concentration, followed with anti-GST polyclonal antibody conjugated to PE, and their fluorescence properties were measured by flow cytometry; fluorescence intensity reflects amount of bound antigen at each concentration. Cells not expressing scFv, as determined by labeling with anti-c-myc monoclonal antibody, followed by goat anti mouse FITC conjugate, were excluded from the analysis. Mean fluorescence intensity is reported in mean fluorescence units (MFU). The pool isolated after affinity maturation exhibits binding at 8 nM approximately equivalent to that observed at 800 nM for the panel isolated from the non-immune library, indicating an approximately 100-fold improvement in affinity.

Clone	Germ-line	CDR H1	CDR H2	CDR H3	CDR L1	CDR L2	CDR L3
0.4.1	Vh6-1, V1-11	GDSVSSNTAAWY	RTYYSSKWFYD	EDD-----YGDYV	SGSTSNIGNNAVN	YDDLPLPS	ATWDDSLNGWV
0.4.2	VH1-69, V1-11	GGTISS--CAIS	GIIPMFDTTN-	TYYHDTSDNDGTYGMDV	SGSTSNIGNNAVN	YDDLPLPS	ASWDDNLNGWV
0.4.3	VH6-1, V1-11	GDSVSSNSAARN	RTYYRSRWYND	DPPIV-----LSTFDI	SGSTSNIGNNAVN	YDDLPLPS	ATWDDSLNGWV
0.4.4	VH1-18, V1-16	GGTISS--CAIS	GIIPMFDTTN-	TYYHDTSDNDGTHGMDV	SGSSSNIGSNTVN	SDNQRPS	ATWDDSLNGWV
0.4.6	VH1-69, V1-11	GGTISS--CAIS	GIIPMFDTTN-	TYYHDTSDNDGTYGMDV	SGSTSNIGNNAVN	YDDLPLPS	ATWDDSLNGWV
0.4.7	VH1-69, V1-11	GGTISS--CAIS	GIIPMFDTTN-	TYYHDTSDNDGTYGMDV	SGSSSNIGSNTVN	ADYERPS	ATWDDSLNGWV
0.4.9	VH1-69, V1-11	GGTISS--CAIS	GIIPMFDTTN-	DDVVA-----TLGGFDI	SGSSSNIGSNTVN	YDALLPS	AAWDDSLDGWV
0.4.10	VH1-69, V1-16	GGTISS--CAIS	GIIPMFDTTN-	TYYHTRDNDGTYGMDV	SGSSSNIGSNTVN	YDDLPLAS	ASWDDNLNGWV
1.4.1	VH6-1, V2-14	GDSVSSNSAAWN	RTYYRSKWNVD	EDD-----YGDYV	GG--TNIDKKS VH	DDSDRPS	TTWDDSLNVVV
1.4.2	VH6-1, V2-14	GCSVSSNRATWH	RTYYSSKWRVD	EDD-----YGDYV	GG--TNIDKKS VH	DDSDRPS	TTWDDSLSGWV
1.4.5	VH1-69, V2-14	GGTISS--CAIS	GIIPMFDTTN-	TYYHDTSDNDGTYGMDV	GG--TNIDKKS VH	DDSDRPS	TTWDDSLNAFV
1.4.8	VH6-1, V2-14	GDSVSSNTAAWY	RTYYSSKWRVD	EDD-----YGCYV	GG--TNIDKKS VH	DDSDRPS	TTWDDSLSGWV
2.4.3	VH1-69, V1-11	GGTISS--CAIS	GIIPMFDTTN-	TYYHDTSDNDGTYGMDV	SGS SN IGSNTVN	YDDLPLAP	ATWDDSLNGWV

Table 4.2

Germline usage and sequences of complementarity determining regions (CDRs) of antibodies before and after affinity maturation. Clones were named according to "rounds of mutation, rounds of FACS sorting, clone number." Germline sequences shown were determined using IgBlast (<http://www.ncbi.nlm.nih.gov/igblast/>). CDR H1 refers to the first CDR of the heavy chain, CDR H2 is the second, etc. Yellow background indicates consensus (residues conserved in at least 11 of the 13 sequences shown). Top, clones isolated from the non-immune human antibody library. Middle, clones obtained after one round of mimicking affinity maturation by using mutagenesis and screening of scFv displayed on the surface of yeast. Bottom, clone obtained after two rounds of affinity maturation. Note high level of conservation in CDR L3.

Chapter 5. Development and characterization of a single domain antibody against htt

In the last chapter, we discussed affinity maturation of the pool of antibodies isolated, to create the scFv 2.4.3. In this chapter, the binding site of 2.4.3 is examined by mutational analysis. Surprisingly, the binding site consisted only of the light chain variable domain. This single domain intrabody was markedly better expressed in the cytoplasm relative to its scFv counterpart, and was able to partially block aggregation of htt in a cellular model of HD. This work demonstrates an approach that may be useful in the development of other single domain intrabodies from a lead scFv.

Materials and Methods

Intracellular antibody expression as YFP fusion protein

Intrabody YFP fusion constructs were generated using homologous recombination in yeast.⁶² The vector plasmid contained YFP on a p414 yeast shuttle vector backbone. XbaI and BamHI were located upstream of YFP and after a galactose inducible promoter; these sites were cleaved to give digested backbone for transformation. A forward PCR primer was designed to contain 30 bp of homology to the region between the galactose promoter and the XbaI site, followed by 20 bp of homology to an HA tag upstream of the antibody in the yeast surface display vector (to use for PCR of the intrabody). The reverse primer contained 30 bp of homology to the N-terminus of YFP, followed by 20 bp homologous to a c-myc tag at the C-terminus of the antibody in the yeast surface

display vector. PCR product and digested vector were transformed into BJ5464 α *S. cerevisiae* to give the final fusion construct. Plasmids were recovered and sequenced, then transformed back into yeast for analysis. YFP fluorescence was measured 24 hours post-induction using a Coulter Epics XL flow cytometer.

Soluble production of V_L

The V_L gene was isolated from the yeast surface display vector by partial digestion with NheI and BamHI and subcloned into an *S. cerevisiae* secretion vector containing an N-terminal flag tag and a C-terminal His₆ tag. The plasmid was transformed into BJ5464 *S. cerevisiae*. Transformants were grown on a plate at 30°C for three days, used to inoculate a starter culture on minimal glucose medium, which grew for two days, and were subsequently transferred to a large (1L) culture in a Tunair flask with the same medium. Thirty six hours later, the medium was replaced with minimal galactose medium for induction and supplemented with 0.5% BSA as a carrier protein. Three days post-induction, the cells were removed from the medium by centrifugation and filtration, and the supernatant was concentrated using an Amicon protein concentrator with a 10 kDa membrane (Millipore). The V_L was purified from the supernatant using a nickel column (Qiagen), and was analyzed by SDS-PAGE and BCA assay (Pierce) to determine purity and concentration.

Cell-free *in vitro* aggregation inhibition assay

Aggregation of httex1Q₆₇ was measured by right angle light scattering on a Varian fluorescence spectrophotometer with excitation and emission filters set to 495 nm. GST-

httx1-Q₆₇ at a concentration of 500 nM (monomer basis), 1 unit thrombin, and various concentrations of VL were mixed in 50 µL total volume with PBS/BSA as a buffer. After a 48 hr incubation at 37 °C, the total volume was brought to 150 µL and the reaction was transferred to a quartz cuvette for measurement. All concentrations were tested in triplicate.

Homology model

The homology model was generated using Web Antibody Modeling (<http://antibody.bath.ac.uk/index.html>). Images of the model were generated using PyMOL software (DeLano Scientific LLC, at <http://www.pymol.org>).

Mammalian cell culture, aggregation assay, and toxicity assays. ST14A cells⁵⁸ were cultured according to standard protocols. C-terminal his₆ tagged intrabody constructs were expressed from a pcDNA3.1 vector under the control of a CMV promoter, as was httx1-Q97-GFP. Cells were transiently transfected using lipofectamine (Invitrogen) or similar reagents and presence of aggregates was monitored by fluorescence microscopy 24 hours post-transfection.

Results

Paratope mapped to variable light chain domain by random mutagenesis

Identification of an antibody's paratope can be useful for guiding the protein engineering process. In order to determine the paratope of the 2.4.3 clone, a library of point mutants was created by error-prone PCR of the entire scFv, followed by FACS

sorting of non-functional but still well-expressed mutants; the location of mutations that result in loss of binding are indicative of the paratope location.

A yeast surface display library with an average of one mutation per clone spread over both domains of the scFv and consisting of approximately 10^7 clones was generated by error prone PCR using Taq polymerase in the presence of $MnSO_4$. The mutation rate used to generate the paratope mapping library was low in order to increase the likelihood that isolated non-functional mutants had only a single point mutation. The presence of multiple point mutations would obscure the contribution of each mutation, and only provides domain-level information about the general location of the paratope when all mutations are constrained to a single domain of the protein.

This library was labeled with the anti-c-myc 9E10 mAb and the monovalent 20aa-biotin peptide antigen at $1 \mu M$ to detect scFv expression and antigen binding, respectively. After labeling with appropriate fluorophore-conjugated secondary reagents, the library was sorted by FACS to obtain mutants that expressed the scFv on the yeast surface, as judged by the presence of a C-terminal c-myc tag, but which lacked binding activity. The sort gate used to accomplish this is shown in Figure 5.1. The antigen concentration was chosen to be ~ 30 times the binding K_d in order to brightly label clones with wild-type affinity, resulting in a high level of discrimination between wild-type clones and non-functional mutants.

Clones isolated after one round of sorting were amplified and re-labeled to ensure undetectable binding activity at $1 \mu M$, corresponding to a $\Delta\Delta G$ of approximately 3 kcal/mol. Twenty-seven of thirty clones selected lost detectable htt peptide binding at $1 \mu M$. These clones were sequenced, and each clone was scored into one of three

categories: those that had only one mutation (3/27), those that had multiple mutations spread over both domains of the scFv (22/27), and those that had multiple mutations constrained to a single domain of the scFv (2/27). In all three clones with only one mutation, the mutation was found to be on the light chain of the scFv, as was the case with the two clones with multiple mutations constrained to a single domain (Figure 5.1B and 5.1C). No non-functional mutants were isolated that had mutations only on the heavy chain. That is, all twenty-seven non-functional mutants isolated contained mutations on the light chain. Isolation of five clones with mutations only on the light chain is statistically significant for mutations randomly distributed between the domains ($P = 0.03$).

The strong bias toward binding-loss mutations occurring only in the light chain is indicative of the light chain contributing the great majority of free energy in the binding interaction. This is consistent with the earlier observation that clones isolated with novel binding activity exhibited highly converged consensus sequence in the light chain, while the heavy chain usage was more flexible. However, it should also be noted that no mutations in the V_L CDR3 loop were isolated in this paratope analysis, despite its conservation in the pool of novel binders. Consequently, the information from this screen was less useful for precise localization of energetic hot spots for binding, and was instead helpful in emphasizing the significance of the V_L domain relative to the V_H .

Single domain expresses well on yeast surface and retains binding affinity

Serendipitously, the light chain of 2.4.3 fused directly to a fragment of Aga2p was isolated from the paratope-mapping library when that library was sorted for improved

binding. Such artifacts may be created during homologous recombination in yeast, because very little homology is required for a cross-over event.⁶¹ The V_L did not exhibit higher affinity, but was slightly better expressed on the yeast cell surface, and was likely isolated from the library for this reason. An Aga2-V_L fusion was constructed with a (Gly₄Ser)₃ linker between the Aga2 and V_L, with a C-terminal c-myc tag included for detection of the fusion protein on the yeast surface. Yeast expressing this construct were labeled with an anti-c-myc antibody followed by goat anti-mouse FITC to detect expression. The result is shown in Figure 5.2, top. The light chain construct was found to express equivalently well on the yeast surface as compared to the scFv. Because the yeast endoplasmic reticulum retains and targets unfolded proteins for degradation,^{38; 39} its ability to reach the yeast cell surface indicates that the light chain variable domain is stable in the absence of its heavy chain partner.

A titration of the light chain-only construct is shown in Figure 5.3 (diamonds). The binding affinity is approximately the same as the 2.4.3, demonstrating that the light chain does in fact contribute essentially all of the binding free energy from the scFv.

Light chain domain has improved intracellular expression in yeast

Intensity of fluorescence from GFP fusion expression has been shown to be a useful tool in gauging and comparing intracellular soluble expression.⁶³ To measure the intracellular expression of the antibody fragments, fusion proteins were expressed consisting of antibody fragments, either the scFv or the V_L alone, and yellow fluorescent protein (YFP-a GFP variant). Fusion proteins were expressed from a cytoplasmic, galactose inducible yeast expression vector. Twenty four hours post induction, cells were

analyzed by flow cytometry. The distribution of fluorescence observed is shown in Figure 5.2. While the scFv-YFP fusion exhibited negligible fluorescence relative to background, the V_L-YFP fusion fluoresced brightly, indicating high levels of protein expression. About 40% of the V_L-YFP cells showed no fluorescence, likely due to plasmid loss, which occurs in 2-50% of yeast cells within a transiently transfected population.

V_L blocks huntingtin aggregation in a cell-free *in vitro* assay

Monoclonal antibodies against polyglutamine have been shown to block huntingtin aggregation in cell-free *in vitro* assays,¹⁶ as have scFvs against the first seventeen amino acids of huntingtin in cell based assays.^{17; 18} These antibodies are thought to block aggregation either by forcing the huntingtin fragment into a conformation that is incapable of aggregating, or by simple steric hindrance of the polyglutamine-polyglutamine interaction that leads to nucleation or elongation of the amyloid fibril. An *in vitro* assay was used to determine if the single domain antibody would inhibit htt aggregation. The V_L was secreted from *S. cerevisiae* as a soluble protein, and purified from the growth medium by affinity chromatography against a C-terminal His₆ epitope tag. The purified yield was approximately 3 mg/L of culture.

An *in vitro* assay was designed based on aggregation of the httex1-Q₆₇ fragment of htt measured by light scattering. The GST-httex1-Q₆₇ contains a thrombin cleavage site between the GST and httex1-Q₆₇, which can be used to initiate aggregation by freeing httex1-Q₆₇ from the stabilizing GST protein. Once cleaved, the httex1-Q₆₇ protein forms aggregates that can be measured by right angle light scattering within 48 hours when

present at 500 nM or greater concentrations. Recombinant V_L was added at various concentrations to evaluate its effect on the aggregation process. The results are shown in Figure 5.4. The V_L antibody completely and reproducibly blocked htt aggregation when it was present at stoichiometric equivalence to httex1-Q₆₇. To ensure that the antibody does not simply inhibit thrombin cleavage, the reaction products were analyzed by SDS-PAGE, and the GST-httex1-Q₆₇ protein was completely cleaved even in the presence of the V_L (Fig. 5.4B).

Single-domain intrabody inhibits htt aggregation in transiently transfected ST14A cells

Finally, we evaluated the ability of the single-domain antibody to inhibit htt aggregation in transiently transfected ST14A cells. Cells were co-transfected with the intrabody and httex1-Q97-GFP at a 2:1 plasmid ratio, and the appearance of aggregates was monitored by fluorescence microscopy 24 hours post-transfection. Cells co-transfected with the VL and htt plasmids were significantly less likely to contain aggregates than those co-transfected with an empty vector in place of the VL (see fig. 5.5).

Discussion

Yeast surface display can facilitate structure/function analysis, as demonstrated with the paratope mapping studies reported here. Typical mutational analysis requires expression and purification of each mutant to be studied, while in yeast surface display

the protein to be studied is expressed directly in a properly folded state, already immobilized on the yeast surface where its binding properties can be analyzed. Combined with the ability to rapidly sort mutant libraries to obtain clones with desired properties, this is an appealing approach to domain-level parsing of binding site contributions; analogous domain-level epitope mapping is also possible.^{64; 65}

We have demonstrated that YSD can be used to derive a single-domain antibody from an scFv, when the binding energy of the scFv is contributed predominantly by one of the two domains. Reduction to a single domain can be advantageous for increasing intracellular expression levels, which is key to the biological activity of intrabodies; it may also be useful for focusing further engineering efforts, such as affinity maturation, on the more relevant domain. However, we did not extract more detailed information about the paratope, such as particular residues that are important for the binding interaction, as are often obtained by alanine scanning.⁶⁶ The clones with single mutations isolated here all involved either proline or glycine, both of which would very likely strongly affect framework secondary structure. We believe these mutations scattered about the entire domain grossly affect folding of the paratope, since they clearly are not positioned to make direct contacts with the antigen (Figure 5.1B). It may be possible to identify particular contact residues in the paratope if the screening approach were modified to find mutants which have only slight decreases in affinity. Alanine scanning studies have shown that individual contact residues often contribute no more than 1.5 kcal/mol of binding energy, which corresponds roughly to a 10-fold decrease in affinity⁶⁷. To achieve a 100-fold or greater decrease in affinity, the threshold for isolation in this

study, multiple mutations or single mutations causing significant structural domain-level changes were apparently required.

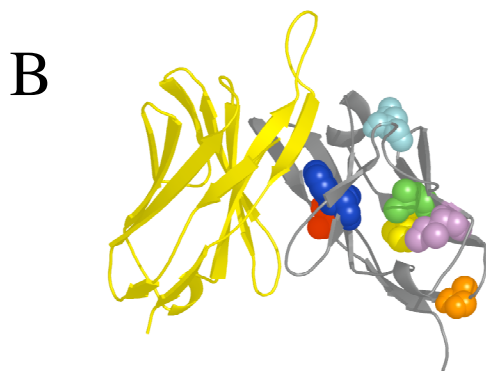
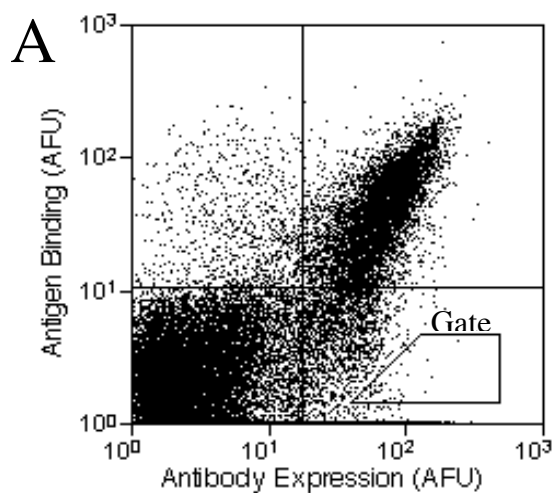
To our knowledge, this is the first reported case where an scFv paratope was mapped entirely to the light chain domain. The fact that the paratope was located only on the light chain of this scFv is contrary to the viewpoint that the interdomain cleft forms the binding pocket for peptide antigens.⁶⁸ Although the crystal structure of this antibody is not available, inspection of a homology model (generated using Web Antibody Modeling (<http://antibody.bath.ac.uk/index.html>)) did not reveal an appropriate cleft which could serve as a substitute. However, it has been reported that peptides can interact with binding pockets which are only moderately concave^{69; 70; 71} which may be the case here.

Although we were successful in isolating an intrabody by this method, a theoretical shortcoming of the yeast surface display platform for application to intrabody engineering might arise from the difference in redox environment on the cell surface as compared to the cytoplasm, where disulfide bonds do not stably form. Antibodies contain highly conserved intradomain disulfide bonds in both the heavy and light chain variable domains that hold the beta-sheet forming framework residues in a rigid conformation. Disruption of these disulfide bonds perturbs the domain structure, reducing protein stability.⁷² This presumably is responsible for the disparity between cell surface expression and cytoplasmic expression levels for the scFv (Figure 5.2, compare top and bottom). Further, the expression of fusion proteins (an scFv is a fusion protein consisting of the heavy and light chain variable domains) is generally cis-dominant; that is, the expression of the fusion protein is only as good as the expression of the member

with the lowest stability, so an alternative explanation of the improvement in expression observed when the heavy chain is eliminated is that the V_H domain of 2.4.3 was significantly less stable than the light chain under reducing conditions.

Although it has been recently reported that single heavy chain variable domains can be used as intracellular antibodies,^{28; 29} to our knowledge this is the first report of a single light chain variable domain intrabody. The increase in expression obtained when using the single V_L domain compared to the entire 2.4.3 scFv is consistent with observations for a heavy chain domain intrabody derived from an scFv.²⁹ The current work supports the value of single domain intrabodies as intracellular antigen recognition units. It has been observed that for immunoglobulin light chains consisting of both the constant and variable regions, dimers can form by interaction of the hydrophobic interdomain face that is exposed in the absence of the heavy chain.⁷³ However, single light chain variable domain antibodies have been shown to form stable monomers,^{27; 74} and should make suitable intrabodies.

A potential advantage to using single-domain intrabodies rather than scFv for treatment of HD via gene therapy arises from the reduced mass of the smaller intrabody. A hallmark of HD is the formation of intranuclear inclusions, so the ability of an intrabody to diffuse into the nucleus and prevent aggregation there may be critical. While scFv, with a molecular weight of 25-30 kDa, are close to the molecular weight cut-off of nuclear pores,⁷⁵ single domain intrabodies are only half that size and should more readily diffuse into the nuclear subcompartment.



C

Clone	Mutation(s)
3.1.1-	A12V (orange), F37S (blue)
3.1.12-	L74P (green)
3.1.13-	I20V (yellow), I76T (violet)
3.1.16-	D52G (cyan)
3.1.29-	G102V (red)

Figure 5.1.

Paratope of scFv 2.4.3 mapped to variable light chain domain by analysis of mutants which had attenuated binding to htt. A library of mutants based on scFv clone 2.4.3 was screened by FACS to isolate mutants that lacked the ability to bind htt. A, FACS data showing typical sorting gate for collecting non-functional mutants. Clones which express the antibody, as detected by presence of c-myc tag with monoclonal antibody followed by goat anti-mouse-FITC, and which do not bind the monovalent 20aa-biotin peptide, detected by streptavidin-PE, were collected. Collected clones were amplified and analyzed individually and those lacking binding activity were submitted for sequencing. B, a homology model (generated using Web Antibody Modeling (<http://antibody.bath.ac.uk/index.html>)) of scFv 2.4.3 showing that mutations that ablated binding were constrained to the variable light chain domain. C, table containing exact location of these mutations.

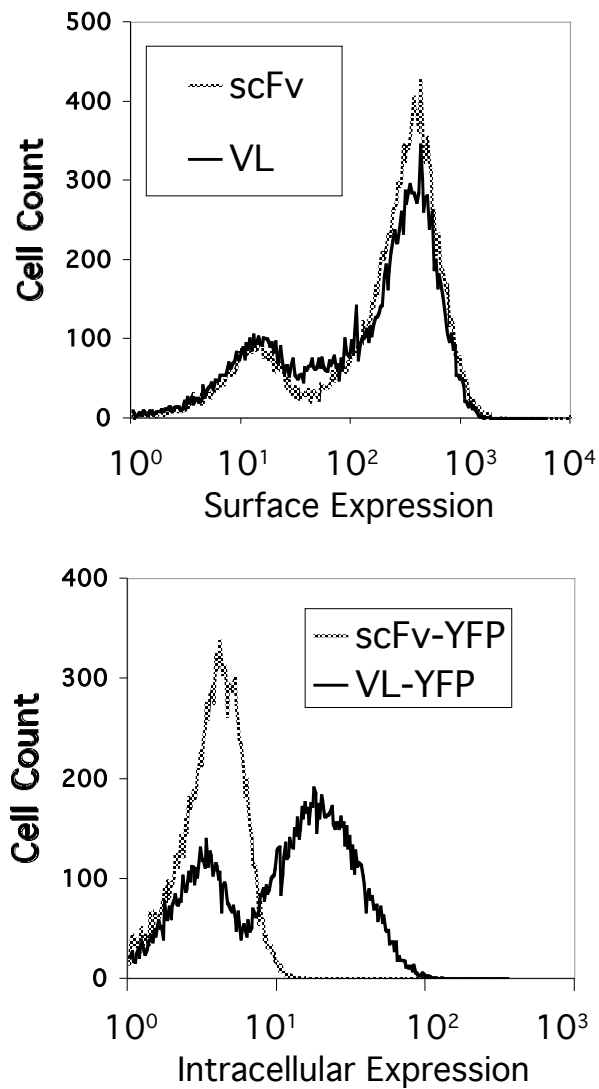


Figure 5.2.

ScFv clone 2.4.3 and the singled-domain V_L of that clone express comparably on the yeast surface, but only the V_L expresses well in the cytoplasm. Top, c-myc tagged V_L and scFv 2.4.3 are equally well expressed on the yeast surface, as detected by anti-c-myc monoclonal antibody and goat anti-mouse-FITC by flow cytometry. Bottom, variable light chain domain intrabody fused to YFP has expression levels at least 5-10 times higher than scFv-YFP fusion. Two peaks can be seen in both panels due to loss of the plasmid containing the antibody, which occurs in 2-50% of cells within transiently transfected yeast cultures.

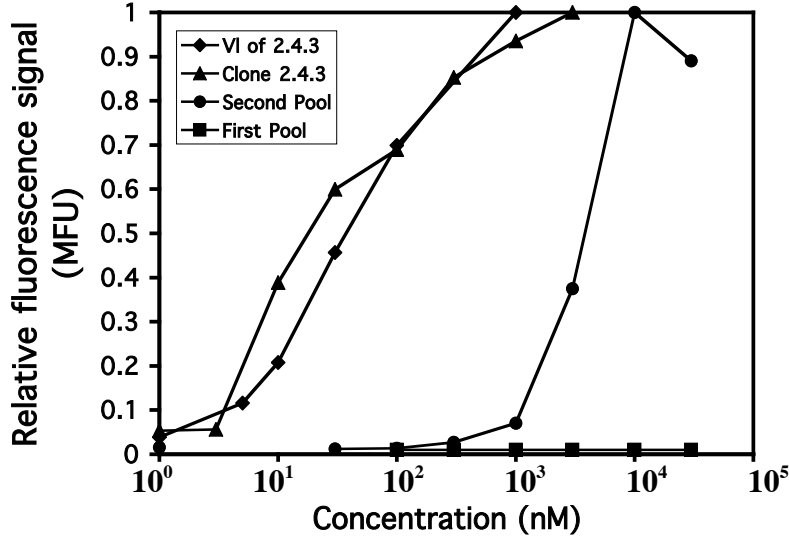


Figure 5.3.

The light chain domain of clone 2.4.3 binds the 20 aa peptide antigen with affinity equivalent to the full scFv. Antibody pools and clones, displayed on the surface of yeast, were titrated with monovalent 20aa-biotin peptide antigen to demonstrate binding affinity. First pool refers to scFvs isolated from the non-immune library; Second pool refers to scFvs isolated after one round of affinity maturation. Cells were incubated with peptide at indicated concentrations, followed by labeling with streptavidin-PE, and mean fluorescence intensity was measured by flow cytometry. Cells not expressing the antibody were excluded from the analysis. Values obtained at each concentration were normalized to the highest value obtained for the clone or panel to give relative fluorescence signal in mean fluorescence units (MFU); except for the first pool, which was normalized to highest value obtained for the second panel, since the first pool did not give signals above background.

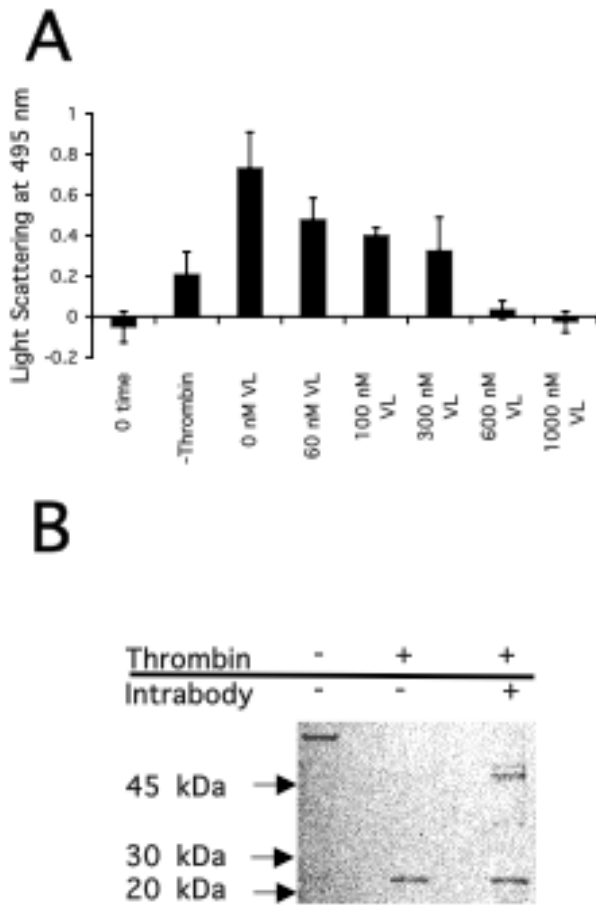


Figure 5.4.

V_L stoichiometrically blocks htt aggregation in an *in vitro* assay. Recombinant GST-htt_{ex1-Q₆₇} protein aggregates rapidly upon GST cleavage by thrombin. A. 500 nM GST-htt_{ex1-Q₆₇}, 1 unit thrombin, and various concentrations of V_L were mixed and aggregation was measured by right angle light scattering 48 hrs later, unless otherwise indicated. At $t=0$, the solution is free of aggregates, but after 48 hrs htt aggregates form in the absence of antibody, even when thrombin is not added (-Thrombin). The dose-response indicates that aggregation inhibition is complete when the V_L is present in stoichiometric proportion (>500 nM) to htt. B. SDS-PAGE gel showing that presence of antibody does not inhibit thrombin cleavage, monitored by presence of GST band at 25 kDa. The polyglutamine-containing htt_{ex1-Q₆₇} runs abnormally high at about 50 kDa, and is not seen in the sample without intrabody because it has aggregated and cannot enter the gel. [Part A generated by Payal Garg under my supervision; part B generated with the assistance of Payal Garg.]

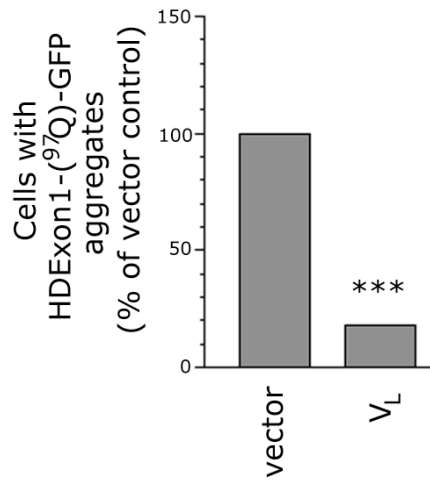


Figure 5.5.

Single-domain intrabody V_L inhibits htt aggregation in transiently transfected ST14A cells. Plasmids for V_L and httx1Q97-GFP were cotransfected into ST14A cells at a 2:1 ratio. Presence of aggregates was observed by fluorescence microscopy 24 hours post-transfection. *** p<0.001 [Data generated by Colin Chu under my supervision.]

Chapter 6. Development and characterization of a high affinity single domain intrabody lacking a disulfide bond

In the last chapter, we described the isolation of a single-chain antibody (scFv) specific for the first 20 amino acids of huntingtin, and its reduction to a single variable light chain (V_L) domain, in order to enable intracellular expression and mild inhibition of htt aggregation²⁴. In this chapter, the V_L intrabody was engineered further for robust and effective inhibition of aggregation and cytotoxicity. This was accomplished by removing the disulfide bond to make intrabody properties independent of redox environment, whether intracellular or extracellular, and performing subsequent engineering. First, the cysteines that form the disulfide bond were mutated to hydrophobic residues (valine and alanine), a technique shown to be effective for obtaining higher yields of active antibody expressed from *E. coli*⁷⁶. This resulted in an unexpectedly large decrease in the intrabody's affinity for its antigen. Iterative rounds of mutation and screening were then applied to improve the intrabody's affinity. We find that the ability to block httx1Q97-GFP aggregation correlates with antigen binding affinity in the absence of disulfide bonds. Disulfide-independent binding affinity and intracellular antibody expression levels^{24; 52; 53; 54}, appear to be the two essential design variables for the development of highly functional intracellular antibodies.

Materials and Methods

Yeast surface display. The cysteine residues of yeast displayed V_L ²⁴ were changed to valine and alanine (C22V, C89A) by site directed mutagenesis of the V_L gene using

QuikChange PCR (Stratagene). Yeast surface display labeling experiments to measure expression and binding were conducted as previously described⁴⁹. A peptide consisting of the first 20 amino acids of htt was used as the antigen (MATLEKLMKAFESLKSFQQQ-biotin, synthesized by the MIT biopolymers lab). The antigen was synthesized to contain three glutamines because the beginning of the polyglutamine region would be an ideal target for interfering with the misfolding of htt exon I. Affinity maturation of $V_{L,C22V,C89A}$ relied upon protocols previously described³³. Briefly, the $V_{L,C22V,C89A}$ gene was used as the template for the creation of a library of point mutants through error prone PCR using nucleotide analogues. The resulting PCR products were amplified and transformed into yeast along with digested pCTCON (a yeast surface display vector) to create a library through homologous recombination⁶². The library had a diversity of 3×10^7 intrabody mutants displayed on the surface of yeast. This library was sorted 4 times by FACS to isolate mutants with approximately 10-fold improvement in affinity, as measured by titration with the 20 amino acid htt peptide. These mutants were then used as the template in the next round of library generation. The entire process, from library generation to isolation of improved mutants, was repeated three times to yield $V_L12.3$. FACS sorting was performed using a Cytomation Moflo FACS machine by the staff of the MIT Flow cytometry core facility. All constructs and clones were sequenced at the MIT biopolymers lab.

Mammalian cell culture, aggregation assay, and toxicity assays. ST14A cells⁵⁸ were cultured according to standard protocols. C-terminal his₆ tagged intrabody constructs were expressed from a pcDNA3.1 vector under the control of a CMV promoter. The

method used to quantify the effect of intrabodies on intracellular htt exon I aggregation in the three cell lines mentioned above is described in detail elsewhere ²⁴; briefly, cells were transiently transfected using Lipofectamine 2000 (Invitrogen) and presence of aggregates was monitored by fluorescence microscopy. Transfection efficiencies and expression levels of httex1Q97-GFP were monitored by flow cytometry on a Moflo FACS machine (Cytomation).

For the MTT (3-(4,5-dimethylthiazol-2-yl)-2,5-diphenyltetrazolium bromide) assay, which was used to measure metabolic activity, transiently transfected ST14A cells were sorted 48 hrs post-transfection based on GFP signal to collect populations expressing GFP or httex1-GFP transgenes (Q25 or Q97). These cells were sorted directly into 96-well plates, 35,000 cells per well in 100 μ l maintenance media. The MTT assay (kit from ATCC) was then performed according to the manufacturer's protocol. A Fluorostar Optima96-well plate reader (BMG Labtechnologies) was used to measure absorbance of the metabolic product at 570 nM.

PC12 cell lines expressing either htt-25Q-EGFP or htt-104Q-EGFP under the control of the inducible ecdysone promoter were obtained from the Housman lab. The construct consists of the first 17 amino acids of htt-Exon1, followed by the polyQ stretch and enhanced GFP in the inducible ecdysone system. The cells are stable transfectants. Cells are grown on RPMI medium supplemented with 15% FBS, 100 units/ml penicillin, 100 ug/ml streptomycin, 2 mM L-glutamine, 200 ug/ml G418, and 100 ug/ml Zeocine.

Intracellular aggregation in yeast. V_L12.3 was expressed cytoplasmically along with htt-x1-Q97-YFP, which forms aggregates in the yeast cytoplasm. Images were taken on

a confocal microscope, and images were analyzed quantitatively to objectively measure the fraction of cells with aggregates. Three images were taken of each sample, with approximately 50-100 cells in each image. Aggregates were scored by applying a threshold value to fluorescence intensity. Because the rate of plasmid loss can be high with non-integrated constructs, the data were corrected by assuming cells which have lost the V_L12.3 plasmid will exhibit a level of aggregation equal to that of the negative control (empty vector).

Viral Delivery of V_L12.3

A strain of adenovirus (Ad-V_L12.3) was created that carries the V_L12.3 gene. V_L12.3 was subcloned into the transfer vector pACCMV2, and the University of Michigan Vector Core facility (<http://www.med.umich.edu/vcore/>) produced the engineered virus.

Results

Elimination of anti-htt V_L intrabody's disulfide bond reduces affinity for huntingtin.

Intracellular expression of antibody fragments leads to incomplete formation of structurally important disulfide bonds. To determine the impact of incomplete disulfide bond formation on V_L expression and affinity for huntingtin, the cysteines of yeast surface-displayed V_L were mutated to valine and alanine (C22V, C89A)⁷⁶, to make mutant V_{L,C22V,C89A}. Yeast cell surface protein expression levels, which can be monitored by the presence of a C-terminal c-myc tag detected by immunofluorescence and flow

cytometry, have been shown to correlate strongly with protein stability^{38;39}.

Significantly, yeast cell surface expression levels of $V_{L, C22V, C89A}$ were comparable to those of V_L , suggesting that the absence of the disulfide bond did not significantly alter stability of the protein (Figure 6.1A). A negative peak can be seen just above a fluorescence value of 10^1 , due to cells that have lost the expression plasmid.

We then measured the affinity of the wild type V_L and mutant $V_{L, C22V, C89A}$ for a biotinylated peptide antigen consisting of the first 20 amino acids of htt, by titration of the yeast surface displayed intrabodies (Figure 6.1B, diamonds and circles, respectively). The mutant lacking a disulfide bond exhibited a binding affinity 2-3 orders of magnitude lower than the wild type intrabody (approximate affinities are $V_L \sim 30$ nM, $V_{L, C22V, C89A} > 10$ μ M), indicating the importance of disulfide bond formation in maintaining the structural integrity of the antigen binding site of the intrabody. Since disulfide bonds are not thermodynamically favored in the reducing environment of the cytoplasm, the intracellular affinity of V_L is expected to be on the order of that of the mutant lacking the disulfide bond.

Elimination of disulfide bond does not affect aggregation inhibition properties of intrabody in transiently transfected mammalian cell model of HD. To ensure that mutation of the cysteine residues that form the disulfide bond of the yeast surface displayed V_L mimics intracellular expression, we measured the effect of disulfide bond elimination on the ability of the intrabody to block htt aggregation when transiently transfected into mammalian cells at a high plasmid ratio relative to htt. ST14A cells were co-transfected with httex1Q₉₇-GFP (also in pcDNA3.1) and either an empty vector,

V_L , or $V_{L,C22V,C89A}$, at a 2:1 intrabody:htt plasmid ratio. Twenty-four hours post-transfection, cells with aggregates were counted. Both the wild type intrabody and the mutant lacking cysteines inhibited aggregation to the same extent (Figure 6.1C), when expressed at high levels. The equivalent aggregation inhibition of V_L and $V_{L,C22V,C89A}$, despite the almost 1,000-fold difference in affinities of the intrabodies under oxidizing extracellular expression conditions, strongly suggests that the disulfide bond in V_L does not form in the cytoplasm.

Intrabody lacking disulfide bond engineered for high affinity by directed evolution.

Since the intracellular affinity of the V_L was relatively low, we hypothesized that more potent aggregation inhibition could be achieved by engineering $V_{L,C22V,C89A}$ for higher affinity. Random mutagenesis of the $V_{L,C22V,C89A}$ gene was carried out using error-prone PCR. The resulting PCR fragments were transformed into yeast along with a yeast surface display vector to create a library through homologous recombination⁶². This library had a diversity of approximately 3×10^7 intrabody mutants displayed on the surface of yeast. Iterative rounds of FACS sorting were used to isolate new mutants with improved affinity. The process of mutagenesis and sorting resulted in an approximately 10-fold improvement in binding affinity. The improved mutants obtained were used as the template for the next round of library creation; the entire mutagenesis and sorting process was repeated three times. After the third round, one mutant designated $V_{L12.3}$ was identified with significantly improved affinity, (titration shown in Figure 6.1B; approximate $K_d \sim 5$ nM).

The improved mutant was sequenced and found to have gained 4 mutations (F37I, Y51D, K67R, A75T); continued absence of the cysteine residues was also confirmed. Three of the four mutations were in framework positions (residues in antibody variable domains that do not generally form contacts with antigens); only one was in a complementarity determining region (Y51D in CDR L2). The locations of the mutations are shown in a homology model (Figure 6.1D; homology model generated at Web Antibody Modeling (<http://antibody.bath.ac.uk/index.html>)).

Engineered intrabody V_L12.3 robustly blocks aggregation in transiently transfected mammalian cell models of HD. To determine whether V_L12.3 has improved huntingtin aggregation inhibition properties, various cell lines were transiently co-transfected with httex1Q₉₇-GFP and V_L12.3, and the formation of aggregates was monitored by fluorescence microscopy and western blotting. In some experiments, an intrabody that lacked specificity for huntingtin (ML3-9) and an empty control vector were tested as a negative controls, and previously reported C4¹⁷ and V_L²⁴ were included for comparison. First, experiments were performed using intrabody to htt plasmid ratios of 5:1. In previous work^{14; 17; 24}, such high levels of intrabody overexpression were required to accomplish moderate reduction of aggregate formation. V_L12.3 exhibited the ability to essentially ablate aggregation at these high levels of expression, as shown in Figure 6.2A (circles), for V_L12.3 in ST14A cells, compared to C4 (triangles) and empty vector (squares). Significantly, aggregation inhibition persisted over a period of several days.

Given the strong capability of V_L12.3 to reduce the formation of aggregates at high expression levels, we then studied the dose response of aggregate formation by

varying the ratio of intrabody to htt plasmid. As shown in Figure 6.2B, V_L12.3 blocked aggregation significantly even when expressed at very low levels (0.5:1 intrabody:htt plasmid ratio). The formation of aggregates was reduced by nearly 80% when the intrabody plasmid was present in a 1:1 ratio with htt plasmid, and greater than 90% when present at higher levels. Sample images with and without V_L12.3 are shown in Figure 2C.

Flow cytometry was used to determine whether expression levels of httex1Q₉₇-GFP were different in the presence of the intrabody; expression levels were comparable for samples with intrabody compared to empty vector (Fig. 6.2D). Therefore, the decrease in aggregation did not occur simply as a result of inhibiting httex1Q₉₇-GFP expression.

Additional characterization of the engineered intrabody in other cells lines is shown in Appendix 2: Results from the Messer lab.

Engineered V_L12.3 inhibits toxicity in neuronal cell culture model of HD. Energy metabolism impairment and mitochondrial dysfunction have been described in cellular models of HD as well as in HD patients^{77;78}. To see if the engineered V_L12.3 intrabody could reduce toxicity in mammalian cells in addition to blocking aggregation, the MTT (3-(4,5-dimethylthiazol-2-yl)-2,5-diphenyltetrazolium bromide) assay was used to measure the mitochondrial activity of transiently transfected ST14A cells⁷⁹. ST14A cells were transfected with either GFP, httex1Q₂₅-GFP, or httex1Q₉₇-GFP. Forty-eight hours post-transfection, live GFP positive cells were sorted by FACS. The ability of the cells to metabolize MTT during four additional hours of culture was measured. Compared to

cells expressing GFP or httex1Q₂₅-GFP, cells expressing httex1Q₉₇-GFP exhibit an attenuated ability to reduce MTT (Figure 6.3). Co-transfection with V_L12.3 at a 2:1 ratio resulted in completely restored ability to metabolize MTT, indicating normal levels of mitochondrial activity.

Viral delivery of VL12.3 inhibits htt aggregation in an established cell line

An established neuronal cell model of HD (Apostol BL, et al, Proc Natl Acad Sci U S A. 2003 May 13) was used to assess the function of the virus. Cells were treated with viral lysates (estimated MOI of 100), or were not treated (negative control). Twenty-four hours post-infection, expression of the huntingtinQ103-GFP transgene was induced using 500 nM mifepristone A (Invitrogen). After an additional twenty-four hours, the aggregation state of huntingtinQ103-GFP was observed using fluorescence microscopy.

Cells which had been exposed to the Ad-VL12.3 virus were significantly less likely to contain aggregates than cells which had not received treatment, as shown in Figure 6.4. Sample images of the cells are shown in Figure 6.5.

Engineered intrabody inhibits huntingtin aggregation in a yeast HD model

We then tested V_L12.3's ability to interfere with huntingtin aggregation in the same yeast HD model that was used in the experiments from chapter 2, in which the original antibodies were found to be ineffective. V_L12.3 was expressed cytoplasmically along with htt-x1-Q97-YFP, which forms aggregates in the yeast cytoplasm. Images were taken on a confocal microscope, and images were analyzed quantitatively to

objectively measure the fraction of cells with aggregates. The engineered intrabody very effectively blocked aggregation in this assay, as shown in Figure 6.7.

Discussion

We have developed a highly potent intracellular antibody against the N-terminal 20 amino acids of the huntingtin protein, htt, which is mutated in Huntington's Disease (HD) and forms intracellular aggregates in medium spiny neurons of the striatum. This new intracellular antibody, V_L12.3, efficiently prevents the aggregation and toxicity of htt-exon1 and may therefore be useful in treatment of HD by gene therapy. We removed the disulfide bond of the single-domain antibody, V_L(1), by site-directed mutagenesis in order to make its properties, such as stability and affinity, independent of the oxidation state of its environment. We next greatly improved the binding affinity of the antibody by mutagenesis and screening for improved binding. In comparison to previously described intrabodies against htt^{14; 17; 24}, this intrabody effectively prevented aggregation at 10-fold lower expression levels or plasmid ratios, and was able to reduce intracellular aggregation of mutant htt-exon1 protein almost completely. Given the relative inefficiency of viral gene delivery to the central nervous system, it is essential that in any proposed gene therapy, the therapeutic protein whose gene is delivered should work as efficiently as possible. For this reason, V_L12.3 may prove useful in treating HD through gene therapy, in addition to use as a research tool in further studies of the role of htt aggregation in HD pathogenesis.

In a cell-based assay, we explored the ability of VL12.3 to eliminate intracellular aggregates of mutant htt-exon1. Recently there has been some discussion of the role that

htt aggregates and aggregation might play in HD⁸⁰. We used the formation of large inclusions in the presence of overexpressed htt exon1 as a measure of intrabody potency, although smaller intermediates in the aggregation process may be responsible for toxicity, or other abnormal protein interactions involving misfolded htt exon1 may be involved. It is therefore noteworthy that when V_L12.3 was expressed along with httex1Q₉₇-GFP, greater than 90% of both aggregation and cell toxicity were prevented.

This study also illustrates the impact of disulfide bond formation (or lack thereof) in the cytoplasm on intracellular binding affinity in intrabody-antigen interactions. Conventional wisdom suggests that disulfide bonds do not form in the cytoplasm. However, disulfide bond formation has been observed following oxidative stress⁸¹, fueling debate within the intrabody research community about whether such bonds form in cytoplasmically expressed antibody fragments. We found a dramatic lowering of the *in vitro* affinity when the cysteines were replaced by the hydrophobic residues alanine and valine (Fig 6.1B). However, these mutations did not alter intracellular intrabody potency, as measured when the intrabody was present at a high plasmid ratio (Fig. 6.1C). This strongly implies that the disulfide bond does not form even when the cysteine residues are present in this case, given the dramatic effect of cysteine mutation on *in vitro* affinity. It is also interesting to note that mutation of the cysteine residues did not significantly alter antibody expression (on the yeast surface in this case, Fig 6.1A) in contrast to other published reports^{34; 72}.

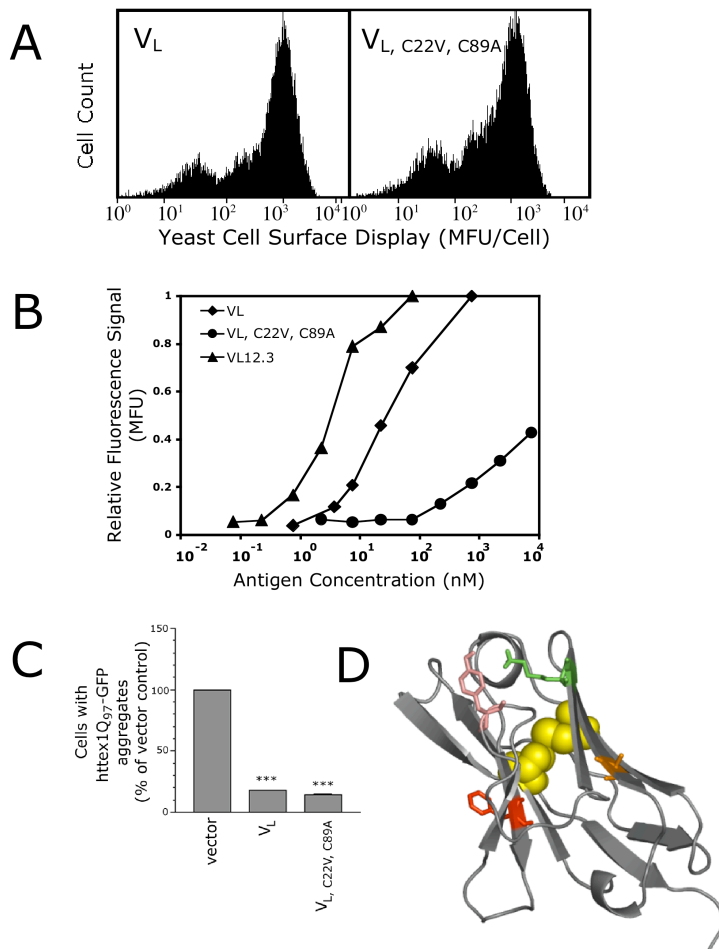


Figure 6.1.

A single domain intrabody against huntingtin was engineered for high affinity in the absence of a disulfide bond. **A.** Histograms of yeast cell surface expression levels for V_L and $V_{L,C22V,C89A}$, indicating comparable levels of expression with and without the disulfide bond. **B.** Antigen binding curves for yeast surface displayed V_L mutants measured by flow cytometry. Values normalized to maximal intensity measured, except for $V_{L,C22V,C89A}$, which was normalized to maximal intensity measured for V_L . V_L (diamonds) has a K_d of approximately 30 nM, while V_L with cysteine mutations ($V_{L,C22V,C89A}$, circles) has significantly lower binding affinity (>10 μ M). Repeated rounds of random mutagenesis of $V_{L,C22V,C89A}$ followed by sorting for improved binding resulted in the mutant $V_{L12.3}$, which has a K_d of approximately 3 nM. **C.** Effect of V_L and $V_{L,C22V,C89A}$ on htt aggregation in ST14A cells transiently transfected with indicated intrabody or vector control and httex1Q₉₇-GFP at a 2:1 plasmid ratio. Both intrabodies are equally capable of partially blocking aggregation when overexpressed at high levels. *** $p < 0.001$. **D.** Homology model showing mutations obtained during engineering; model contains residues present before mutagenesis. Cysteine residues are shown in yellow. Mutations observed after mutagenesis and sorting are F37I (red), Y51D (pink), K67R (green), A75T (orange). [Data in part C was generated by Colin Chu under my supervision.]

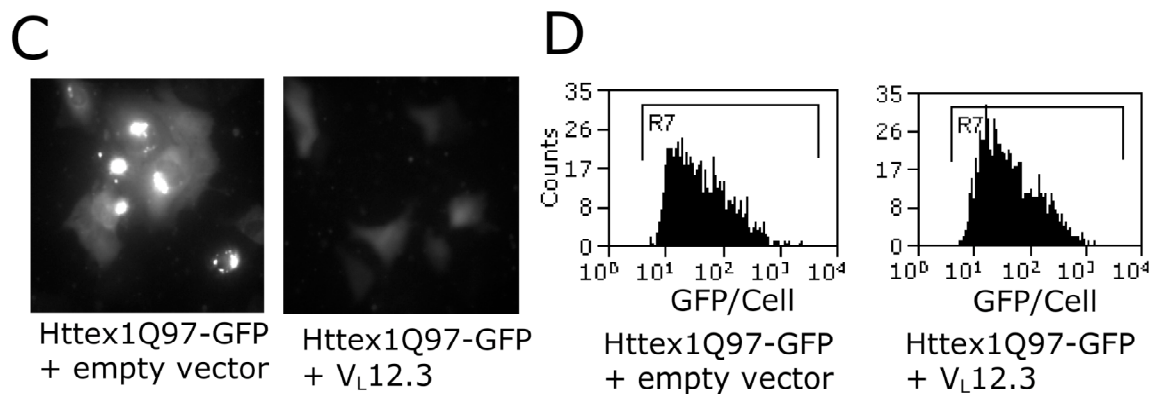


Figure 6.2.

Engineered V_L12.3 robustly blocks htt aggregation. A. ST14A cells were transiently co-transfected with httex1Q₉₇-GFP and either an intrabody (C4¹⁷ or V_L12.3) or an empty control vector, and cells with visible aggregates were counted 1, 2 and 3 days post-transfection (5:1 intrabody:htt plasmid ratio, N=3). V_L12.3 (circles) persistently eliminated htt aggregation over three days. B. Dose response of V_L12.3 was measured at two days by varying intrabody:htt plasmid ratios (N=3). C. Fluorescence microscopy images of typical cells. D. Flow cytometry histograms showing expression level per cell of httex1Q₉₇-GFP in transfected cells in the presence of intrabody compared to empty vector (mean fluorescence intensity 82 MFU vs. 76 MFU, respectively; transfection efficiencies were comparable in both samples, at 13% and 11%, respectively). [Data in A,B,D generated by Colin Chu under my supervision].

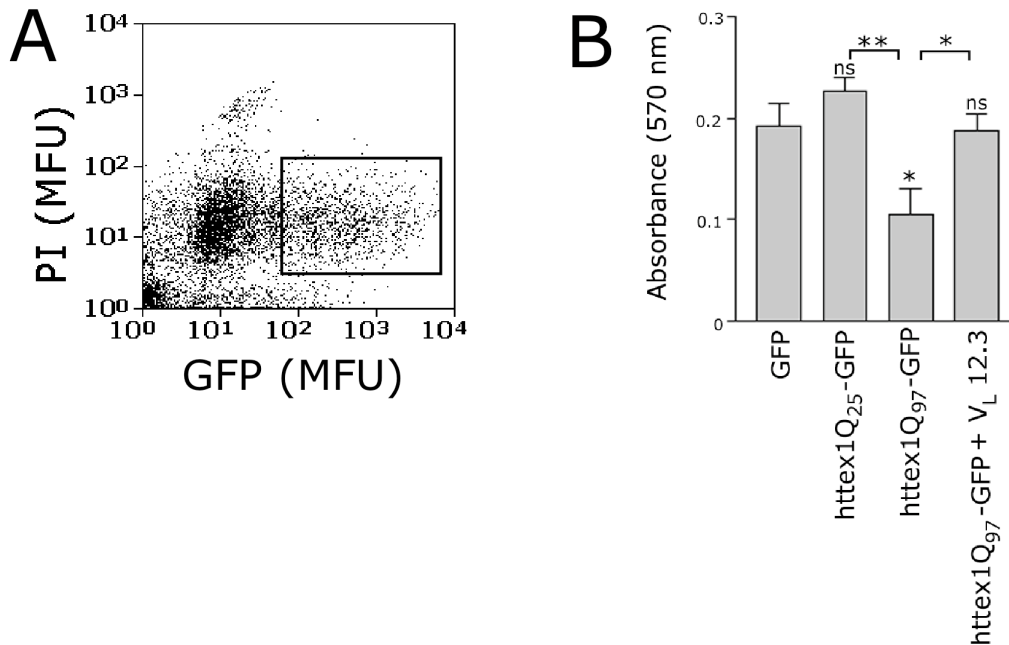


Figure 6.3.

Engineered intrabody $V_L12.3$ inhibits metabolic dysfunction in neuronal model of HD. ST14A cells were transfected with a plasmid encoding either GFP, httex1 Q_{25} -GFP, httex1 Q_{97} -GFP, or httex1 Q_{97} -GFP with $V_L12.3$ in a 2:1 ratio. A. Live GFP positive cells were collected by FACS in a 96-well plate, 35,000 cells per well 48 hrs post-transfection; typical dot plot is shown for a GFP sample. Other samples showed similar pattern, and the sorting gate (box shown) was the same in all instances. B. Cells were incubated with MTT reagent for 3 hours, solubilized, and the A570 was measured; mean values from 3 separate experiments containing all four samples are shown. Statistics directly over error bars are for comparison to GFP, ns, not significant, * $p < 0.05$, ** $p < 0.01$. Statistics over brackets are comparisons between the two samples indicated. Four additional pairwise comparisons may be made between httex1 Q_{97} -GFP and httex1 Q_{97} -GFP + $V_L12.3$; the pooled results indicate a 56 +/- 25% increase in A570, $p < 0.001$. Expression of httex1 Q_{97} -GFP significantly reduced the ability of cells to reduce MTT, but this effect was reversed by the co-expression of $V_L12.3$. [Data in this figure generated by John Cassady under my supervision.]

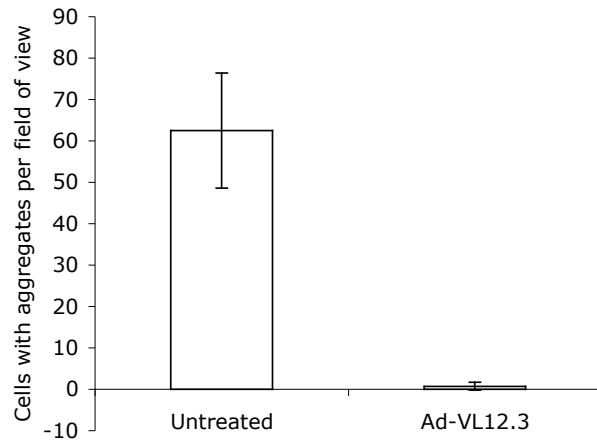


Figure 6.4. Adenovirus encoding VL12.3 (Ad-VL12.3) reduces huntingtinQ103-GFP aggregation in a neuronal cell culture model of HD. PC12 cells expressing httN17Q103-GFP on ecdysone promoter were treated with Ad-VL12.3 at time of induction with muristerone A (500 nM). Cells with aggregates were counted 24-hrs post-transfection.

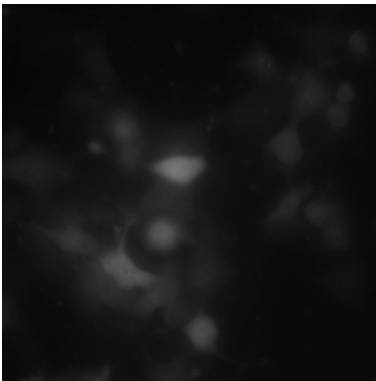
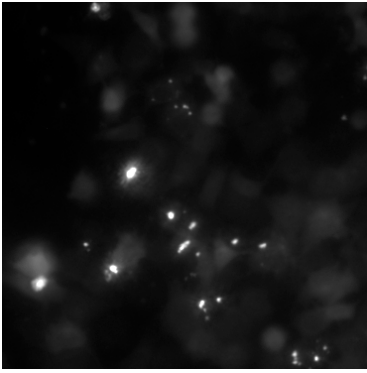


Figure 6.5.
Sample images of untreated cells expressing httN17Q103-GFP (top), and Ad-V_L12.3 treated cells expressing httN17Q103-GFP (bottom). Adenovirus encoding VL12.3 (Ad-VL12.3) reduces huntinginQ103-GFP aggregation in a neuronal cell culture model of HD. PC12 cells expressing httN17Q103-GFP on ecdysone promoter were treated with Ad-VL12.3 at time of induction with muristerone A (500 nM).

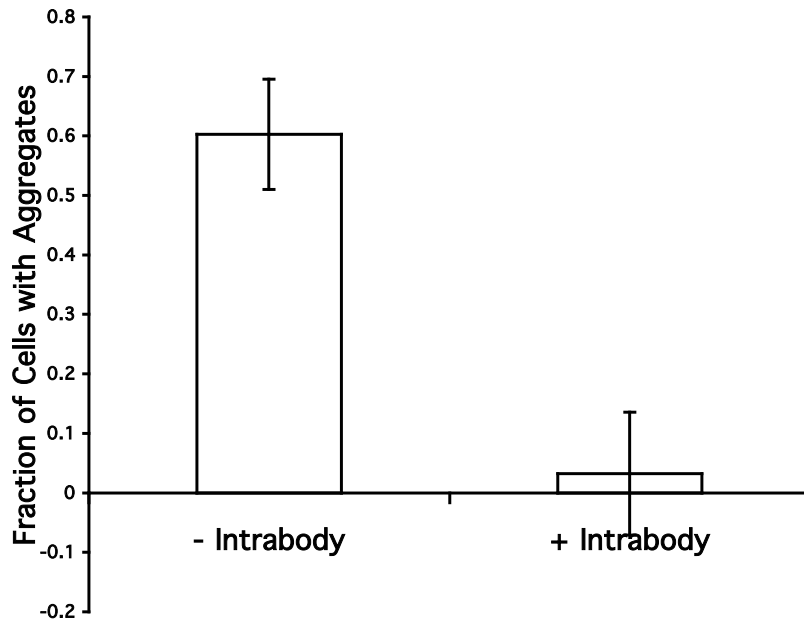


Figure 6.6. Aggregation inhibition resulting from co-expression of engineered intrabody with htx1Q97-YFP. Yeast cells expressing htx1Q97-YFP and either VL12.3 or empty vector (both transgenes under the control of a galactose promoter) were examined by confocal microscopy 18 hours post induction.

Chapter 7. Conclusions

We have developed a highly potent intracellular antibody against the N-terminal 20 amino acids of the huntingtin protein, htt, which is just upstream of the polyglutamine expansion that causes Huntington's Disease (HD). The protein forms intracellular aggregates in medium spiny neurons of the striatum in patients with the disease. This new intracellular antibody, V_L12.3, efficiently prevents the aggregation and toxicity of htt-exon1 and may therefore be useful in treatment of HD by gene therapy.

Intracellular antibodies are attracting interest as tools to manipulate and study biological systems intracellularly. However, robust, effective protocols for intrabody construction have not been definitively identified. In this work, we isolated human anti-htt scFv antibodies from a yeast surface display library (chapter 2). However, these antibodies were not effective at blocking htt aggregation in a yeast model of HD. We analyzed the problems which would lead to inactivity, identifying two parameters (antibody expression and binding affinity) that are key to the activity of intrabodies. We also developed a mathematical model of the aggregation phenomenon and used this to help estimate appropriate values for the expression levels and binding affinities required for potent inhibition of htt aggregation (chapter 3). Antibody affinity for htt was engineered to ~30 nM (chapter 4). The paratope was mapped to the VL domain of the intrabody, which was found to have superior intracellular expression relative to the full scFv; this intrabody fragment was partially effective at blocking htt aggregation in mammalian cell models of HD (chapter 5). However, the intrabody was still not fully effective at blocking htt aggregation. We surmised that the absence of disulfide bond formation in the cytoplasm may affect intrabody binding affinity, and demonstrated that

this was the case by knocking out the disulfide bonds of the intrabody expressed on the yeast surface. We then applied affinity maturation to improve the mutant lacking its disulfide bond (chapter 6). The final intrabody robustly blocked aggregation in transiently transfected mammalian cell models of HD and two yeast HD models. We also demonstrated that the intrabody inhibited htt aggregation in an established HD cell line when delivered by adenovirus.

Previous attempts at intrabody generation have either coupled phage display with screening in mammalian cells or the yeast two hybrid system, or relied exclusively on yeast two hybrid technology.^{17; 19; 21; 22; 29} Here we have demonstrated a novel approach to the isolation of functional intrabodies using engineering and analysis by YSD. Significantly, a functional intrabody was derived through molecular evolution and rational design (i.e. reduction to a single domain and mutating residues that form the disulfide bond) from an scFv which had no function in cell assays initially, and which consequently could not have been identified in an initial yeast two-hybrid screen. Given the importance of isolating functional intracellular antibodies, availability of multiple complementary strategies will raise the probability of success.

Several reports have brought into question the relevance of antibody affinity in predicting efficacy of intracellular antibodies^{52; 53}, suggesting that only expression levels are relevant. However, V_L is expressed at levels equivalent to or even above V_L12.3 (see Appendix 2), but is significantly less active. Therefore, affinity is clearly a key determinant in intrabody efficacy in the present case, consistent with the equilibrium relationship:

$$\frac{[Intrabody \cdot Antigen]}{[Antigen]} = \frac{[Intrabody]}{K_d} \quad (1)$$

where [Intrabody•Antigen] is the concentration of the bound complex. From this relationship, it is clear that high level intrabody overexpression can at least partially compensate for diminished intracellular affinity, as we demonstrate here for the wild-type V_L intrabody and $V_{L,C22V,C89A}$. For a micromolar-affinity intrabody, however, micromolar expression levels are necessary even when antigen concentration is much lower than micromolar, as it is likely to be in striatal neurons *in vivo*. $V_L12.3$, with 3 nM affinity, should be effective at nanomolar level concentrations. In earlier reports, the role of affinity was obscured by measuring antibody affinity in oxidizing (extracellular) environments, where disulfide bonds will form, for comparison to intracellular assays for activity, in which disulfide bonds are unlikely to form. By mutating the cysteines of V_L so that no disulfide bond will form, we assessed the protein's properties under oxidizing, extracellular conditions while maintaining the structurally relevant cytoplasmic form. Subsequent affinity maturation of the disulfide bond-free mutant allowed the conferment of improved properties to the intracellular environment.

Although we have made a significant step toward the treatment of HD by gene therapy, many challenges must be overcome before gene therapy can be used in practice. Viral delivery of genes to the CNS is limited both by the immune response to the viral delivery vehicles, which decreases the infectivity of the virus, and by the limited diffusion of viral particles from injection sites in the brain. In general, the safety of gene therapy with regards to subsequent development of cancer and immune responses which can be harmful to treated tissue must also be dealt with.

Will the $V_L12.3$ intrabody also bind to wild-type htt in HD heterozygote, and will that alter wild-type function? Unfortunately this cannot be determined presently because

the function or functions of wt-htt are still being investigated and are not conclusively known at present. However, co-transfection of V_L12.3 with httex1Q97-GFP did not decrease httex1Q97-GFP expression levels, so the intrabody should not affect the stability and turn over of htt. Further, the intrabody did not cause cell death or apoptosis when expressed in mammalian cells.

Single-domain intrabodies without disulfide bonds, such as V_L12.3, are a minimal and versatile unit for antigen recognition. Single-domain antibodies²⁷ and structurally analogous domains⁸² are increasingly being exploited as alternatives to single chain antibodies for molecular recognition. The approach demonstrated here may find application in engineering existing intrabodies for increased potency against other disease targets, including Parkinson's⁸³ and Alzheimer's diseases, HIV, and cancer.

Appendix 1: Methods for Affinity Maturation by Yeast Surface Display

The following methods for affinity maturation using yeast surface display were developed and described by myself and coworkers; I collected and rewrote the methods for publication.³³

The original YSD protocols were described earlier,⁴⁹ but new and refined methods have been developed, in particular improved vectors, mutagenesis methods, and efficient ligation-free yeast transformation procedures. Here, we provide up to date protocols for engineering single chain antibodies by YSD.

This appendix contains methods for creating mutant libraries and sorting libraries for improved clones. The constructs and strains required for yeast surface display are described in the introduction to this thesis. The first section contains the method for creating large mutant libraries using homologous recombination, including the precise conditions used for error prone PCR using nucleotide analogues. We have also included protocols for labeling yeast with fluorophores and sorting by FACS for improved affinity.

Generating Large Mutant Antibody Libraries in Yeast

The most efficient way to make a mutant library in yeast is to use homologous recombination, thereby eliminating the need for ligation and *E.coli* transformation.⁸⁴ In brief, cut plasmid and an insert containing the mutated gene are prepared separately, with

significant homology (30-50 bp or more) shared by the insert and plasmid at each end. These DNA fragments are then taken up by yeast during electroporation, and re-assembled *in vivo*. Libraries prepared by this method typically include at least 10^7 transformants, and are often over 10^8 in diversity, which approximates the amount that can be sorted by state of the art cell sorters in an hour.

In the following section we describe how to prepare scFv insert DNA with random point mutations by error prone PCR with nucleotide analogues. However, this may be replaced with DNA shuffling with slight modification using one of many published protocols.^{85; 86; 87}

Preparation of Insert: Error Prone PCR using Nucleotide Analogues

Nucleotide analog mutagenesis allows the frequency of mutation to be tuned based on the number of PCR cycles and the relative concentration of the mutagenic analogues.^{88; 89} The two analogues, 8-oxo-2'-deoxyguanosine-5'-triphosphate and 2'-deoxy-p-nucleoside-5'-triphosphate (8-oxo-dGTP and dPTP respectively, TriLink Biotech), create both transition and transversion mutations. In order to ensure that some fraction of the library created is sufficiently mutated to generate improvements, but not so highly mutated as to completely ablate binding, a range of several different mutagenesis levels are used in parallel. The conditions reported here are the ones we typically use to create antibody libraries; these conditions give an error rate ranging from 0.2%-5%.

If the gene to be mutated is already in pCTCON, then the following primers may be used to carry out the mutagenesis and subsequent amplification. These primers are

designed to have >50 bp of homology to pCTCON for use during homologous recombination.

Forward primer: cgacgattgaaggtagataccatacgcaggtccagactacgctctgcag

Reverse primer: cagatctcgagctattacaagtcttcttcagaaataagctttgttc

1. Set up six 50 μ l PCR reactions

	<u>Final Concentration</u>
10X PCR Buffer (without MgCl ₂)	
MgCl ₂	2 mM
Forward Primer	0.5 μ M
Reverse Primer	0.5 μ M
dNTP's	200 μ M
Template	0.1-1 ng
8-oxo-dGTP	2-200 μ M
dPTP	2-200 μ M
dH ₂ O	to final volume
Taq polymerase	2.5 units

Of the six PCR reactions, two should contain 200 μ M nucleotide analogues, two should contain 20 μ M nucleotide analogues, and two should contain 2 μ M nucleotide analogues.

2. Run the PCR for the number of cycles specified below. The cycles should have the following incubation temperatures and times: denature at 94 °C for 45 sec, anneal at 55 °C for 30 sec, extend at 72 °C for 1 min. One should also include a 3 min

denaturation step at 94 °C before the cycles begin and a 10 min extension step after the cycles are completed (the 10 min extension may be done on a heating block to run all reactions simultaneously).

<u>Nucleotide Analogue Concentration</u>	<u>Number of PCR cycles</u>
200 µM	5
200 µM	10
20 µM	10
20 µM	20
2 µM	10
2 µM	20

3. Run the entire mutagenic PCR products out on a 1% low melt agarose gel. PCR products cycled 20 times are easily visible on a gel stained with SYBR Gold (Molecular Probes). Reactions cycled 10 times or less may not be visible on the gel; however, it is important to gel purify anyway to remove the non-mutated template before amplification (next step). Cut out and purify using Qiagen gel purification kit following manufacturer's protocol.

4. Amplify each reaction in the absence of nucleotide analogues to generate sufficient insert DNA for the transformation. Three 100 µl reactions should be set up for each mutagenic reaction, and 1 µl or more of the gel purified product should be used as

template in the new reaction. Do not add nucleotide analogues. Cycle 25-30 times as you would for a normal PCR.

5. Optional. Gel purify the PCR products from step 4. Purification will eliminate many PCR artifacts from the library, but may also result in significant loss of PCR product.

6. Concentrate the PCR products using Pellet Paint (Novagen). After pellet has dried, dissolve in water to a final concentration of 5 $\mu\text{g}/\mu\text{l}$. This protocol typically produces 40-100 μg of PCR product.

Preparation of Vector

1. Miniprep 10 μg or more of pCTCON.
2. Digest with NheI (New England Biolabs) for at least two hours in NEB2 buffer.
3. Adjust salt concentration by adding one-tenth of the total volume of 1 M NaCl.
4. Double digest with BamHI and Sall for two additional hours, to ensure complete digestion of pCTCON and reduce reclosure of the acceptor vector. (Note that the plasmid is cut in three places to ensure that the vector will not transform yeast cells in the absence of insert.)

5. Use Qiagen nucleotide removal kit to purify DNA from enzymes, keeping in mind that a single column saturates with 10 μg DNA.

6. Concentrate DNA using Paint Pellet reagent. After drying pellet, dissolve in water to 2 $\mu\text{g}/\mu\text{l}$.

Preparation of Electrocompetent Yeast Cells

This protocol has been adapted from E. Meilhoc et. al.,⁸⁴ and generates enough cells for transformation of ~60 µg of insert DNA and ~6 µg of vector, which typically produces ~5 x 10⁷ yeast transformants.

1. Inoculate 100 mL of YPD to OD₆₀₀ 0.1 from a fresh overnight culture of EBY100 (or appropriate yeast strain).
2. Grow cells with vigorous shaking at 30°C to an OD₆₀₀ of 1.3 - 1.5 (about 6 hours).
3. Add 1 mL filter sterilized 1,4-dithiothreitol (DTT, Mallinckrodt) solution (1 M tris, pH 8.0, 2.5 M DTT). DTT is unstable and the solution must be made fresh just before use. Continue to grow with shaking at 30°C for 20 min.
4. Harvest cells at 3500 rpm, 5 min, 4°C. Discard supernatant. All centrifugation steps should be carried out in autoclaved centrifuge tubes or sterile Falcon tubes.
5. Wash with 25 mL of E buffer (10 mM tris, pH 7.5, 270 mM sucrose, 1 mM MgCl₂) at room temperature. Spin down again.
6. Transfer to two 1.5 mL microcentrifuge tubes and wash a second time with 1 mL of E buffer each. Spin down.
7. Resuspend both pellets in E buffer to a final combined volume of 300 µl. Any extra cells that will not be used immediately may be frozen down in 50 µl aliquots for future use. Note that using frozen cells results in a 3-10-fold loss in transformation efficiency.

Transformation of competent yeast cells using electroporation

Electroporation is carried out using a Biorad Gene Pulser device.

1. In a microcentrifuge tube, mix 0.5 μ L vector (1 μ g), 4.5 μ L insert (9 μ g), and 50 μ L electrocompetent yeast cells. Add the mixture to a sterile 0.2 cm electroporation cuvette (Biorad). Incubate on ice 5 min. Prepare additional cuvettes until all of the DNA is used.
2. Set Gene pulser settings to 25 μ F (capacitance) and 0.54 kV (voltage), which gives an electric field strength of 2.7 kV/cm with 0.2 cm cuvettes; time constant should be about 18 ms with 55 μ L volumes. The pulse controller accessory is not used.
3. Carry out pulsing at room temperature. Insert cuvette into slide chamber. Push both red buttons simultaneously until pulsing tone is heard, then release.
4. After pulsing, immediately add 1 mL of room temperature YPD media⁸ to the cuvette. Incubate at 30 °C for 1 hour in 15 mL round bottom falcon tubes with shaking (250 rpm).
5. Spin down cells at 3500 rpm in a microcentrifuge. Resuspend in selective media (SD+CAA, ⁸ 50 mL/electroporation reaction). Plate out serial 10-fold dilutions to determine transformation efficiency. The library may be propagated directly in liquid culture without significant bias, due to repression of scFv expression in glucose-containing medium such as SD+CAA.³²

Transformation efficiency should be at least $10^5/\mu\text{g}$, but is typically around $10^6/\mu\text{g}$. In addition to the electroporation mixture described here, one should perform a control where no insert is added and determine the transformation efficiency. This is the background efficiency and should be less than $\sim 1\%$ of that obtained in the presence of insert DNA.

Labeling yeast cells for flow cytometry or FACS.

Labeling yeast that are displaying an antibody or antibody library with a fluorescent or biotinylated antigen allows quantification of binding affinity and enables library sorting by FACS. Typically a second fluorophore conjugated to an antibody is used to detect the epitope tag C-terminal to the scFv, which allows for normalization of expression and eliminates non-displaying yeast from quantification. A short protocol follows for labeling with a biotinylated antigen and the 9E10 monoclonal antibody against the C-terminal epitope tag c-myc. This protocol is for analytical labeling; for labeling large libraries, adjust volumes as describe at the end of the protocol.

1. Grow transformed yeast overnight in SD+CAA. OD_{600} should be greater than one.

As a general approximation, $\text{OD}_{600} = 1$ represents 10^7 cells/mL.

2. Inoculate a 5 mL culture of SG+CAA⁸ (inducing media) with the overnight culture. The final OD_{600} of the new culture should be ~ 1 .

3. Induce at 20 °C with shaking (250 rpm) for at least 18 hrs. Appropriate induction temperature should be tested for each scFv, from 20, 25, 30, or 37 °C.

4. Collect 0.2 OD₆₀₀-mL of induced yeast in a 1.5 mL microcentrifuge tube. Several such aliquots may be necessary to sample the full diversity of the library, since this aliquot will correspond to approximately 2×10^6 cells.
5. Spin down in table top centrifuge for 30 sec at max speed. Discard supernatant.
6. Rinse with PBS/BSA (phosphate buffered saline plus 0.1% BSA). Centrifuge for 10 sec, discard supernatant.
7. Incubate with primary reagents. Add desired concentration of biotinylated antigen and 1 μ L 9e10 (1:100, Covance) to a final volume of 100 μ L in PBS/BSA. Incubate at desired temperature for 30 min. Larger volumes and longer incubation times are required for very low (<10 nM) antigen concentrations (see notes at end of protocol).
8. Centrifuge, discard supernatant, and rinse with ice cold PBS/BSA. Centrifuge, discard supernatant from rinse.
9. On ice, incubate with secondary reagents. Add 97 μ l ice cold PBS/BSA, 2 μ l goat anti-mouse FITC conjugate (1:50, Sigma), and 1 μ l streptavidin phycoerythrin conjugate (1:100, Molecular Probes). Incubate 30 min.
10. Centrifuge, discard supernatant, and rinse with ice cold PBS/BSA. Centrifuge, discard supernatant from rinse.
11. Resuspend cells in 500 μ l ice cold PBS/BSA and transfer to tubes for flow cytometry or FACS sorting.

An important consideration when labeling high affinity antibodies (<30 nM) is depletion of antigen from the labeling mixture. This results in a lower than expected concentration of soluble (free) antigen, and hence a lower signal. Sorting libraries under

depletion conditions can reduce the difference in signal observed for improved clones compared to their wild-type counterparts. The equivalent concentration of yeast surface-displayed proteins when 0.2 OD₆₀₀-mL of yeast is added to a 100 µl volume is approximately 3 nM or less. To avoid depletion, always use at least a 10-fold excess of antigen by adjusting the total volume and/or reducing the number of yeast added (as little as 0.05 OD₆₀₀-mL can be used).

Note that for labeling large libraries, it is advisable not to scale up directly. Instead use 1 mL volume per 10⁸ cells labeled, keeping the reagent dilutions constant. Depletion can be especially severe with such high cell densities, however, and the experiment must be designed to avoid such conditions.

Analyzing Clones and Libraries by Flow Cytometry

Once a yeast population is labeled, it can be analyzed by flow cytometry. This allows quantification of binding affinity by titrating antigen concentration. In addition to the samples that one wishes to analyze, a negative control (no fluorophores) and two single positive controls (just one fluorophore in each) should be prepared. With standard filters installed, FITC will be detected in the FL1 channel, while PE will be detected by FL2 for the settings on most flow cytometers. However, some “bleed over” or spectral overlap will be present in each channel, which must be compensated out. One should use the negative control to set the voltage and gain on each of the detectors so that the negative population has order of magnitude intensity of one to ten. The single positive controls are used to adjust compensation so that no FITC signal is detected in FL2 and no PE signal in FL1.

In a titration, one generally sets a gate on cells that express the antibody (i.e. FITC positive cells if the preceding labeling protocol is used) to eliminate non-expressing cells from quantification.

For sorting or analyzing a library, it is helpful to also prepare a labeled sample of the wild-type antibody and saturated library for comparison and to aid in drawing sort windows.

Sorting Yeast Surface Display Libraries by FACS

FACS is the most efficient and accurate way to sort yeast surface display libraries, although magnetic particle strategies have also been employed.⁴² To sort a library by FACS, one labels cells according to the protocol above, taking into consideration the notes that follow the protocol. Equations describing the optimum labeling concentration for a first library sort are available,⁴⁹ or one can simply choose a concentration that results in a weak signal (say, one fourth of the K_d value). One should typically screen 10-100 times the number of independent clones that are in the library. When drawing a gate for collecting cells, it is advisable to use a window with a diagonal edge to normalize for expression, if a double positive diagonal is present (Fig. A1.1). If no diagonal is observed (little or no binding), the entire double positive quadrant should be collected. Cells should be sorted directly into SD+CAA with antibiotics such as penicillin and streptomycin to diminish the risk of bacterial contamination. Cells will grow to saturation in one (if $>10^5$ cells are collected) or two ($<10^5$) days.

The very first time a library is sorted, gates are drawn conservatively (0.5% to 1% of the library is collected) to minimize the likelihood that an improved clone is missed.

After the first sort, care should be taken to note the number of cells collected, as this is the maximum number of independent clones remaining in the library. In subsequent sorts, when the library size has been reduced and the amount of sorting time necessary decreases, one should bring several samples labeled under different conditions for sorting. These samples should be sorted at increasing stringency to rapidly isolate the best clones. Sort gates should cover the range of 0.01% of cells collected to 0.5%. All samples should be analyzed and the one with the greatest improvement should be chosen for further sorting. Typically the single best clone, or clones containing a consensus mutation, are isolated within 4 sorts.

The cells collected in the final sort are plated out for clonal analysis. The mutant plasmids may be recovered from yeast using the Zymoprep kit (Zymo Research). The following primers may be used for sequencing:

Forward Sequencing Primer: gttccagactacgctctgcagg

Reverse Sequencing Primer: gattttgtacatctacactgttg

Summary

The protocols and methods described here enable engineering of scFv's by yeast surface display. Each protocol is up to date, and has been verified and optimized through several years of application. The directed evolution process is often applied iteratively until the desired affinity is achieved. A single round of mutagenesis and screening typically results in 10- to 100-fold improvement in the K_d value, with largest improvements obtained when the wild-type affinity is low (say, low micromolar binding

constant). A complete cycle of mutagenesis and screening, from wild-type clone to improved mutant clone, requires conservatively approximately 3-6 weeks.

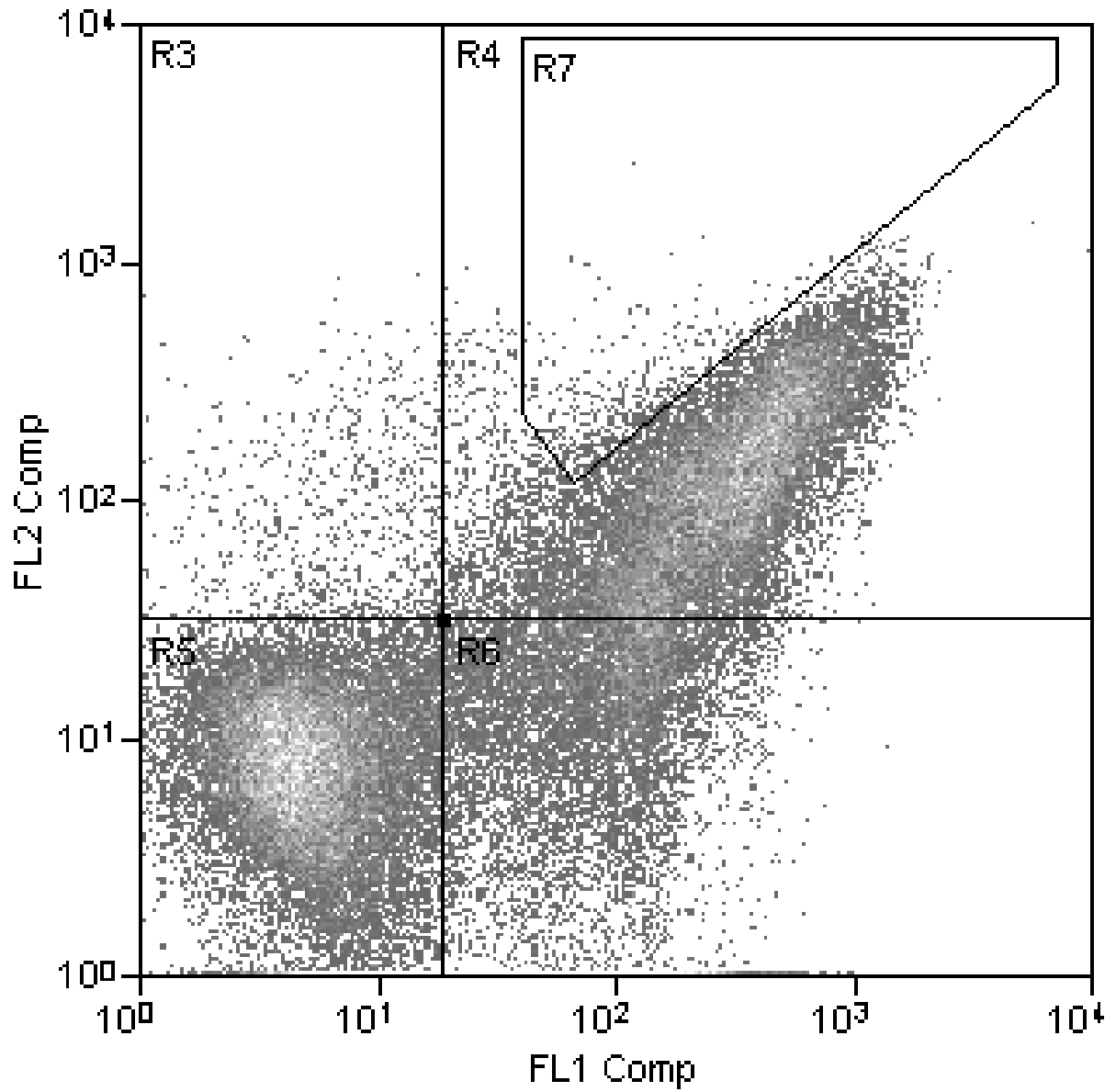


Figure A1.1.
Sort gate. If a diagonal population is present in the library, a sort gate such as the one labeled R7 should be drawn to take full advantage of expression normalization.

Appendix 2: Results from the Messer lab

The work in this section was performed by Jack Webster under the supervision of Anne Messer at the Wadsworth Institute in Albany, NY.

Materials and Methods

Mammalian cell aggregation inhibition assay

HEK293, and SH-SY5Y cells were cultured according to standard protocols. Cells were cotransfected, using Fugene 6 reagent(Roche), with httex1-Q₉₇-GFP and an intrabody at a plasmid ratio of 1:5, respectively. Cells were plated in 12 well dishes with 2×10^5 cells per well the day before the transfection. Transfections were carried out with 3 μ l of Fugene and 1 μ g of total DNA per well. Transfection efficiencies were consistent for all samples within each experiment. Aggregates were visualized by fluorescence microscopy and the number of cells with aggregates per well were counted approximately 24 hours after transfection. Data were normalized to the number of aggregates in empty vector co-transfections (pcDNA3.1).

Cell lysis, preparation of Triton soluble lysates and immunoblots were carried out as described⁹⁰. Triton insoluble fractions were prepared by resuspending the Triton X-100 insoluble pellet in water, followed by sonication and centrifugation at 16,000 g for 10 min.; the final pellet was resuspended in SDS gel loading buffer before processing in immunoblots with a monoclonal anti-htt recognizing the first 17 amino acids of the htt protein (m445).

Intracellular expression levels of intrabodies were measured by anti-His (antibody from Santa Cruz Biotechnology) western blot.

Results

Single domain intrabody efficiently blocks huntingtin aggregation in mammalian cells

We tested the ability of the single domain antibody to block htt aggregation when transiently co-expressed with httex1-Q₉₇-GFP in HEK293 cells. Vectors were derived from pcDNA3.1 with a CMV promoter driving expression of either httex1-Q₉₇-GFP or V_L. As negative controls, an empty pcDNA3.1 vector or a vector expressing the ML3-9 scFv recognizing an irrelevant antigen¹ (ErbB2) was used. As a positive control, the anti-htt C4 scFv was tested along with the V_L intrabody, since C4 has previously been shown to reduce httex1-GFP aggregate formation in cellular models of HD.¹⁷ HEK 293 cells were transiently co-transfected with httex1-Q₉₇-GFP and the appropriate intrabody expression vector or empty vector. Twenty-four hours post-transfection, cells with aggregates were counted by fluorescence microscopy. The results are shown in Figure A2.1. The V_L intrabody was at least as effective as the C4 scFv at blocking htt aggregation, demonstrating that single variable light chain domain intrabodies can function intracellularly.

Efficacy of V_L12.3 was characterized and compared to two previously described intrabodies (C4 and V_L) in other cell lines, both by fluorescence microscopy and western blotting analysis. In SH-SY5Y human neuroblastoma cells at a 1:1 intrabody:htt ratio only V_L12.3, and not earlier intrabodies, effectively reduced aggregation (Fig. A2.2E). Aggregation inhibition properties of V_L12.3 in HEK293 cells (Fig. A2.2F) were comparable to those observed in ST14A and SH-SY5Y cells. Partial dose response

curves are shown for each intrabody. Especially noteworthy is the ability of V_L12.3 to inhibit aggregation when used at a plasmid ratio (1:1 intrabody to htt) which was completely ineffective with previously reported intrabodies.

While microscopy confirmed that fewer cells contain visible aggregates when cotransfected with V_L12.3, we also sought to confirm a reduction in total aggregated htt protein. Western blotting analysis of Triton-soluble and Triton-insoluble htt fractions was performed on cell lysates obtained from HEK293 cells (Fig. A2.2G), transiently transfected using a 2:1 ratio of intrabody:htt plasmid. Significantly reduced levels of aggregated material were detected in the Triton-insoluble fractions for cells cotransfected with V_L12.3 and httex1Q₉₇-GFP, while co-transfection of httex1Q₉₇-GFP with any of the other intrabodies resulted in amounts of aggregated material comparable to negative control. Coexpression of intrabodies did not decrease the amount of material in the Triton-soluble fraction.

V_L was expressed at levels equivalent to or slightly higher than V_L12.3, as measured by anti-His₆ western blot (Fig. A2.2H).

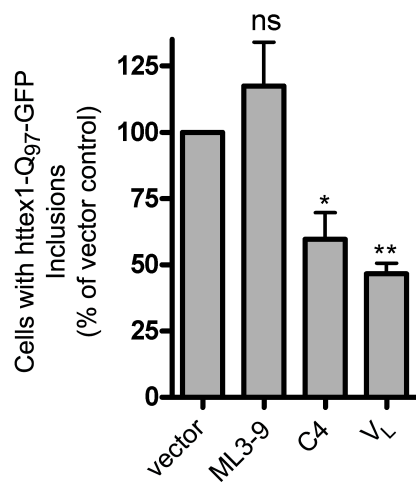


Figure. A2.1.

VL blocks intracellular aggregation of httex1-Q97-GFP in transiently transfected HEK 293 cells. Cells with aggregates were counted by fluorescence microscopy 24 hrs post-transfection and normalized to a negative control. ML3-9 is an intrabody not specific for huntingtin, C4 is a previously reported¹⁷ scFv against the first 17 amino acids of huntingtin, VL is the single domain intrabody described in the current work. Ns, not significant, * $p < 0.05$, ** $p < 0.01$, $N \geq 3$.

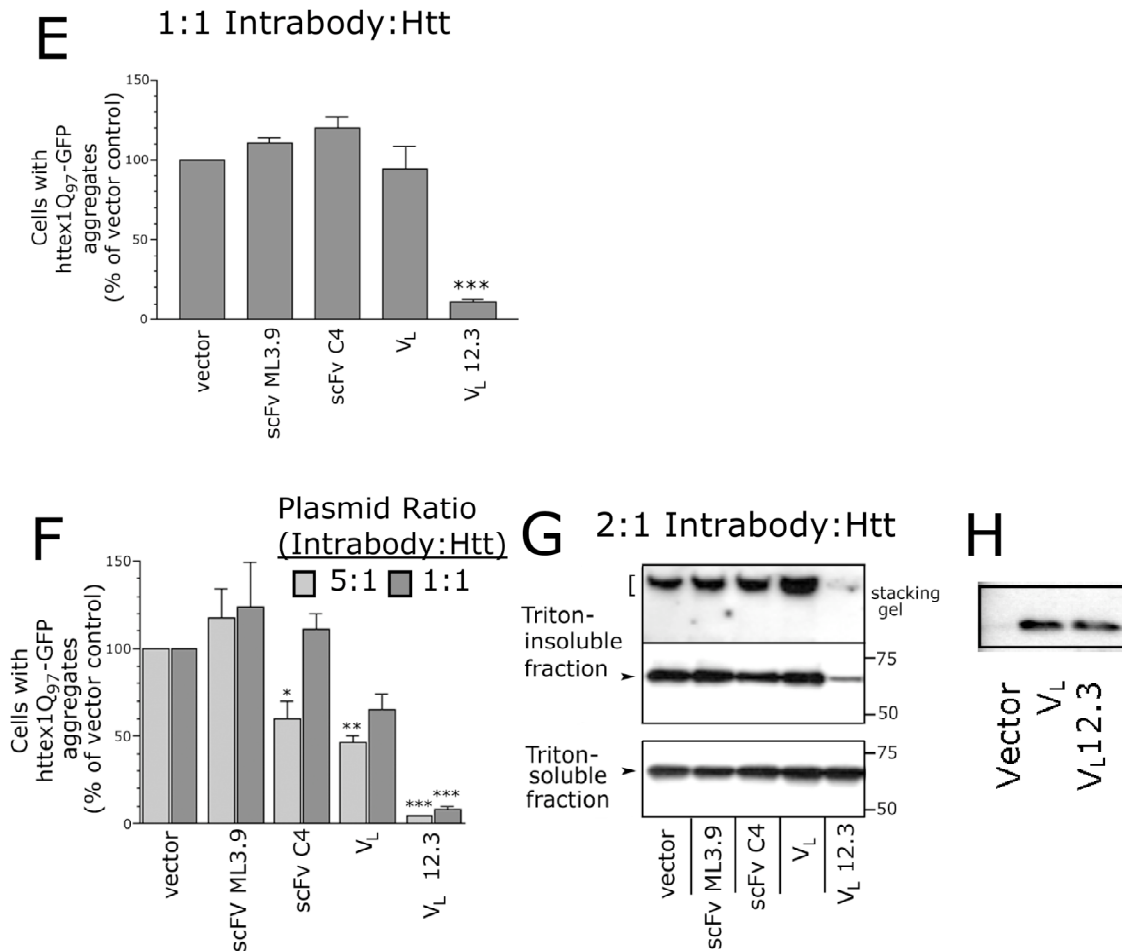


Figure A2.2.

Engineered V_L12.3 robustly blocks htt aggregation. Cells were transiently co-transfected with httex1Q₉₇-GFP and either an intrabody (C4¹⁷ or V_L12.3) or an empty control vector, and cells with visible aggregates were counted. E. Comparison of intrabody activity for the intrabodies mentioned above and a non-huntingtin binding intrabody (scFv ML3.9) and wild-type V_L, at 1:1 intrabody:htt plasmid ratio (***, p<0.001) in SH-SY5Y human neuroblastoma cells. F. Partial dose response for the same intrabodies in HEK293 cells. G. Western blot of Triton-soluble and Triton-insoluble fractions of cells lysed 24 hours after cotransfection at a 2:1 intrabody:htt ratio. H. Anti-His₆ western blot of intrabody expression levels in transiently transfected HEK293 cells.

Appendix 3: Results from the Lindquist lab

The work in this section was performed by Martin Duenwald and Helen Zazulak under the supervision of Prof. Susan Lindquist at the Whitehead Institute for Biomedical Research in Cambridge, Massachusetts.

Materials and Methods

Yeast cell culture, aggregation, and toxicity. Yeast media was prepared based on standard protocols⁹¹ using complete supplemental mixtures (BIO101). Transformation of yeast was performed as described previously⁹². Yeast integrating plasmids containing galactose inducible promoters (pRS303 backbone⁹³) for the expression of huntingtin exon-fragments were linearized by digestion with BstXI prior to transformation. V_L12.3-YFP was subcloned into p414 (ATCC), which also contains a galactose inducible promoter. Filter retardation assays of aggregated material were done essentially as described previously⁹⁴. For the induction of expression of the huntingtin fragment in yeast, cultures were grown at 30°C in raffinose-containing liquid media and transferred to galactose-containing media. In order to measure growth, yeast cells were diluted to a final OD_{600nm} of 0.05 and transferred to a microtiter plate. Yeast cultures were grown at 30°C with intermittent, intensive shaking on the Bioscreen C (Growth Curves USA) for 48 hrs with OD measurements taken every 2 hours. Western blot analysis of V_L12.3-YFP and httex1Q₇₂-CFP with anti-GFP antibodies indicated that the intrabody was present at lower protein concentrations than the htt exon I fragment (data not shown).

Results

Engineered V_L12.3 blocks aggregation and cytotoxicity in a yeast model of HD. *S. Cerevisiae* is likely the simplest *in vivo* model of HD, exhibiting both huntingtin aggregation and cytotoxicity^{50;95}. To determine whether the engineered intrabody could prevent these HD phenotypes in yeast, *S. cerevisiae* strains expressing both a huntingtin exon I protein (with either Q₂₅ or Q₇₂) fused to cyan fluorescent protein (httex1Q₂₅-CFP and httex1Q₇₂-CFP) and a V_L12.3-yellow fluorescent protein fusion (V_L12.3-YFP) on galactose-inducible promoters were made. Negative control strains were also constructed with an empty vector in place of V_L12.3-YFP.

The aggregation state of huntingtin in the presence and absence of V_L12.3-YFP was measured eight hours post-induction by a filter retardation assay. This assay consists of lysing cells and passing the lysate through a filter with 0.2 μm pores, trapping aggregates. The amount of aggregated httex1Q₇₂-CFP is then visualized by CFP fluorescence. As shown in Figure A3.1A, cells expressing the intrabody had much less aggregated httex1Q₇₂-CFP. This result was confirmed by fluorescence microscopy; expression of V_L12.3-YFP resulted in significantly reduced aggregation when measured by this method as well (data not shown).

Finally, we tested the ability of the intrabody to inhibit HD related cytotoxicity in yeast. *S. cerevisiae* expressing huntingtin with long polyglutamine tracts have been shown to grow slower than those expressing huntingtin with shorter polyglutamine tracts⁹⁵.

Growth assays were performed on the cell lines mentioned above. The cell line expressing both V_L12.3-YFP and httex1Q₇₂-CFP grew at a significantly faster rate than that which expressed the empty vector and httex1Q₇₂-CFP, as demonstrated by a spotting

assay in which the cells were plated on solid media (Figure A3.1B). Growth curves were also collected by measuring the optical density (OD) of cultures at 600 nM as a function of time (Figure A3.1C). The inhibition of aggregation and toxicity observed in the yeast system upon expression of V_L12.3 suggests that a conserved mechanism for htt toxicity is conserved in mammalian and yeast HD models. This confirms the value of *S. cerevisiae* models in screening and testing potential therapeutic molecules.

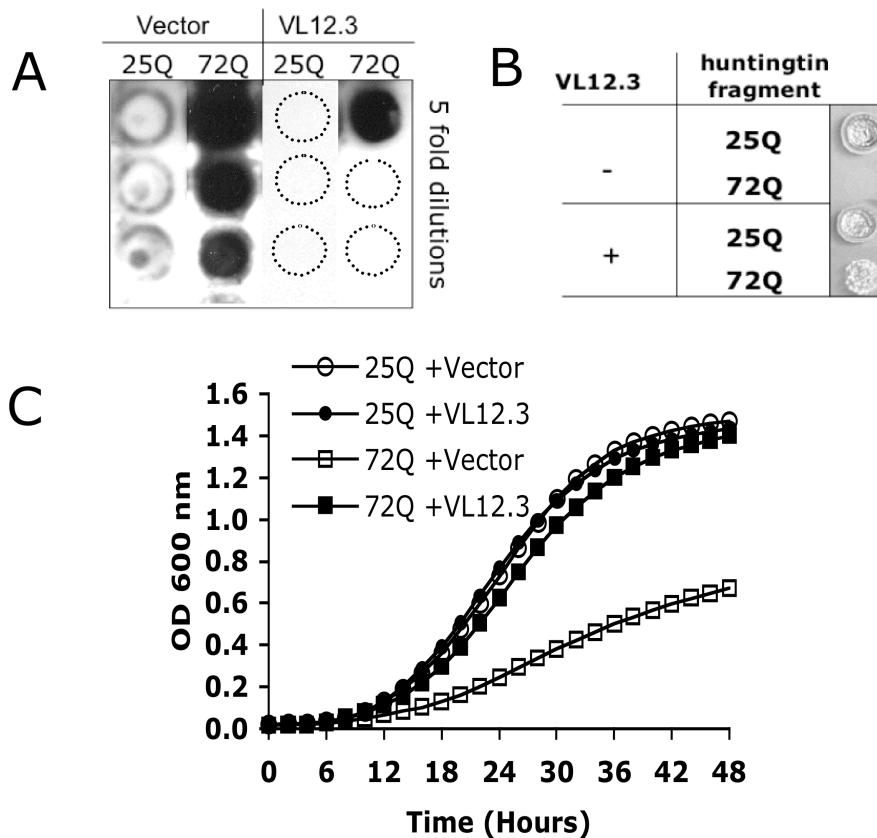


Figure A3.1.

V_L12.3 suppresses aggregation and rescues toxicity in a *S. cerevisiae* model of HD. A. Filter retardation assay showing httex1Q₇₂-CFP aggregates (dark) from lysates of cells expressing httex1Q₂₅-CFP or httex1Q₇₂-CFP with either V_L12.3 or an empty vector control. Dashed circles indicate where insoluble material would appear. Difference between 25Q with and without VL12.3 is insignificant and within variance usually observed for the assay. B. Spotting of yeast strains indicating ability to grow on solid media. C. Growth curves obtained by measuring the optical density of yeast cultures at 600 nm. Yeast expressing V_L12.3-YFP along with httex1Q₇₂-CFP grow at rates comparable to those expressing htt with non-pathological polyglutamine repeat lengths, in contrast to those carrying an empty vector only.

Appendix 4: Genbank Summary of V_L12.3

LOCUS AY818434 366 bp DNA linear SYN 12-DEC-2004
DEFINITION Synthetic construct immunoglobulin variable light chain domain
VL12.3 gene, complete cds.
ACCESSION AY818434
VERSION AY818434.1 GI:56404255
KEYWORDS .
SOURCE synthetic construct
ORGANISM [synthetic construct](#)
other sequences; artificial sequences.
REFERENCE 1 (bases 1 to 366)
AUTHORS Colby,D.W., Wittrup,K.D. and Ingram,V.M.
TITLE Potent inhibition of huntingtin aggregation and cytotoxicity by a
disulfide bond-free single domain intrabody
JOURNAL Unpublished
REFERENCE 2 (bases 1 to 366)
AUTHORS Colby,D.W., Wittrup,K.D. and Ingram,V.M.
TITLE Direct Submission
JOURNAL Submitted (04-NOV-2004) Chemical Engineering, MIT, 400 Main St.
Bldg. 56-491, Cambridge, MA 02139, USA
FEATURES Location/Qualifiers
source 1..366
/organism="synthetic construct"
/mol_type="other DNA"
/db_xref="taxon:32630"
[CDS](#) 1..366
/note="single domain antibody fragment"
/codon_start=1
/transl_table=[11](#)
/product="immunoglobulin variable light chain domain
VL12.3"
/protein_id="[AAV87178.1](#)"
/db_xref="GI:56404256"

/translation="MGSQPVLVTQSPSVSAAPRQRVTISVSGSNSNIGSNTVNWIQQLP
GRAPELLMYDDDLLAPGVSDRFSGSRSGTSASLTISGLQSEDEADYYAATWDDS
LNGW
VFGGGTKVTVLSGHHHHHH"
ORIGIN
1 atgggttctc agcctgtgct gactcagtea ccttcggtct ctgcagcccc cggc aaagg
61 gtcaccatct ccgtgtctgg aagcaactcc aacatcggaa gtaatactgt aaactggatc
121 cagcagctcc caggaagggc tcccagctc ctcattgtacg atgacgatct attggcccca
181 ggggtctctg accgatttc tggctctagg tctggcacct cagctcct gaccatcagt

241 gggctccagt ctgaggatga ggctgattat tacgcagcaa catgggatga cagcctgaat
301 ggttgggtgt tcggcggagg gaccaaggtc accgtctat cggacatca ccatcacat
361 cactag

//

References

1. The Huntington's Disease Collaborative Research Group (1993). A novel gene containing a trinucleotide repeat that is expanded and unstable on Huntington's disease chromosomes. *Cell* 72, 971-83.
2. Poirier, M. A., Jiang, H. & Ross, C. A. (2005). A structure-based analysis of huntingtin mutant polyglutamine aggregation and toxicity: evidence for a compact beta-sheet structure. *Hum Mol Genet* 14, 765-74.
3. DiFiglia, M., Sapp, E., Chase, K. O., Davies, S. W., Bates, G. P., Vonsattel, J. P. & Aronin, N. (1997). Aggregation of huntingtin in neuronal intranuclear inclusions and dystrophic neurites in brain. *Science* 277, 1990-3.
4. Zhang, Y., Li, M., Drozda, M., Chen, M., Ren, S., Mejia Sanchez, R. O., Leavitt, B. R., Cattaneo, E., Ferrante, R. J., Hayden, M. R. & Friedlander, R. M. (2003). Depletion of wild-type huntingtin in mouse models of neurologic diseases. *J Neurochem* 87, 101-6.
5. Busch, A., Engemann, S., Lurz, R., Okazawa, H., Lehrach, H. & Wanker, E. E. (2003). Mutant huntingtin promotes the fibrillogenesis of wild-type huntingtin: a potential mechanism for loss of huntingtin function in Huntington's disease. *J Biol Chem* 278, 41452-61.
6. Perutz, M. F., Johnson, T., Suzuki, M. & Finch, J. T. (1994). Glutamine repeats as polar zippers: their possible role in inherited neurodegenerative diseases. *Proc Natl Acad Sci U S A* 91, 5355-8.
7. Perutz, M. F., Finch, J. T., Berriman, J. & Lesk, A. (2002). Amyloid fibers are water-filled nanotubes. *Proc Natl Acad Sci U S A* 99, 5591-5.
8. Scherzinger, E., Lurz, R., Turmaine, M., Mangiarini, L., Hollenbach, B., Hasenbank, R., Bates, G. P., Davies, S. W., Lehrach, H. & Wanker, E. E. (1997). Huntingtin-encoded polyglutamine expansions form amyloid-like protein aggregates in vitro and in vivo. *Cell* 90, 549-58.
9. Nucifora, F. C., Jr., Sasaki, M., Peters, M. F., Huang, H., Cooper, J. K., Yamada, M., Takahashi, H., Tsuji, S., Troncoso, J., Dawson, V. L., Dawson, T. M. & Ross, C. A. (2001). Interference by huntingtin and atrophin-1 with cbp-mediated transcription leading to cellular toxicity. *Science* 291, 2423-8.
10. Bence, N. F., Sampat, R. M. & Kopito, R. R. (2001). Impairment of the ubiquitin-proteasome system by protein aggregation. *Science* 292, 1552-5.
11. Scherzinger, E., Sittler, A., Schweiger, K., Heiser, V., Lurz, R., Hasenbank, R., Bates, G. P., Lehrach, H. & Wanker, E. E. (1999). Self-assembly of polyglutamine-containing huntingtin fragments into amyloid-like fibrils: implications for Huntington's disease pathology. *Proc Natl Acad Sci U S A* 96, 4604-9.
12. Perutz, M. F. & Windle, A. H. (2001). Cause of neural death in neurodegenerative diseases attributable to expansion of glutamine repeats. *Nature* 412, 143-4.
13. Wheeler, Y. Y., Kute, T. E., Willingham, M. C., Chen, S. Y. & Sane, D. C. (2003). Intrabody-based strategies for inhibition of vascular endothelial growth factor receptor-2: effects on apoptosis, cell growth, and angiogenesis. *Faseb J* 17, 1733-5.

14. Khoshnan, A., Ko, J. & Patterson, P. H. (2002). Effects of intracellular expression of anti-huntingtin antibodies of various specificities on mutant huntingtin aggregation and toxicity. *Proc Natl Acad Sci U S A* 99, 1002-7.
15. Alvarez, R. D., Barnes, M. N., Gomez-Navarro, J., Wang, M., Strong, T. V., Arafat, W., Arani, R. B., Johnson, M. R., Roberts, B. L., Siegal, G. P. & Curiel, D. T. (2000). A cancer gene therapy approach utilizing an anti-erbB-2 single-chain antibody-encoding adenovirus (AD21): a phase I trial. *Clin Cancer Res* 6, 3081-7.
16. Heiser, V., Scherzinger, E., Boeddrich, A., Nordhoff, E., Lurz, R., Schugardt, N., Lehrach, H. & Wanker, E. E. (2000). Inhibition of huntingtin fibrillogenesis by specific antibodies and small molecules: implications for Huntington's disease therapy. *Proc Natl Acad Sci U S A* 97, 6739-44.
17. Lecerf, J. M., Shirley, T. L., Zhu, Q., Kazantsev, A., Amersdorfer, P., Housman, D. E., Messer, A. & Huston, J. S. (2001). Human single-chain Fv intrabodies counteract in situ huntingtin aggregation in cellular models of Huntington's disease. *Proc Natl Acad Sci U S A* 98, 4764-9.
18. Murphy, R. C. & Messer, A. (2004). A single-chain Fv intrabody provides functional protection against the effects of mutant protein in an organotypic slice culture model of Huntington's disease. *Brain Res Mol Brain Res* 121, 141-5.
19. Gennari, F., Mehta, S., Wang, Y., St Clair Tallarico, A., Palu, G. & Marasco, W. A. (2004). Direct phage to intrabody screening (DPIS): demonstration by isolation of cytosolic intrabodies against the TES1 site of Epstein Barr virus latent membrane protein 1 (LMP1) that block NF-kappaB transactivation. *J Mol Biol* 335, 193-207.
20. Emadi, S., Liu, R., Yuan, B., Schulz, P., McAllister, C., Lyubchenko, Y., Messer, A. & Sierks, M. R. (2004). Inhibiting aggregation of alpha-synuclein with human single chain antibody fragments. *Biochemistry* 43, 2871-8.
21. Tse, E., Lobato, M. N., Forster, A., Tanaka, T., Chung, G. T. & Rabbitts, T. H. (2002). Intracellular antibody capture technology: application to selection of intracellular antibodies recognising the BCR-ABL oncogenic protein. *J Mol Biol* 317, 85-94.
22. Tanaka, T. & Rabbitts, T. H. (2003). Intrabodies based on intracellular capture frameworks that bind the RAS protein with high affinity and impair oncogenic transformation. *Embo J* 22, 1025-35.
23. Visintin, M., Tse, E., Axelson, H., Rabbitts, T. H. & Cattaneo, A. (1999). Selection of antibodies for intracellular function using a two-hybrid in vivo system. *Proc Natl Acad Sci U S A* 96, 11723-8.
24. Colby, D. W., Garg, P., Holden, T., Chao, G., Webster, J. M., Messer, A., Ingram, V. M. & Wittrup, K. D. (2004). *J Mol Biol* 342, 901-12.
25. Jager, M. & Pluckthun, A. (1999). Domain interactions in antibody Fv and scFv fragments: effects on unfolding kinetics and equilibria. *FEBS Lett* 462, 307-12.
26. Ewert, S., Huber, T., Honegger, A. & Pluckthun, A. (2003). Biophysical properties of human antibody variable domains. *J Mol Biol* 325, 531-53.
27. Holt, L. J., Herring, C., Jespers, L. S., Woolven, B. P. & Tomlinson, I. M. (2003). Domain antibodies: proteins for therapy. *Trends Biotechnol* 21, 484-90.

28. Jobling, S. A., Jarman, C., Teh, M. M., Holmberg, N., Blake, C. & Verhoeyen, M. E. (2003). Immunomodulation of enzyme function in plants by single-domain antibody fragments. *Nat Biotechnol* 21, 77-80.
29. Tanaka, T., Lobato, M. N. & Rabbitts, T. H. (2003). Single domain intracellular antibodies: a minimal fragment for direct in vivo selection of antigen-specific intrabodies. *J Mol Biol* 331, 1109-20.
30. Roth, J. A. & Grammer, S. F. (2004). Gene replacement therapy for non-small cell lung cancer: a review. *Hematol Oncol Clin North Am* 18, 215-29.
31. Boder, E. T. & Wittrup, K. D. (1997). Yeast surface display for screening combinatorial polypeptide libraries. *Nat Biotechnol* 15, 553-7.
32. Feldhaus, M. J., Siegel, R. W., Opresko, L. K., Coleman, J. R., Feldhaus, J. M., Yeung, Y. A., Cochran, J. R., Heinzelman, P., Colby, D., Swers, J., Graff, C., Wiley, H. S. & Wittrup, K. D. (2003). Flow-cytometric isolation of human antibodies from a nonimmune *Saccharomyces cerevisiae* surface display library. *Nat Biotechnol* 21, 163-70.
33. Colby, D. W., Kellogg, B. A., Graff, C. P., Yeung, Y. A., Swers, J. S. & Wittrup, K. D. (2004). Engineering antibody affinity by yeast surface display. *Methods Enzymol* 388, 348-58.
34. Graff, C. P., Chester, K., Begent, R. & Wittrup, K. D. (2004). Directed evolution of an anti-carcinoembryonic antigen scFv with a 4-day monovalent dissociation half-time at 37{degrees}C. *Protein Eng Des Sel* 17, 293-304.
35. Rao, B. M., Girvin, A. T., Ciardelli, T., Lauffenburger, D. A. & Wittrup, K. D. (2003). Interleukin-2 mutants with enhanced alpha-receptor subunit binding affinity. *Protein Eng* 16, 1081-7.
36. Boder, E. T., Midelfort, K. S. & Wittrup, K. D. (2000). Directed evolution of antibody fragments with monovalent femtomolar antigen-binding affinity. *Proc Natl Acad Sci U S A* 97, 10701-5.
37. Cochran, J. R., Kim, Y. S., Olsen, M. J., Bhandari, R. & Wittrup, K. D. (2004). Domain-level antibody epitope mapping through yeast surface display of epidermal growth factor receptor fragments. *J Immunol Methods* 287, 147-58.
38. Orr, B. A., Carr, L. M., Wittrup, K. D., Roy, E. J. & Kranz, D. M. (2003). Rapid method for measuring ScFv thermal stability by yeast surface display. *Biotechnol Prog* 19, 631-8.
39. Shusta, E. V., Kieke, M. C., Parke, E., Kranz, D. M. & Wittrup, K. D. (1999). Yeast polypeptide fusion surface display levels predict thermal stability and soluble secretion efficiency. *J Mol Biol* 292, 949-56.
40. Shusta, E. V., Holler, P. D., Kieke, M. C., Kranz, D. M. & Wittrup, K. D. (2000). Directed evolution of a stable scaffold for T-cell receptor engineering. *Nat Biotechnol* 18, 754-9.
41. VanAntwerp, J. J. & Wittrup, K. D. (2000). Fine affinity discrimination by yeast surface display and flow cytometry. *Biotechnol Prog* 16, 31-7.
42. Yeung, Y. A. & Wittrup, K. D. (2002). Quantitative screening of yeast surface-displayed polypeptide libraries by magnetic bead capture. *Biotechnol Prog* 18, 212-20.

43. Kieke, M. C., Cho, B. K., Boder, E. T., Kranz, D. M. & Wittrup, K. D. (1997). Isolation of anti-T cell receptor scFv mutants by yeast surface display. *Protein Eng* 10, 1303-10.
44. Holler, P. D., Holman, P. O., Shusta, E. V., O'Herrin, S., Wittrup, K. D. & Kranz, D. M. (2000). In vitro evolution of a T cell receptor with high affinity for peptide/MHC. *Proc Natl Acad Sci U S A* 97, 5387-92.
45. Kieke, M. C., Shusta, E. V., Boder, E. T., Teyton, L., Wittrup, K. D. & Kranz, D. M. (1999). Selection of functional T cell receptor mutants from a yeast surface-display library. *Proc Natl Acad Sci U S A* 96, 5651-6.
46. Kieke, M. C., Sundberg, E., Shusta, E. V., Mariuzza, R. A., Wittrup, K. D. & Kranz, D. M. (2001). High affinity T cell receptors from yeast display libraries block T cell activation by superantigens. *J Mol Biol* 307, 1305-15.
47. Colby, D. W., Chu, Y., Cassady, J. P., Duennwald, M., Zazulak, H., Webster, J. M., Messer, A., Lindquist, S., Ingram, V. M. & Wittrup, K. D. (2004). Potent inhibition of huntingtin aggregation and cytotoxicity by a disulfide bond-free single-domain intracellular antibody. *Proc Natl Acad Sci U S A* 101, 17616-21.
48. Colby, D. W., Garg, P., Holden, T., Chao, G., Webster, J. M., Messer, A., Ingram, V. M. & Wittrup, K. D. (2004). Development of a human light chain variable domain (V(L)) intracellular antibody specific for the amino terminus of huntingtin via yeast surface display. *J Mol Biol* 342, 901-12.
49. Boder, E. T. & Wittrup, K. D. (2000). Yeast surface display for directed evolution of protein expression, affinity, and stability. *Methods Enzymol* 328, 430-44.
50. Krobitch, S. & Lindquist, S. (2000). Aggregation of huntingtin in yeast varies with the length of the polyglutamine expansion and the expression of chaperone proteins. *Proc Natl Acad Sci U S A* 97, 1589-94.
51. Marks, J. D., Hoogenboom, H. R., Bonnert, T. P., McCafferty, J., Griffiths, A. D. & Winter, G. (1991). By-passing immunization. Human antibodies from V-gene libraries displayed on phage. *J Mol Biol* 222, 581-97.
52. Arafat, W., Gomez-Navarro, J., Xiang, J., Siegal, G. P., Alvarez, R. D. & Curiel, D. T. (2000). Antineoplastic effect of anti-erbB-2 intrabody is not correlated with scFv affinity for its target. *Cancer Gene Ther* 7, 1250-6.
53. Rajpal, A. & Turi, T. G. (2001). Intracellular stability of anti-caspase-3 intrabodies determines efficacy in retargeting the antigen. *J Biol Chem* 276, 33139-46.
54. Zhu, Q., Zeng, C., Huhlov, A., Yao, J., Turi, T. G., Danley, D., Hynes, T., Cong, Y., DiMattia, D., Kennedy, S., Daumy, G., Schaeffer, E., Marasco, W. A. & Huston, J. S. (1999). Extended half-life and elevated steady-state level of a single-chain Fv intrabody are critical for specific intracellular retargeting of its antigen, caspase-7. *J Immunol Methods* 231, 207-22.
55. Arrasate, M., Mitra, S., Schweitzer, E. S., Segal, M. R. & Finkbeiner, S. (2004). Inclusion body formation reduces levels of mutant huntingtin and the risk of neuronal death. *Nature* 431, 805-10.
56. Clarke, G., Collins, R. A., Leavitt, B. R., Andrews, D. F., Hayden, M. R., Lumsden, C. J. & McInnes, R. R. (2000). A one-hit model of cell death in inherited neuronal degenerations. *Nature* 406, 195-9.

57. Chen, S., Ferrone, F. A. & Wetzel, R. (2002). Huntington's disease age-of-onset linked to polyglutamine aggregation nucleation. *Proc Natl Acad Sci U S A* 99, 11884-9.
58. Cattaneo, E. & Conti, L. (1998). Generation and characterization of embryonic striatal conditionally immortalized ST14A cells. *J Neurosci Res* 53, 223-34.
59. Wexler, N. S., Lorimer, J., Porter, J., Gomez, F., Moskowitz, C., Shackell, E., Marder, K., Penchaszadeh, G., Roberts, S. A., Gayan, J., Brocklebank, D., Cherny, S. S., Cardon, L. R., Gray, J., Dlouhy, S. R., Wiktorski, S., Hodes, M. E., Conneally, P. M., Penney, J. B., Gusella, J., Cha, J. H., Irizarry, M., Rosas, D., Hersch, S., Hollingsworth, Z., MacDonald, M., Young, A. B., Andresen, J. M., Housman, D. E., De Young, M. M., Bonilla, E., Stillings, T., Negrette, A., Snodgrass, S. R., Martinez-Jaurrieta, M. D., Ramos-Arroyo, M. A., Bickham, J., Ramos, J. S., Marshall, F., Shoulson, I., Rey, G. J., Feigin, A., Arnheim, N., Acevedo-Cruz, A., Acosta, L., Alvir, J., Fischbeck, K., Thompson, L. M., Young, A., Dure, L., O'Brien, C. J., Paulsen, J., Brickman, A., Krch, D., Peery, S., Hogarth, P., Higgins, D. S., Jr. & Landwehrmeyer, B. (2004). Venezuelan kindreds reveal that genetic and environmental factors modulate Huntington's disease age of onset. *Proc Natl Acad Sci U S A* 101, 3498-503.
60. Colby, D. W., Kellog, B., Graff, C. P., Yeung, Y. A., Swers, J. S. & Wittrup, K. D. (2004). Engineering Antibody Affinity by Yeast Surface Display. In *Methods Enzymol*, Vol. 388.
61. Swers, J. S., Kellogg, B. A. & Wittrup, K. D. (2004). Shuffled antibody libraries created by in vivo homologous recombination and yeast surface display. *Nucleic Acids Res* 32, e36.
62. Raymond, C. K., Pownder, T. A. & Sexson, S. L. (1999). General method for plasmid construction using homologous recombination. *Biotechniques* 26, 134-8, 140-1.
63. Pedelacq, J. D., Piltch, E., Liang, E. C., Berendzen, J., Kim, C. Y., Rho, B. S., Park, M. S., Terwilliger, T. C. & Waldo, G. S. (2002). Engineering soluble proteins for structural genomics. *Nat Biotechnol* 20, 927-32.
64. Cochran, J. R., Kim, Y. S., Olsen, M. J., Bhandari, R. & Wittrup, K. D. (2004). Domain-level antibody epitope mapping through yeast surface display of epidermal growth factor receptor fragments. *J Immunol Meth* 287, 147-158.
65. Johns, T. G., Adams, T. E., Cochran, J. R., Hall, N. E., Hoyne, P. A., Olsen, M. J., Kim, Y. S., Rothacker, J., Nice, E. C., Walker, F., Old, L. J., Ward, C. W., Burgess, A. W., Wittrup, K. D. & Scott, A. M. (2004). Identification of the epitope for the EGFR-specific monoclonal antibody 806 reveals that it preferentially recognizes an untethered form of the receptor. *J Biol Chem*.
66. Vajdos, F. F., Adams, C. W., Breece, T. N., Presta, L. G., de Vos, A. M. & Sidhu, S. S. (2002). Comprehensive functional maps of the antigen-binding site of an anti-ErbB2 antibody obtained with shotgun scanning mutagenesis. *J Mol Biol* 320, 415-28.
67. Thorn, K. S. & Bogan, A. A. (2001). ASEdb: a database of alanine mutations and their effects on the free energy of binding in protein interactions. *Bioinformatics* 17, 284-5.

68. MacCallum, R. M., Martin, A. C. & Thornton, J. M. (1996). Antibody-antigen interactions: contact analysis and binding site topography. *J Mol Biol* 262, 732-45.
69. Wilson, I. A. & Stanfield, R. L. (1993). Antibody-Antigen Interactions. *Cur Op Struct Biol* 3, 113-118.
70. Wilson, I. A. & Stanfield, R. L. (1994). Antibody-antigen interactions: new structures and new conformational changes. *Curr Opin Struct Biol* 4, 857-67.
71. Rini, J. M., Stanfield, R. L., Stura, E. A., Salinas, P. A., Profy, A. T. & Wilson, I. A. (1993). Crystal structure of a human immunodeficiency virus type 1 neutralizing antibody, 50.1, in complex with its V3 loop peptide antigen. *Proc Natl Acad Sci U S A* 90, 6325-9.
72. Ramm, K., Gehrig, P. & Pluckthun, A. (1999). Removal of the conserved disulfide bridges from the scFv fragment of an antibody: effects on folding kinetics and aggregation. *J Mol Biol* 290, 535-46.
73. Stevens, F. J. & Schiffer, M. (1995). Structure and properties of human immunoglobulin light-chain dimers. *Methods Mol Biol* 51, 51-81.
74. van den Beucken, T., van Neer, N., Sablon, E., Desmet, J., Celis, L., Hoogenboom, H. R. & Hufton, S. E. (2001). Building novel binding ligands to B7.1 and B7.2 based on human antibody single variable light chain domains. *J Mol Biol* 310, 591-601.
75. Bonner, W. M. (1978). Protein migration and accumulation in nuclei. In *The Cell Nucleus* (Busch, H., ed.), Vol. 6, part C, pp. 97-148. Academic Press, New York, NY.
76. Proba, K., Worn, A., Honegger, A. & Pluckthun, A. (1998). Antibody scFv fragments without disulfide bonds made by molecular evolution. *J Mol Biol* 275, 245-53.
77. Choo, Y. S., Johnson, G. V., MacDonald, M., Detloff, P. J. & Lesort, M. (2004). Mutant huntingtin directly increases susceptibility of mitochondria to the calcium-induced permeability transition and cytochrome c release. *Hum Mol Genet* 13, 1407-20.
78. Leenders, K. L., Frackowiak, R. S., Quinn, N. & Marsden, C. D. (1986). Brain energy metabolism and dopaminergic function in Huntington's disease measured in vivo using positron emission tomography. *Mov Disord* 1, 69-77.
79. Mosmann, T. (1983). Rapid colorimetric assay for cellular growth and survival: application to proliferation and cytotoxicity assays. *J Immunol Methods* 65, 55-63.
80. Schaffar, G., Breuer, P., Boteva, R., Behrends, C., Tzvetkov, N., Strippel, N., Sakahira, H., Siegers, K., Hayer-Hartl, M. & Hartl, F. U. (2004). Cellular toxicity of polyglutamine expansion proteins: mechanism of transcription factor deactivation. *Mol Cell* 15, 95-105.
81. Cumming, R. C., Andon, N. L., Haynes, P. A., Park, M., Fischer, W. H. & Schubert, D. (2004). Protein disulfide bond formation in the cytoplasm during oxidative stress. *J Biol Chem* 279, 21749-58.
82. Xu, L., Aha, P., Gu, K., Kuimelis, R. G., Kurz, M., Lam, T., Lim, A. C., Liu, H., Lohse, P. A., Sun, L., Weng, S., Wagner, R. W. & Lipovsek, D. (2002). Directed

- evolution of high-affinity antibody mimics using mRNA display. *Chem Biol* 9, 933-42.
83. Zhou, C., Emadi, S., Sierks, M. R. & Messer, A. (2004). *Mol Ther* In Press.
 84. Meilhoc, E., Masson, J. M. & Teissie, J. (1990). High efficiency transformation of intact yeast cells by electric field pulses. *Biotechnology (N Y)* 8, 223-7.
 85. Stemmer, W. P. (1994). Rapid evolution of a protein in vitro by DNA shuffling. *Nature* 370, 389-91.
 86. Stemmer, W. P. (1994). DNA shuffling by random fragmentation and reassembly: in vitro recombination for molecular evolution. *Proc Natl Acad Sci U S A* 91, 10747-51.
 87. Volkov, A. A. & Arnold, F. H. (2000). Methods for in vitro DNA recombination and random chimeragenesis. *Methods Enzymol* 328, 447-56.
 88. Zacco, M. & Gherardi, E. (1999). The effect of high-frequency random mutagenesis on in vitro protein evolution: a study on TEM-1 beta-lactamase. *J Mol Biol* 285, 775-83.
 89. Zacco, M., Williams, D. M., Brown, D. M. & Gherardi, E. (1996). An approach to random mutagenesis of DNA using mixtures of triphosphate derivatives of nucleoside analogues. *J Mol Biol* 255, 589-603.
 90. Webster, J. M., Tiwari, S., Weissman, A. M. & Wojcikiewicz, R. J. (2003). Inositol 1,4,5-trisphosphate receptor ubiquitination is mediated by mammalian Ubc7, a component of the endoplasmic reticulum-associated degradation pathway, and is inhibited by chelation of intracellular Zn²⁺. *J Biol Chem* 278, 38238-46.
 91. (1991). *Methods in Enzymology*. Guide to Yeast Genetics and Molecular Biology (Fink, G. R. & Guthrie, C., Eds.), 194.
 92. Ito, H., Fukuda, Y., Murata, K. & Kimura, A. (1983). Transformation of intact yeast cells treated with alkali cations. *J Bacteriol* 153, 163-8.
 93. Sikorski, R. S. & Hieter, P. (1989). A system of shuttle vectors and yeast host strains designed for efficient manipulation of DNA in *Saccharomyces cerevisiae*. *Genetics* 122, 19-27.
 94. Muchowski, P. J., Schaffar, G., Sittler, A., Wanker, E. E., Hayer-Hartl, M. K. & Hartl, F. U. (2000). Hsp70 and hsp40 chaperones can inhibit self-assembly of polyglutamine proteins into amyloid-like fibrils. *Proc Natl Acad Sci U S A* 97, 7841-6.
 95. Meriin, A. B., Zhang, X., He, X., Newnam, G. P., Chernoff, Y. O. & Sherman, M. Y. (2002). Huntington toxicity in yeast model depends on polyglutamine aggregation mediated by a prion-like protein Rnq1. *J Cell Biol* 157, 997-1004.

Curriculum Vitae

David W. Colby

Curriculum Vitae

400 Main St. Bldg. 56-491
Cambridge, MA 02139

(617) 258-5293
dcolby@mit.edu

<http://web.mit.edu/cheme/kdw-lab/colby.htm>

EDUCATION

Massachusetts Institute of Technology

Ph.D. Candidate, Chemical Engineering

- Thesis: Intracellular Antibodies Engineered to Prevent Protein Aggregation in Huntington's Disease
- Minor in Computational Biology
- **National Science Foundation Graduate Research Fellow**
- Ph.D. anticipated June 2005

Virginia Commonwealth University

BS Chemical Engineering May 2000

BS Chemistry May 2000

- Minor in Mathematics
- Graduated *summa cum laude*

RESEARCH EXPERIENCE

University of California, San Francisco, Department of Neurology

Post-doctoral Researcher

Advisor: Stanley Prusiner

To begin in July 2005

MIT Departments of Chemical Engineering and Biology

Graduate Research Assistant

2000-Present

- Advisors: K. Dane Wittrup and Vernon Ingram
- Isolated and **engineered intracellular antibodies** against the huntingtin protein
- Studied effect of intracellular antibody expression in **neuronal cell culture models** of Huntington's disease
- Developed and validated **mathematical models of cellular huntingtin aggregation**

VCU Department of Chemical Engineering

Undergraduate Research Assistant

1997-2000

- Senior design project: Design of a **microarray reader** (Advisor: Anthony Guiseppie)
- **Biosensors** for monitoring **Schwan cell growth** (Advisors: Gary Wnek and Oliver Bogler)
- Development of environmentally friendly solders using electrically conducting polymers (Advisor: Gary Wnek)
- Design, construction, and evaluation of a pervaporator for membrane based separations (Advisor: Wayne Erickson)

**RESEARCH
EXPERIENCE,
CONTINUED**

Sentor Technologies, Inc.

Laboratory Specialist
1999-2000

- Analysis of polymers processed by rapid expansion of supercritical solutions

Foster-Miller, Inc.

Laboratory Specialist
Summer 2000

- Development of environmentally friendly solders using electrically conducting polymers

**TEACHING
EXPERIENCE**

MIT Department of Chemical Engineering

Teaching Assistant course 10.28 **Biological Engineering Lab**
Fall 2003

- Assisted in course development for the first offering of this new subject
- Taught undergraduates basic molecular biology and microbiology techniques
- Gave pre-lab lectures

VCU Department of Physics

Laboratory Instructor
Spring 1998

- Gave pre-lab lectures and supervised students in a General Physics Laboratory.

VCU Department of Chemical Engineering

Teaching Assistant
Fall 1997

- Tutored students in introductory chemical engineering course individually and in small groups; gave review lectures.

**AWARDS AND
HONORS**

National Science Foundation Graduate Research Fellow
John Grover Fellow (MIT)
Entrepreneurial Scholarship in Chemical Engineering (VCU)
Tau Beta Pi Honor Society
Phi Kappa Phi Honor Society
Golden Key National Honor Society
VCU Undergraduate Research Grant

**SUPERVISED
UNDERGRADUATE
PROJECTS (MIT)**

Dobrin Draganov (*Current Affiliation: Harvard University*) Effect of huntingtin-binding peptides on cell viability

Nancy Chen Quantitative analysis of peptide transduction domain mediated peptide uptake

Yijia (Colin) Chu Effect of engineered intracellular antibodies on huntingtin aggregation in transiently transfected neuronal cells

Payal Garg (*Current Affiliation: Merck & Co., Inc*) Inhibition of huntingtin aggregation by a single domain antibody against huntingtin monitored by light scattering

**SUPERVISED
UNDERGRADUATE
PROJECTS,
CONTINUED**

Katarzyna Puchala Analysis of apoptosis in neuronal cells expressing the huntingtin transgene
Grace Lin Quantitative analysis of neuronal huntingtin aggregation
John Cassady Effect of huntingtin expression on cell viability
Christine Nee Small molecule inhibitors of huntingtin aggregation

**PAPERS AND
PATENTS**

David W. Colby, Yijia Chu, John Cassady, Helen Zazulak, Martin Duenwald, Jack M. Webster, Anne Messer, Susan Lindquist, Vernon Ingram, K. Dane Wittrup. Potent inhibition of huntingtin aggregation and cytotoxicity by a disulfide bond-free single domain intrabody. *Proc. Natl. Acad. Sci.* **v.101**, pp. 17616-21, 2004
David W. Colby, Payal Garg, Tina Holden, Ginger Chao, Jack M. Webster, Anne Messer, Vernon M. Ingram, K. Dane Wittrup. Development of a Human Light Chain Variable Domain (V_L) Intracellular Antibody against Huntingtin via Yeast Surface Display. *J. Mol. Biol.* **v.342**, pp. 901-12, 2004
David W. Colby, Brenda Kellog, Christilynn P. Graff, Yik A. Yeung, Jeffrey S. Swers, K. Dane Wittrup. Engineering Antibody Affinity by Yeast Surface Display. *Methods in Enzymology* **v.388**, pp. 348-58, 2004
Feldhaus MJ, Siegel RW, Opresko LK, Coleman JR, Feldhaus JM, Yeung YA, Cochran JR, Heinzelman P, Colby D, Swers J, Graff C, Wiley HS, Wittrup KD. Flow-cytometric isolation of human antibodies from a nonimmune *Saccharomyces cerevisiae* surface display library. *Nat Biotechnol.* **v.21** pp.163-70, 2003.
David W. Colby, K. Dane Wittrup, Vernon M. Ingram. Single-Domain Antibodies and Uses Thereof. (Provisional patent application) November 2003.
D. Pestov, N. Levit, D. Colby, G. Tepper, "Chemically Sensitive Nanoparticles Developed from Rapid Expansion of Supercritical Solutions", American Chemical Society, Division of Polymeric Materials: Science and Engineering, PMSE, 2000, **83**, pp. 538-539

PRESENTATIONS

Invited Oral Presentations:

Biomedical Engineering Society, October 2004
CAGn Hereditary Disease Foundation Conference, May 2004
American Institute of Chemical Engineers Annual Conference, Nov 2003
13th Annual Mid Atlantic Bio-Engineering Consortium, April 2000
Engineering the Future of Medicine, Seminar Series, Virginia Commonwealth University, Feb 2000
Second Conference on the Development of Technology in Medicine for Virginia, Nov 1999

Poster Presentations:

Gordon Conference on CAG triplet repeat disorders, May 2003
CAGn Hereditary Disease Foundation Conference, May 2002
Gordon Conference on CAG triplet repeat disorders, May 2001
Merging Micro-Technologies: The Biochip and the Microchip, Jan 2000
Advanced Polymers via Macromolecular Engineering, Aug 1999
High Technology Materials Center Eighth Annual Symposium, Nov 1999
5th International Symposium of Supercritical Fluid Technology, April 2000

**FUNDED
PROPOSALS**

"Therapeutic antibodies for Huntington's disease," David Colby and K.
Dane Wittrup, **Hereditary Disease Foundation**, \$38,000, approved
March 2002
Renewed 4/2003, \$53,000
Renewed 5/2004, \$68,000